

ENERGY TRANSFER IN MIXTURES OF CARBON DIOXIDE-POLYATOMIC MOLECULES USING LASER INDUCED FLUORESCENCE

A Thesis Submitted
In Partial Fulfilment of the Requirements
for the Degree of
DOCTOR OF PHILOSOPHY

by
PALADUGU RAMAMOHANA RAO

to the

DEPARTMENT OF CHEMICAL ENGINEERING
INDIAN INSTITUTE OF TECHNOLOGY KANPUR
APRIL, 1977

CHE-1977-D-RAD-ENE

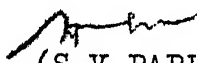
U.S. AIR FORCE
CENTRAL LIBRARY

Acc. No. **53989**

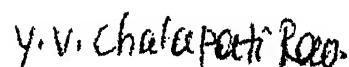
1978

CERTIFICATE:

This is to certify that the work described in this thesis is the original work of Mr. PALADUGU RAMAMOHANA RAO done under our supervision, and has not been submitted elsewhere for a degree.



(S.V.BABU)
Assistant Professor
Dept. of Chem. Engg.
Indian Institute of Technology
Kanpur



(Y.V.CHALAPATI RAO)
Assistant Professor
Dept. of Chem. Engg.
Indian Institute of Technology
Kanpur

POST GRADUATE OFFICE
This thesis has been approved
for the award of the Degree of
Doctor of Philosophy (Ph.D.)
in accordance with the
regulations of the Indian
Institute of Technology Kanpur
Dated:

POST GRADUATE OFFICE
This thesis has been approved
for the award of the Degree of
Doctor of Philosophy (Ph.D.)
in accordance with the
regulations of the Indian
Institute of Technology Kanpur
Dated: 6/3/78

TABLE OF CONTENTS

	Page
LIST OF FIGURES	iv
LIST OF TABLES	v
ABSTRACT	vii
CHAPTER I INTRODUCTION	1
CHAPTER II LASER INDUCED FLUORESCENCE TECHNIQUE	9
CHAPTER III EXPERIMENTAL SET-UP	15
CHAPTER IV RESULTS AND DISCUSSION	25
CHAPTER V CONCLUSIONS	116
REFERENCES	119

LIST OF FIGURES

Figure		Page
1	Block diagram of the experimental set-up	16
2	Sectional view of the test cell	19
3	Typical fluorescence decay curve	23
4	Semilogarithmic plot of fluorescence signal intensity versus time	28
5	The dependence of τ^{-1} on P	29
6	The composition dependence of decay rate constant, K_{obs}	31
7	Temperature dependence of $K_{\text{CO}_2-\text{CH}_3\text{OH}}$	32
8	Temperature dependence of $K_{\text{CO}_2-\text{CH}_3\text{OD}}$	53
9	Temperature dependence of $K_{\text{CO}_2-\text{C}_2\text{H}_5\text{OH}}$	64
10	Temperature dependence of $K_{\text{CO}_2-\text{C}_2\text{H}_4\text{O}}$	69
11	Temperature dependence of $K_{\text{CO}_2-\text{CH}_3\text{CHO}}$	83
12	Temperature dependence of $K_{\text{CO}_2-\text{HCOOH}}$	99
13	Temperature dependence of $K_{\text{CO}_2-\text{CH}_3\text{COOH}}$	111

LIST OF TABLES

Table		Page
1	Rate constants, cross-sections and probabilities for $\text{CO}_2\text{-CH}_3\text{OH}$ system	33
2-4	Experimental data for $\text{CO}_2\text{-CH}_3\text{OH}$ system	34-36
5	Molecular and other constants used in Sharma-Brau theory calculations	44
6	Calculated probabilities for $\text{CO}_2\text{-CH}_3\text{OH}$ system	45
7-11	Experimental data for $\text{CO}_2\text{-CH}_3\text{OD}$ system	48-52
12	Rate constants, cross-sections and probabilities for $\text{CO}_2\text{-CH}_3\text{OD}$ system	47
13	Calculated probabilities for $\text{CO}_2\text{-CH}_3\text{OH}$ system	56
14-18	Experimental data for $\text{CO}_2\text{-C}_2\text{H}_5\text{OH}$ system	59-63
19	Rate constants, cross-sections and probabilities for $\text{CO}_2\text{-C}_2\text{H}_5\text{OH}$ system	58
20	Calculated probabilities for $\text{CO}_2\text{-C}_2\text{H}_5\text{OH}$ system	67
21-28	Experimental data for $\text{CO}_2\text{-C}_2\text{H}_4\text{O}$ system	70-77
29	Rate constants, cross-sections and probabilities for $\text{CO}_2\text{-C}_2\text{H}_4\text{O}$ system	78
30	Calculated probabilities for $\text{CO}_2\text{-C}_2\text{H}_4\text{O}$ system	80
31-36	Experimental data for $\text{CO}_2\text{-CH}_3\text{CHO}$ system	84-89
37	Rate constants, cross-sections and probabilities for $\text{CO}_2\text{-CH}_3\text{CHO}$ system	90

Table		Page
38	Calculated probabilities for $\text{CO}_2\text{-CH}_3\text{CHO}$ system	92
39-41	Experimental data for $\text{CO}_2\text{-HCOOH}$ system	96-98
42	Rate constants, cross-sections and probabilities for $\text{CO}_2\text{-HCOOH}$ system	95
43-50	Experimental data for $\text{CO}_2\text{-CH}_3\text{COOH}$ system	103-110
51	Rate constants, cross-sections and probabilities for $\text{CO}_2\text{-CH}_3\text{COOH}$ system	112

ABSTRACT

Name of student	:	Paladugu Ramamohana Rao
Programme	:	Ph.D.
Department	:	Chemical Engineering
Title of the Thesis	:	Energy Transfer in mixtures of Carbon dioxide-polyatomic molecules using Laser Induced Fluorescence
Supervisors	:	Dr. S.V. Babu Dr. Y.V. Chalapati Rao Department of Chemical Engg.
Institute	:	Indian Institute of Technology Kanpur-208016, India

The collisional deactivation rates of the $\text{CO}_2(00^01)$ mode in binary mixtures with CH_3OH , CH_3OD , $\text{C}_2\text{H}_5\text{OH}$, $\text{C}_2\text{H}_4\text{O}$, CH_3CHO , HCOOH and CH_3COOH are experimentally measured in the temperature range of 300-750°K using the Laser Induced Fluorescence technique. The measured deactivation rates are in the range of 20-400($\text{msec}^{-1}\text{torr}^{-1}$) and decrease with increasing temperature suggesting that near-resonant V-V energy transfer processes are responsible for the deactivation. The processes are discussed for each binary system. In the alcohols, the C-O stretch mode dominates the deactivation process. In the other molecules, in addition to some fundamental bands around 1000 cm^{-1} , some weak bands around 2350 cm^{-1} also participate. The dipole moments of the transitions involved in these processes are estimated using Sharma-Brau theory and our experimental results. This could not be done for the two acids, primarily because of substantial dimer concentration in the vapor phase at lower temperatures.

CHAPTER I

INTRODUCTION

The measurement and prediction of energy transfer rates in gases and gas mixtures is of practical importance in the design of new laser systems, chemical kinetics, gas dynamics, electrical discharges etc.

The importance of the knowledge of energy transfer rates in laser technology can be viewed from the tremendous impact that such a knowledge made on the CO_2 laser output power. From a level of 30 mW in pure CO_2 , the power output has gone up to a few kilowatts in mixtures of $\text{CO}_2\text{-N}_2\text{-He}^{1-6}$. This power enhancement and higher efficiency is closely related to the efficient energy transfer that occurs between the vibrational modes of CO_2 and N_2 and between the vibrational and translational modes of CO_2 and He. If the rate of excitation of the upper laser level becomes comparable to the decay rate of the lower laser level, overpopulation of the lower level limits the power output⁷.

The performance limiting factors in molecular lasers are determined by the various energy transfer processes for the self deactivation and vibrational energy transfer of the constituent gases. At present not many molecules exhibit

laser action (even though the reported laser lines run into several hundreds) and it is reasonable to expect that more and more new molecular lasers will be developed as additional knowledge of energy transfer mechanisms and pathways in these molecules becomes available.

Atomic recombination and unimolecular chemical decomposition depend on the inter- and intramolecular energy transfer processes. Chemical reactions proceed through the rupture or weakening of chemical bonds. In conventional thermal reactions, energy is supplied to the translational degrees of freedom of the reactants which then has to be transferred into the internal degrees of freedom before the bond rupture or weakening takes place. However, vibrationally hot molecules undergo reaction even if their translational temperature is low. Thus, the rate at which energy is exchanged between the translational and vibrational (T-V) degrees of freedom and between vibrational and vibrational (V-V) degrees of freedom of the reacting molecules plays an important role in determining the rate of these reactions.

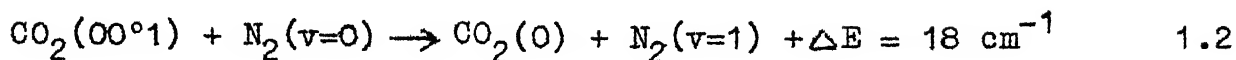
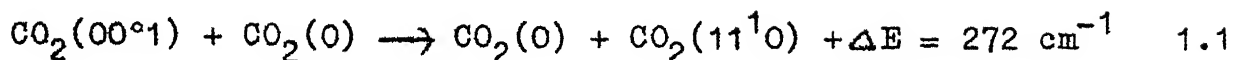
With the development of lasers, their application to induce and stimulate chemical reactions by vibrationally exciting the reactant molecules at even lower translational temperatures has attracted much attention⁸⁻¹⁰. When the

reactant molecule is excited using a laser, it is possible that the energy gets redistributed among the translational and the various internal modes of the molecule by collisions before the chemical bond weakens. To understand the effect of laser radiation on chemical reaction rates, product yields etc. as well as the mechanism of unimolecular decomposition, information regarding different energy transfer processes like V-T and V-V is required.

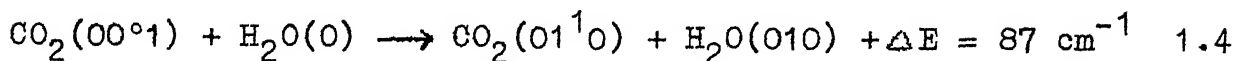
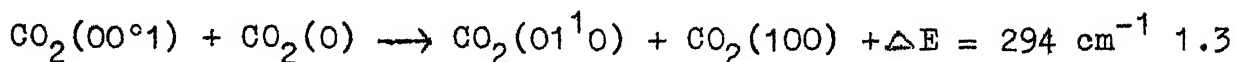
However, in most systems it is difficult to measure these rates directly. So it will be useful to have at least some well tested theories, even if they are only approximate, to predict these rates.

Before mentioning the energy transfer theories, it is useful to classify the energy transfer processes. In general they can be divided into several types like vibration to vibration (V-V), vibration to translation (V-T), vibration to rotation (V-R) and rotation to rotation (R-R) processes. It is well established that R-R and V-R rates are faster than V-V rates which are faster than V-T rates. Of these, only the V-V energy transfer processes are studied in this thesis. These can be further divided as¹¹

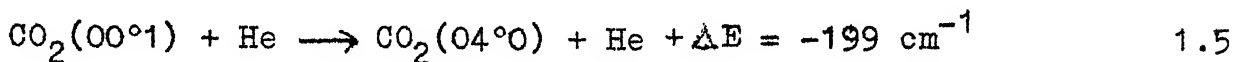
1. Intermolecular V-V energy transfer



2. Intermolecular V-V energy sharing



3. Intramolecular V-V energy sharing.



Each of the processes in the above classes may again be divided into

- a) near-resonant processes i.e., those with small energy mismatch (processes 1.2 and 1.4) and
- b) nonresonant processes i.e., those with high energy mismatch (processes 1.1 and 1.3).

The observed V-V energy transfer probability in a polyatomic molecule may be due to one or more of the above class of processes¹¹. For near-resonant V-V processes the energy transfer probabilities may be predicted using Sharma and Brau (SB) theory¹², whereas for nonresonant processes,

Schwartz, Slawsky and Herzfeld (SSH) theory¹³ and its refinements¹⁴⁻¹⁷ may be used. SB theory takes into account only the long range multipole interactions and predicts comparatively large values for the energy transfer probability. It also predicts a negative temperature dependence for the energy transfer probability. However, it appears that this temperature dependence is not necessarily due to the long range nature of the intermolecular forces but arises, as pointed out by Moore¹⁸, because of the "impact parameter, constant velocity, straight line form of the Born approximation" used in the theory. There is, infact, some recent controversy on this point¹⁹⁻²¹. On the other hand, the probabilities predicted by SSH theory, which assumes the presence of only short range repulsive forces, are generally considerably small even for near-resonant processes. In addition, this theory also predicts a positive temperature dependence for the probability. Hence, it may be said that whenever fairly large probabilities are encountered SB theory or some refinement of it^{22,23} has to be used. Exceptions exist as in the case of Hydrogen halides, but in these systems it is now accepted that rotational effects are important²⁴. SB theory has, infact, been extensively applied to many near resonant energy transfer processes involving small molecules like CO_2 , N_2 ¹⁴, N_2 ¹⁵,

$C^{12}O, C^{13}O, N_2^{14}O, N_2^{15}O, N^{14}O, N^{15}O$ etc¹⁸. So it should be useful to extend these studies to processes involving larger molecules.

The collisional energy transfer rates in gases and gas mixtures can be studied by creating large enough changes in the equilibrium populations among the vibrational levels and the subsequent observation of the rate at which the excess population relaxes to its equilibrium value. A number of experimental methods are available to study these rates^{11,16}. Some of the widely used methods are

1. Ultrasonic and shock tube techniques
2. Optical excitation without lasers
3. Flash photolysis
4. Monochromatically excited electronic fluorescence.
5. Chemical excitation.
6. Molecular beams
7. Laser excitation methods
 - (a) Laser induced fluorescence
 - (b) Laser - Laser double resonance
 - (c) Time resolved thermal lensing

All these methods have been thoroughly reviewed by Moore¹¹, Amme²⁵ and Ormonde²⁶ and the references cited therein. Among these, the laser excitation methods have been

widely used to obtain specific energy transfer rates^{11,18,30} since lasers provide monochromatic and intense radiation which can be used to create large changes in energy level populations and to selectively excite any particular level among the internal degrees of freedom of a molecule. The possibility of exciting any given level in a molecule is becoming increasingly feasible with the availability of more and more tunable lasers.

In the present work, the rate of collisional transfer of energy from the $\text{CO}_2(00^01)$ mode in binary mixtures of CO_2 with several polyatomic molecules has been experimentally measured in the temperature range 300-750°K using the laser induced fluorescence technique. The polyatomic molecules studied are CH_3OH , CH_3OD , $\text{C}_2\text{H}_5\text{OH}$, $\text{C}_2\text{H}_4\text{O}$, CH_3CHO , HCOOH and CH_3COOH . It has been observed that the deactivation rates are fairly large ($20\text{-}400\text{ msec}^{-1}\text{ torr}^{-1}$) in all these systems and that they decrease with temperature. It is also shown in the following that several near-resonant processes are possible in each of these systems, and that the observed rate is due to a combination of all of them. Using the experimentally measured probabilities, the dipole moments of the transitions involved in these processes (except in the case of HCOOH and CH_3COOH) are estimated assuming that SB theory is reasonably accurate in estimating the probabilities for

these processes. The estimated transition moments are necessarily approximate in view of the limitations of the SB theory pointed out above. However, these calculated moments are in accord with the relative spectral absorption intensities of the corresponding IR bands. Hence, if the values of these transition moments can be obtained through independent experiments, these estimates may be regarded as providing a basis to test the applicability of SB theory to near-resonant processes involving polyatomic molecules.

The remainder of the thesis is organised as follows. The laser induced fluorescence technique which is employed in the present work is described in detail in chapter II. The experimental setup along with a description of its components - namely a) Q-switched CO_2 laser, b) signal detection units and c) signal processing units - have been briefly described in chapter III. In chapter IV, the collisional energy transfer rates obtained from the experiments in binary mixtures of ~~the~~ CO_2 (~~0001~~) ~~mode~~ with the polyatomic molecules listed earlier are discussed. The processes that are responsible for the energy transfer have been identified for each system and SB theory has been used to estimate the unknown transition dipole moments in these molecules. Finally, the conclusions are presented in chapter V.

CHAPTER II

LASER INDUCED FLUORESCENCE TECHNIQUE

The laser induced fluorescence technique which has been employed for V-V energy transfer studies in CO₂-polyatomic molecules is discussed briefly in this chapter. Ever since this technique was reported^{27,28} in 1966, it has been widely used to study V-V and V-T/R energy transfer rates in gases and gas mixtures in the temperature range of 77°K - 1000°K^{11,18,29-33}.

In general, any gas laser operating on a particular vibrational transition permits that transition to be excited in that gas (or a transition which can absorb that frequency if a different gas is used) when a sample of it is placed either inside or outside the laser cavity. A non-equilibrium population results among the vibrational levels of the absorbing gas following such an excitation. As the population returns to equilibrium, primarily due to collisional exchange of energy between the internal modes, fluorescence emitted by any individual level can be followed by an appropriate combination of filters and detectors to obtain the rate of pumping^{to} or the rate of removal of energy from the fluorescing level. It is also possible to excite molecules of one gas in a mixture of gases and follow the

fluorescence, if any, from the molecules of any of the other components of the gas mixture.

In the present work, a Q-switched CO_2 laser is used to excite the CO_2 molecules present in a test cell along with those of a polyatomic gas M. During the laser pulse the transitions ($100, 020 \rightarrow 00^{\circ}1$) in CO_2 are saturated creating a non-equilibrium population among these levels. Immediately after the excitation pulse ceases, the excess population pumped into the ($00^{\circ}1$) level, which leads to the emission of 4.3μ fluorescence, starts decaying. The time constant τ , of this decay, which is obtained by monitoring the 4.3μ fluorescence, may be called the relaxation time or the life time of that level of the sample. In all our experimental runs single exponential decay of the fluorescence has been observed. This means that, if $n(t)$ is the excess population in the ($00^{\circ}1$) level at any time t after the excitation pulse is turned off, then the rate of change of this excess population is proportional to the excess population itself and is given by

$$\frac{dn}{dt} = - \frac{n}{\tau} \quad 2.1$$

where τ is the relaxation time of the fluorescing level.

The solution of this first order rate equation is

$$n = n_0 \exp(-t/\tau) \quad 2.2$$

where n_0 is the excess population of the level at time $t = 0$.

The excess population of the ($00^{\circ}1$) level returns to the equilibrium value through i) radiative decay, ii) collisions with CO_2 molecules and the molecules of the added gas, if any, and iii) diffusion to and subsequent decay by collisions with the walls of the container. Therefore, the total relaxation rate ($1/\tau$) at a given pressure P can be written as

$$\frac{1}{\tau} = \frac{1}{\tau_{\text{rad}}} + \frac{1}{\tau_{\text{coll}}} + \frac{1}{\tau_{\text{diff}}} \quad 2.3$$

The radiative decay rate ($1/\tau_{\text{rad}}$) is constant and is independent of gas pressure, while the collisional decay rate ($1/\tau_{\text{coll}}$) is directly proportional to the gas pressure P as long as only binary collisions are predominant. However, the diffusion rate ($1/\tau_{\text{diff}}$) varies inversely with the pressure and is important only if the sample pressure is low (< 1 torr)³⁴. Therefore, the slope of the plot of τ^{-1} versus P yields $(P\tau_{\text{coll}})^{-1}$ directly, if we limit ourselves to $P < 1$ torr. This slope is called K_{obs} in this thesis.

Since the $\text{CO}_2(00^{\circ}1)$ level is optically connected to the ground state, it emits spontaneous radiation at 4.3μ . The intensity of the emitted radiation is proportional to the excess number of molecules in that level. The rate at

which the excess population attains its equilibrium value can be studied by monitoring the rate of decay of the fluorescence signal intensity with a Ge: Au detector maintained at 77°K. If the decay is according to the exponential form (equation 2.2), a semilogarithmic plot of the fluorescence signal intensity versus time should yield a straight line from which the relaxation time τ can be obtained. By measuring τ at different pressures and then plotting τ^{-1} against pressure P , one can obtain the collisional decay rate K_{obs} . In a mixture of CO_2 and a polyatomic gas M , the collisional rate thus obtained is due to: i) collisions with CO_2 molecules and ii) collisions with molecules M . By studying the composition dependence of K_{obs} , and then extrapolating K_{obs} to zero percent composition of CO_2 in the mixture, it is possible to deduce the collisional deactivation rate constant K_{CO_2-M} of the $\text{CO}_2(00^{\circ}1)$ mode with only M . The above studies are carried out at different temperatures, to obtain the temperature dependence of the collisional deactivation rates K_{CO_2-M} .

This laser excited fluorescence method has several advantages over the conventional methods like flash photolysis, ultrasonic absorption, shock waves etc., for the measurement of energy transfer rates in gases and gas mixtures¹¹. The initial excited level of a molecule can be

precisely specified in laser experiments since the exciting pulse emitted by the laser has very narrow band width. The fact that this excitation can be achieved, without directly disturbing the adjacent energy levels, has been used in laser double resonance experiments. Thus, the excitation is specific, and since decay from any other specific level can be followed, deactivation rates can be measured experimentally for specific levels. The other experimental methods are, in comparison, limited by the fact that the excitation must proceed through the translational degrees of freedom. Thus, in these methods the excitation is not specific, and when dealing with polyatomic molecules the analysis of the resulting data is quite complex. Secondly, the high power densities of the exciting radiation produced by lasers are very useful in the study of fast V-V energy transfer rates in gases and gas mixtures, since this enables one to saturate the upper energy level of the absorbing transition, which in turn yields a strong fluorescence signal with a correspondingly high signal to noise ratio. The narrow band width can be used to excite specific energy levels which is not possible with other conventional methods.

The experimental data on energy transfer is generally reported in terms of the deactivation rate constant $K_{\text{CO}_2-\text{M}}$, the collision cross-section for energy transfer σ , and the

energy transfer probability per collision P . These are interrelated as follows.

$$\bar{v} = K/nV \quad 2.4$$

$$P = \bar{v}/\pi d^2 \quad 2.5$$

where n = number density of molecules

V = average relative velocity of the colliding pair

and d = average diameter of the colliding pair.

Thus for CO_2 -M collisions

$$d = \frac{1}{2} [d(\text{CO}_2) + d(\text{M})]$$

CHAPTER III

EXPERIMENTAL SET UP

A brief description of the experimental set-up used to study Laser Induced Fluorescence had been reported^{35,36}. A block diagram of the experimental set-up is shown in Fig.1. The main components of the set-up are

- a) A Q-switched CO₂ laser
- b) Fluorescence signal detection units
- c) Signal processing units

A description of the above components is presented below.

- a) Q-switched CO₂ Laser

The laser consists of a discharge tube; 25 mm ID, 3.5 m. long thick walled Pyrex glass. Glass 'T' joints are attached at both ends. The side projections are used as gas inlet and exit ports. One end of the discharge tube is sealed at Brewster's angle with a polished NaCl window (60 mm dia, 5 mm thick), and the other end is attached to a fixed mirror mount through flexible metal bellows. The gas inlet port is in turn connected to a copper tube which acts as a hollow cylindrical anode. The exit port is connected to a 160 l/m Welch mechanical pump through a water cooled copper tube, which acts as the cathode. The discharge tube is held

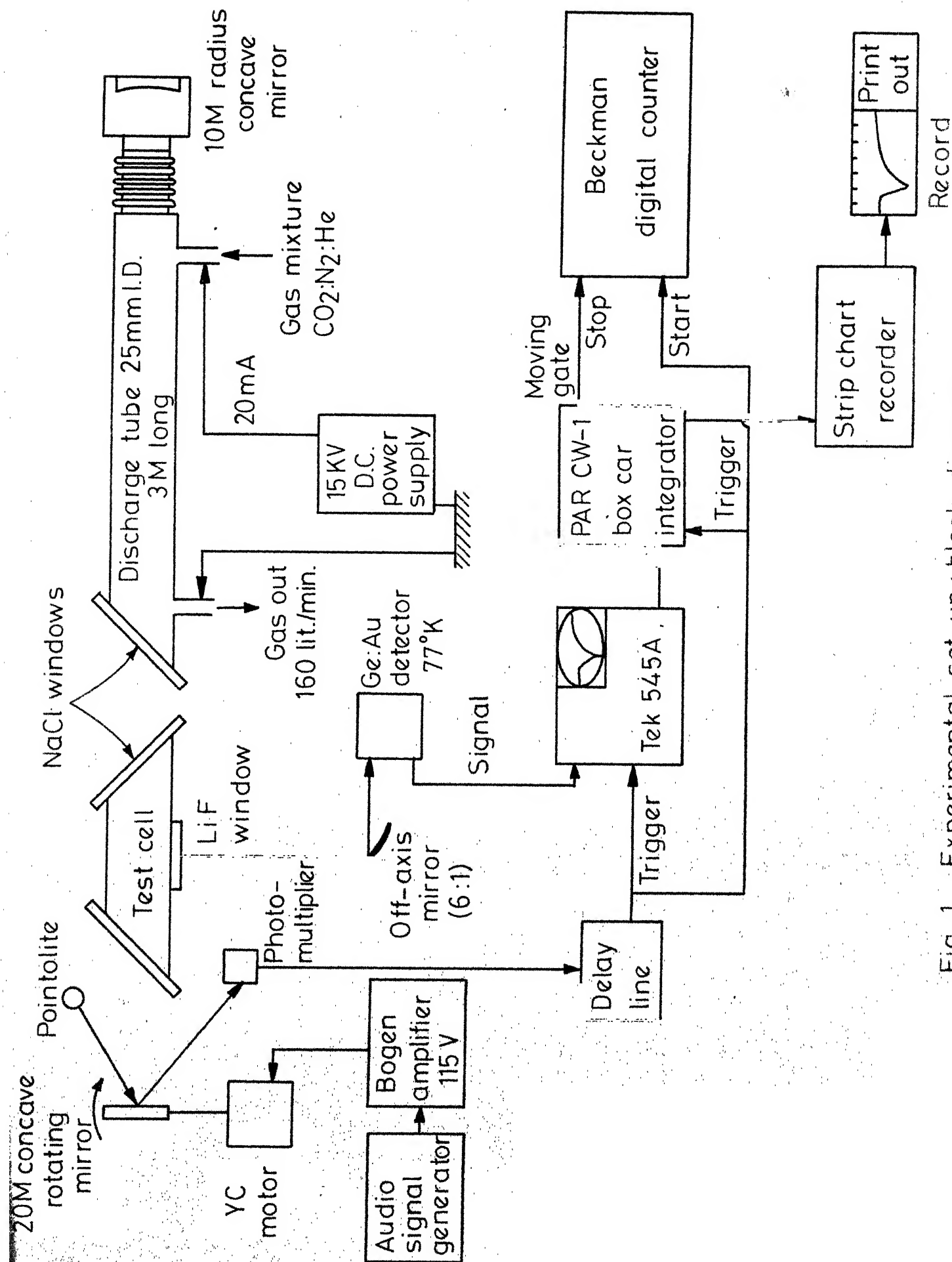


Fig. 1 -Experimental set-up : block diagram

concentric inside a 50 mm dia, 3 m long thick walled Pyrex glass tube. Cold water is circulated through the annulus to cool the plasma tube while in operation. The entire assembly is supported by 'V' blocks on a steel channel which is rigidly mounted on vibration proof concrete foundations.

Gold coated high reflectivity mirrors are used in the present work. The mirrors have been developed by vacuum deposition of gold on polished pyrex blanks. A 10 m. radius of curvature mirror with a 6 mm dia. central hole for laser power output coupling, is mounted in the stationary mirror mount. This hole is blanked by a NaCl window. The orientation of the mirror can be adjusted by two micrometer screws. The other mirror of 20 m. radius of curvature is mounted on the shaft of a Globe YC motor. This motor is located a meter away from the window fixed at Brewster's angle to facilitate the insertion of the fluorescence cell. Audio signal of 400 Hz is generated by an Exact Electronics function generator and amplified to 115 V through a Bogen amplifier. This power is used to run the YC motor at 40 Hz to Q-switch the laser. The motor is mounted on a steel plate which can traverse along both the horizontal and vertical axes. This plate is supported on a steel frame which can be tilted. These motions facilitate the easy alignment of the mirror.

The gases used in the laser are commercial grade Nitrogen supplied by Indian Oxygen Limited, Bone Dry grade CO_2 and high purity He both supplied by Matheson gas Co. The gases are mixed in the ratio of $\text{CO}_2:\text{N}_2:\text{He} = 1:2:1$ in a brass mixing chamber which is fitted with micrometer needle valves to regulate the flow of gases. The pressure in the mixing chamber is maintained at approximately 12 torr. The mixing chamber is connected to the discharge tube by a 10 m. long, 12 mm dia. teflon tube. The length of the teflon tube is selected such that the distance between the anode and the metal mixing chamber is at least twice that of the distance between the two electrodes to prevent the discharge occurring between the anode and the mixing chamber.

An optimum current of 18-20 mA. through the discharge tube required a potential difference of 12 KV DC across the electrodes. The DC power supply for the laser consists of a high voltage transformer (15 KV-0-15 KV, 500 mA) and a series of rectifier diodes. The rectified voltage is filtered through a low pass filter net work and the output is taken to the plasma tube through a $100\text{K}\Omega$ ballast resistor.

b) Fluorescence Signal detection units

The fluorescence cell which can be used upto 1000°K is described by I.V. Rao³⁷ and is shown in Fig.2. The cell

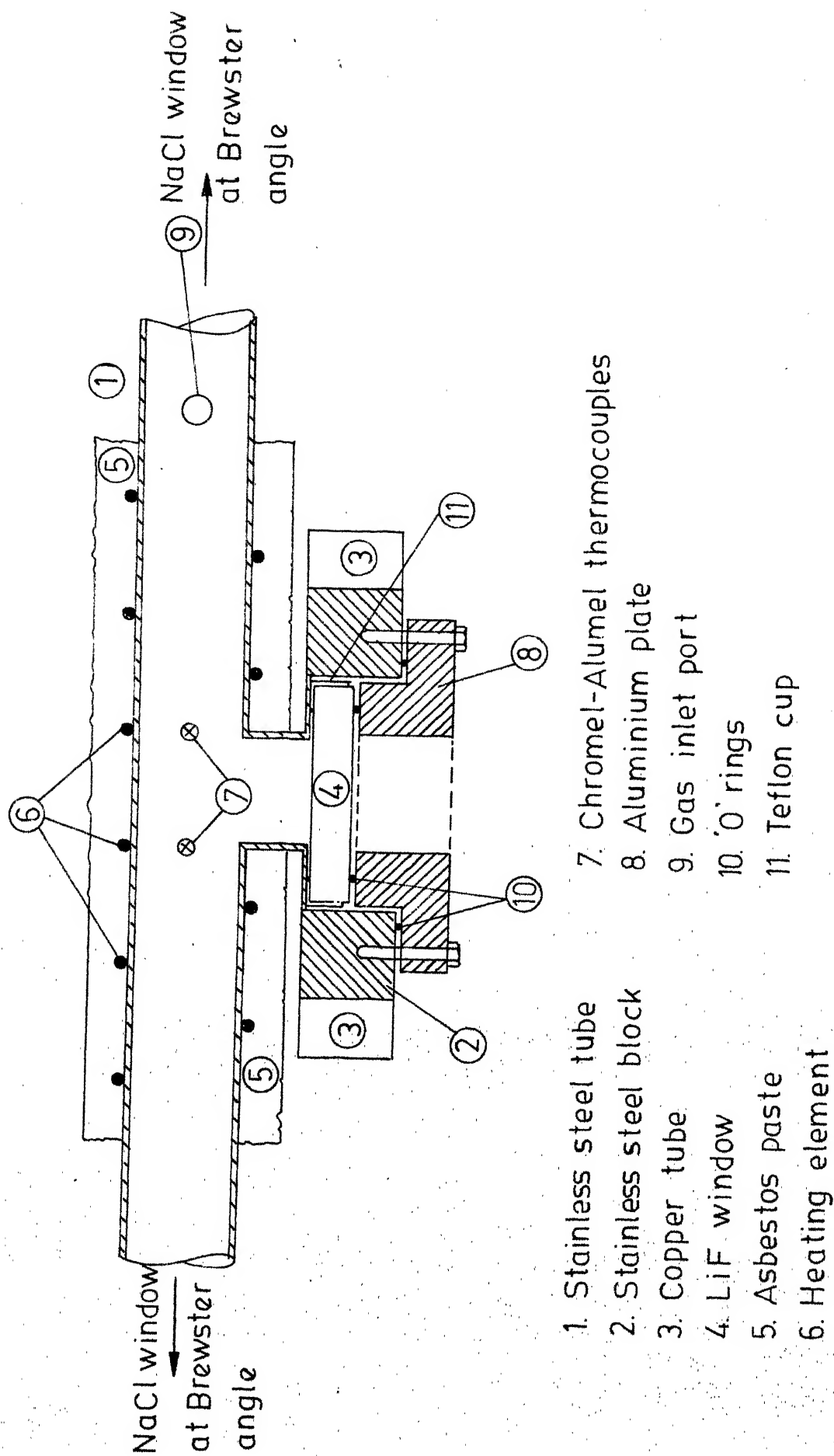


Fig. 2 -Sectional plan of the test cell.

is made of 35 cm long, 25 mm ID, 4 mm thick SS tube. To either side of the SS tube, short glass tubes of the same ID are attached by flanges. The ends of the glass tubes are cut at Brewster's angle and sealed with NaCl windows. A 25-mm hole is drilled at the center of the SS tube normal to the axis on one side and a very short SS tube is then welded after ensuring that its axis is perpendicular to the axis of the main tube. A heavy SS block (10x10 cmx12mm) with a 25 mm central hole is welded to the short side tube. This block, which is kept cool by passing cold water through coils welded to it, houses the LiF window which transmits $4.3\ \mu$ fluorescence radiation and blocks not only the $10.6\ \mu$ laser radiation but also any possible fluorescence from the polyatomic molecule. On one side of the cell, a 6 mm hole is drilled at the top which is connected through flexible metal bellows to a 6 mm Pyrex ball joint, which can be coupled to the gas handling station for evacuation and filling purposes. The cell is wound with a 1000 W nichrome wire and insulated. Two Chromel-Alumel thermocouples are located 2.5 cms. apart at the centre of the cell to monitor the cell temperature. One of them is used to measure and the other to control the temperature through a Honey-Well on - off controller. The cell temperature is maintained constant within $\pm 2^\circ\text{C}$. The cell is placed in the laser cavity between the discharge tube and the Q-switch motor.

The test cell is evacuated down to 10^{-4} torr and the test gas mixture is filled at a known pressure. During the CO_2 Q-switched laser pulse, the transitions $(100,020) \rightarrow 001$ in CO_2 gas present in the test cell are saturated. The CO_2 molecules excited to the ν_3 state lose energy due to collisions with other molecules. The spontaneous emission from the transition $001 \rightarrow 000$ in CO_2 at 4.3μ is viewed through the LiF window. The fluorescence is collected by an off-axis elliptical mirror (6:1) and focussed on to a liquid Nitrogen cooled Ge: Au detector (SBRC) loaded with 10K Ω . The response time of the detector under these conditions is estimated to be less than 2 μ sec.

c) Signal Processing Units

A point source of light is focussed on to the rotating mirror and its reflection is intercepted by an IP 28 photomultiplier biased at 900 V. The PMT output is used to trigger the Tektronix 545A Oscilloscope with predetermined delay. The detector output is displayed on the CRO with 1A7A plugin unit. The low and high frequency cut offs are adjusted to 1Hz and 1 MHz. The vertical amplifier output is fed to a PAR CW-1 Boxcar integrator to improve the signal to noise ratio. The delayed trigger output from the CRO is used to trigger the Boxcar and a Beckman digital counter.

Typical integration times are 20 μ sec with a time constant of 0.1 ms, gate width of 1 μ sec, to scan a time base of 100 μ sec with a 40 PPS pulse repetition rate. The moving gate of the Boxcar is used to stop the counter. The output from the Boxcar is recorded on a Bausch-Lomb VOM-6 Strip Chart recorder. A typical fluorescence decay curve as obtained on the recorder is presented in Fig.3.

TEST SAMPLES

The polyatomic molecules chosen in this study are liquids at room temperature with the exception of Ethylene oxide. The test samples of these liquids are prepared as follows. The liquid is taken into a 50 cc bottle which is connected to the glass vacuum station. The trapped air is first pumped out from this bottle. Then the sample is frozen at liquid nitrogen temperature while evacuation is continued for about 15 minutes. Then the sample is allowed to warm up to room temperature and the vapors are pumped out for another 15 minutes to get rid of any volatile impurities that may be present. The vapors are then collected in thoroughly evacuated ($\approx 10^{-4}$ torr) glass bulbs at different pressures. Then these bulbs are filled with CO₂ gas to bring the total pressure upto about 400 torr. The composition of the sample in the bulbs is determined from partial

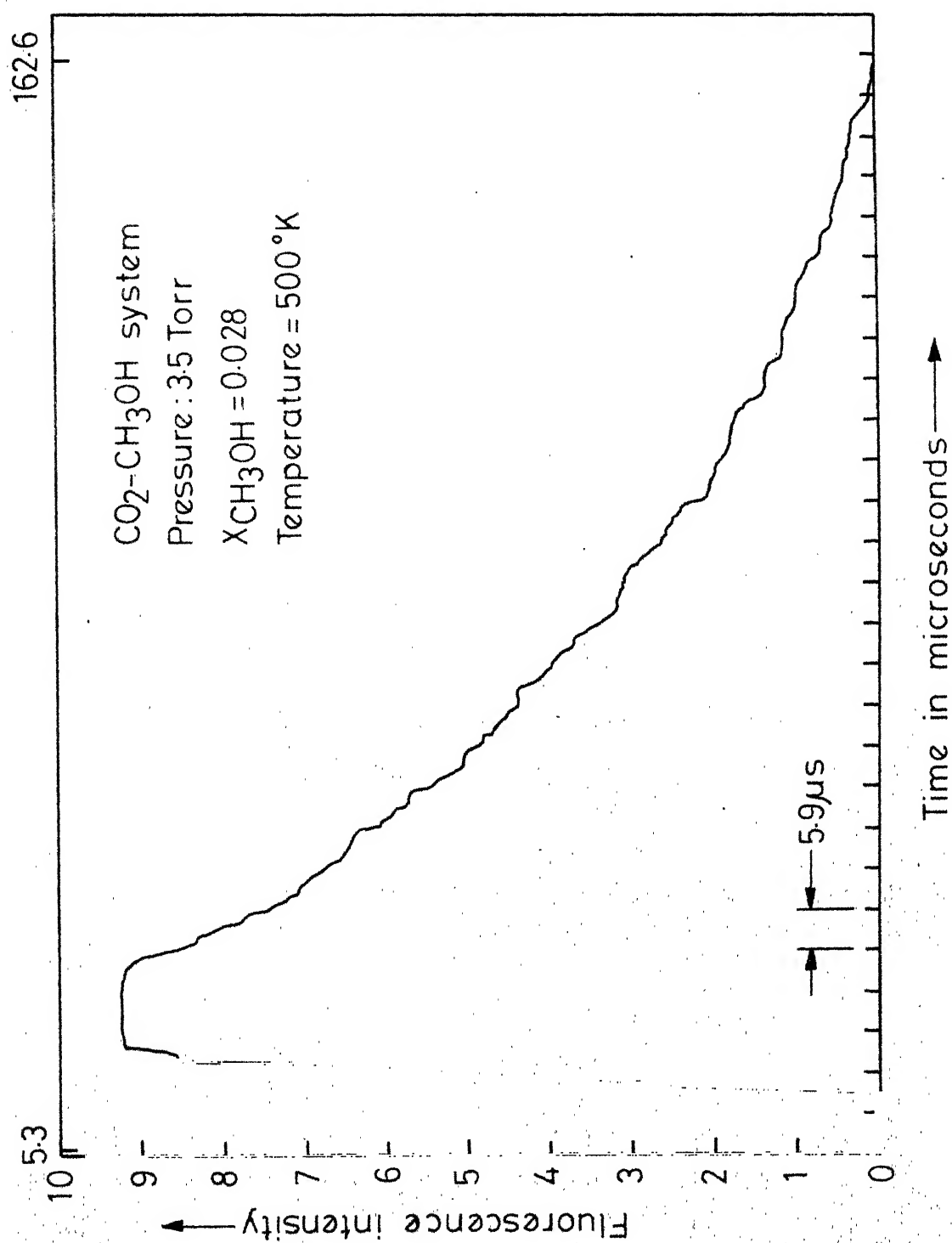


Fig. 3 - Typical fluorescence decay curve

pressure measurements. Pressures upto 25 torr are measured with a Silicone oil (Dow Corning 702 fluid) manometer, (accuracy 0.2 torr) while pressures higher than 25 torr are measured with a mercury manometer.

Same procedure is followed in the case of Ethylene oxide except that the bulbs are filled directly from the gas cylinder. In all the cases the mixtures are left for 24-36 hours to ensure complete mixing before a sample is withdrawn for fluorescence studies.

The purity of the samples used are as follows. CO_2 is 99.8% pure (Bone Dry grade, Matheson gas Co.) and $\text{C}_2\text{H}_4\text{O}$ is specified to be 99.7% pure (Union Carbide Co.). Among the liquids, the isotope CH_3OD (supplied by Isotopes Division, BARC, Bombay) is stated to be greater than 95% isotopic purity. The purity of the samples HCOOH , CH_3COOH and CH_3CHO is stated to be 99%, 99.7% and 99.5% respectively (BDH, Analar grade).

The alcohols CH_3OH and $\text{C}_2\text{H}_5\text{OH}$ are purified as follows. About 250 cc of laboratory grade alcohol is distilled over activated Calcium oxide. The distillate is mixed with about 2 grms. of Magnesium and a few crystals of Iodine and left over for 2-3 hours. Then the solution is distilled for two hours. The distillate, whose purity is greater than 99.5%, is used for subsequent sample preparation as described above.

CHAPTER IV

RESULTS AND DISCUSSION

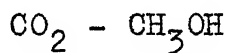
The deactivation of $\text{CO}_2(00^{\circ}1)$ mode in collisions with different polyatomic molecules has been studied using the Laser Induced Fluorescence technique as described in chapter II and III. The collision partners studied are CH_3OH , CH_3OD , $\text{C}_2\text{H}_5\text{OH}$, $\text{C}_2\text{H}_4\text{O}$, CH_3CHO , HCOOH and CH_3COOH . With each of these molecules as a collision partner, experiments have been carried out at different compositions of the mixtures and at different temperatures. The measurements are limited to those compositions of the mixtures for which the measured relaxation times are about three to four times larger than the response time of the detector and the associated electronic circuitry, which is less than $2\text{ }\mu\text{secs}$. The observed decay rate K_{obs} increases linearly with the composition X_M of the colliding partner M in all the systems studied. The deactivation rate constant $K_{\text{CO}_2-\text{M}}$ is evaluated by linearly extrapolating K_{obs} to zero percent of CO_2 since $K_{\text{CO}_2-\text{M}}$ refers to collisions between CO_2 and M only.

To check if dissociation is occurring in any of the samples in the temperature range studied, the following method has been used. The relaxation time τ of the sample at a pressure P is first measured at room temperature and

the temperature of the sample is then raised to the desired value and maintained there for an hour. Then the sample is cooled rapidly down to room temperature and the relaxation time and the pressure are measured again. If these agreed within the experimental error with the earlier ones, then it has been concluded that dissociation is unimportant. Each system is checked in this manner and the temperature range of the experiments is restricted such that no dissociation occurs.

In the temperature range of our measurements the deactivation rate constant is found to decrease with increasing temperature for all the systems studied. The magnitude of these rates and their decrease with temperature suggest that near-resonant vibration to vibration (V-V) energy transfer processes are primarily responsible for the transfer of energy from the asymmetric stretch mode of CO_2 to all the above mentioned molecules. As discussed in subsequent pages, the magnitude of the transition dipole moments of the transitions involved in CH_3OH , CH_3OD , $\text{C}_2\text{H}_5\text{OH}$, $\text{C}_2\text{H}_4\text{O}$ and CH_3CHO in the deactivation of $\text{CO}_2(00^01)$ mode have been estimated using the experimentally derived probabilities at different temperatures and SB theory.

The experimental results and their analysis are discussed for the individual systems in the following. The $\text{CO}_2\text{-CH}_3\text{OH}$ system is chosen as a prototype for a detailed discussion. Since the analysis of the data is similar for all the other systems, only a brief discussion is presented afterwards for the remaining systems.



The energy transfer rates for the deactivation of $\text{CO}_2(00^01)$ mode have been measured for five compositions, all below 12.5%, of Methyl alcohol at three different temperatures, namely 305, 400 and 500°K. A typical fluorescence decay curve ($P=3.5$ torr, $X_{\text{CH}_3\text{OH}} = 0.028$ and $T = 500^\circ\text{K}$) is shown in Fig.3. A semilogarithmic plot of this fluorescence signal intensity versus time, shown in Fig.4, resulted in a straight line, implying a single exponential decay which is also the case with all other signals. The slope of this line yields the relaxation time τ due to collisions. The relaxation times are measured at different total pressures for the same composition, in the range of 2-30 torr. Fig.5 shows the dependence of τ^{-1} on P , which is a straight line, suggesting that the deactivation is only through binary collisions in this pressure range. The slope of this line, which is the collisional decay rate $K_{\text{obs}} = (P \tau_{\text{coll}})^{-1}$, is found to be $2.75 \pm 0.09 \text{ msec}^{-1} \text{ torr}^{-1}$.

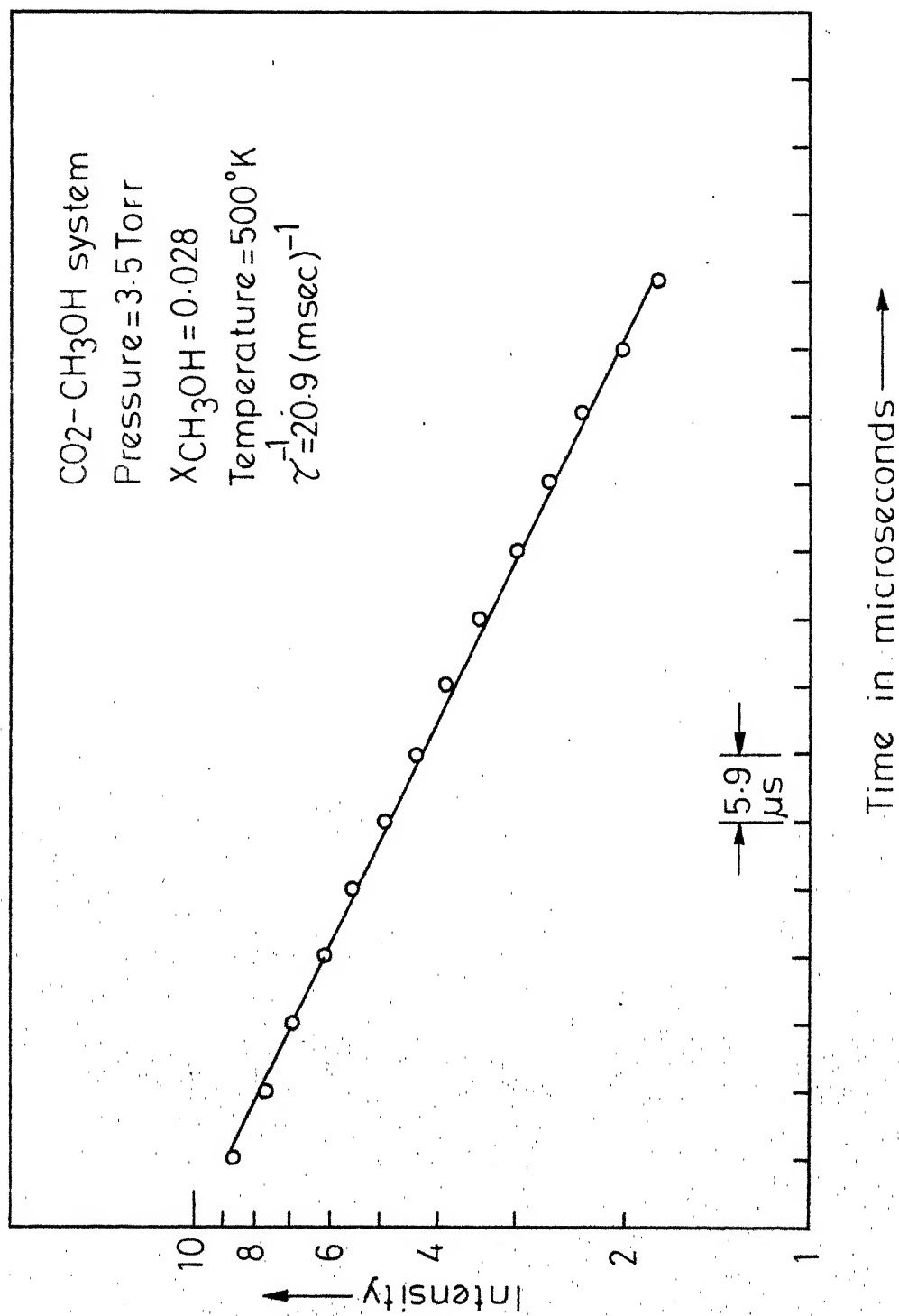


Fig. 4 - Semi logarithmic plot of fluorescence signal intensity vs. time.

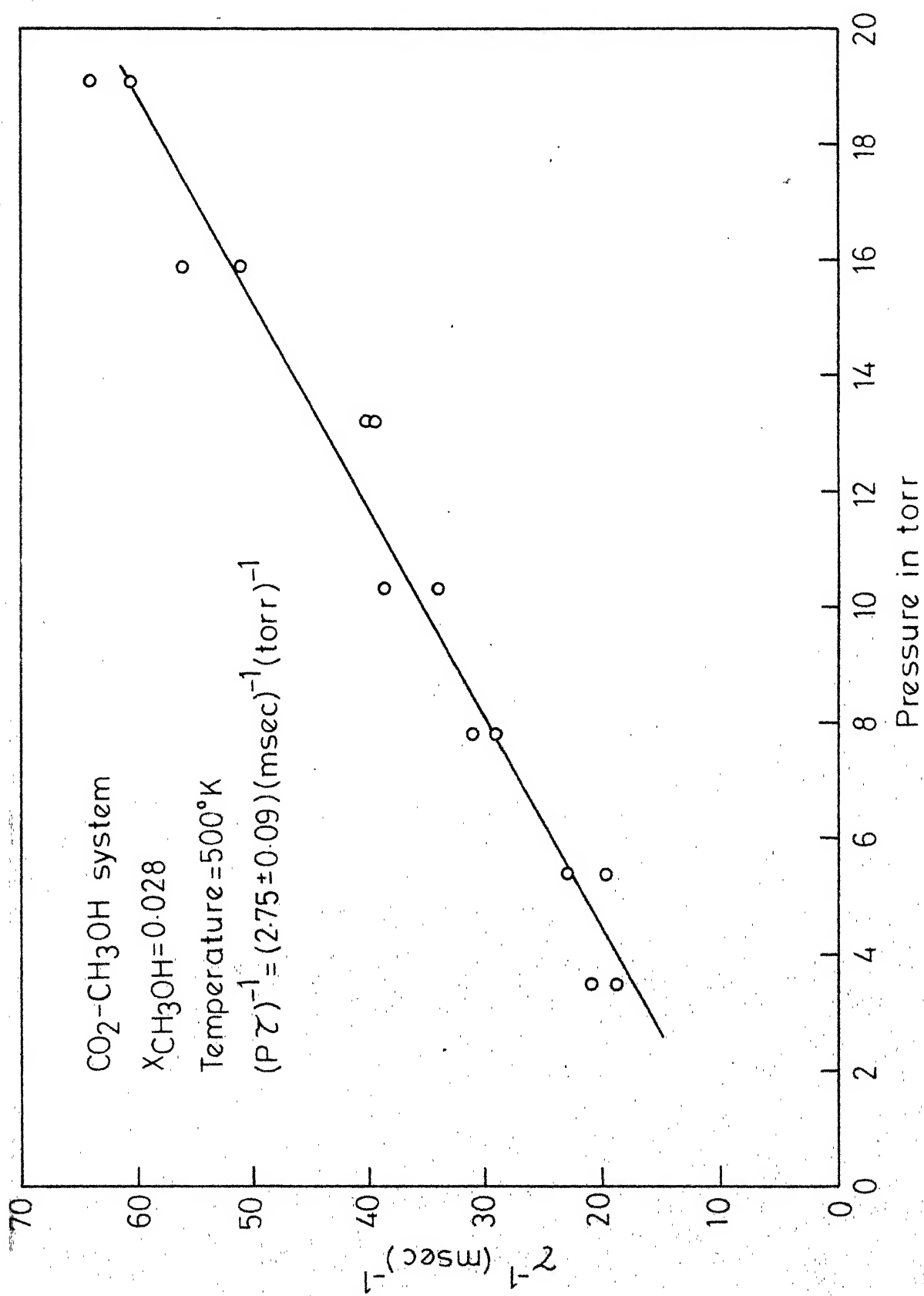


Fig. 5 - Plot of τ^{-1} with pressure.

These measurements have been repeated for different compositions of the mixture and the observed decay rate increased with increasing mole fraction of the alcohol. This increase suggests that Methyl alcohol is more efficient in deactivating the $\text{CO}_2(00^{\circ}1)$ mode than CO_2 itself. The composition dependence of the decay rate constant is shown in Fig.6. It can be seen from this plot that K_{obs} varies linearly with the composition, X_M , of the colliding partner M in the mixture according to the relation

$$K_{\text{obs}} = K_{\text{CO}_2-\text{CO}_2} X_{\text{CO}_2} + K_{\text{CO}_2-\text{M}} X_M \quad 4.1$$

Here, $K_{\text{CO}_2-\text{CO}_2}$ is the deactivation rate constant of the $\text{CO}_2(00^{\circ}1)$ mode due to collisions with CO_2 molecules only³⁸, while $K_{\text{CO}_2-\text{M}}$ is the deactivation rate due to collisions with molecules M only and can therefore be obtained by extrapolating K_{obs} to zero percent of CO_2 in the mixture.

This linear composition dependence of K_{obs} has been found to hold in all the mixtures $\text{CO}_2\text{-M}$ studied in this thesis. Therefore this extrapolation to zero percent CO_2 has been used in all the mixtures to obtain $K_{\text{CO}_2-\text{M}}$.

Experiments have been carried out at different temperatures and the results are shown in the form of a plot of $K_{\text{CO}_2-\text{CH}_3\text{OH}}$ versus temperature in Fig.7. It should be

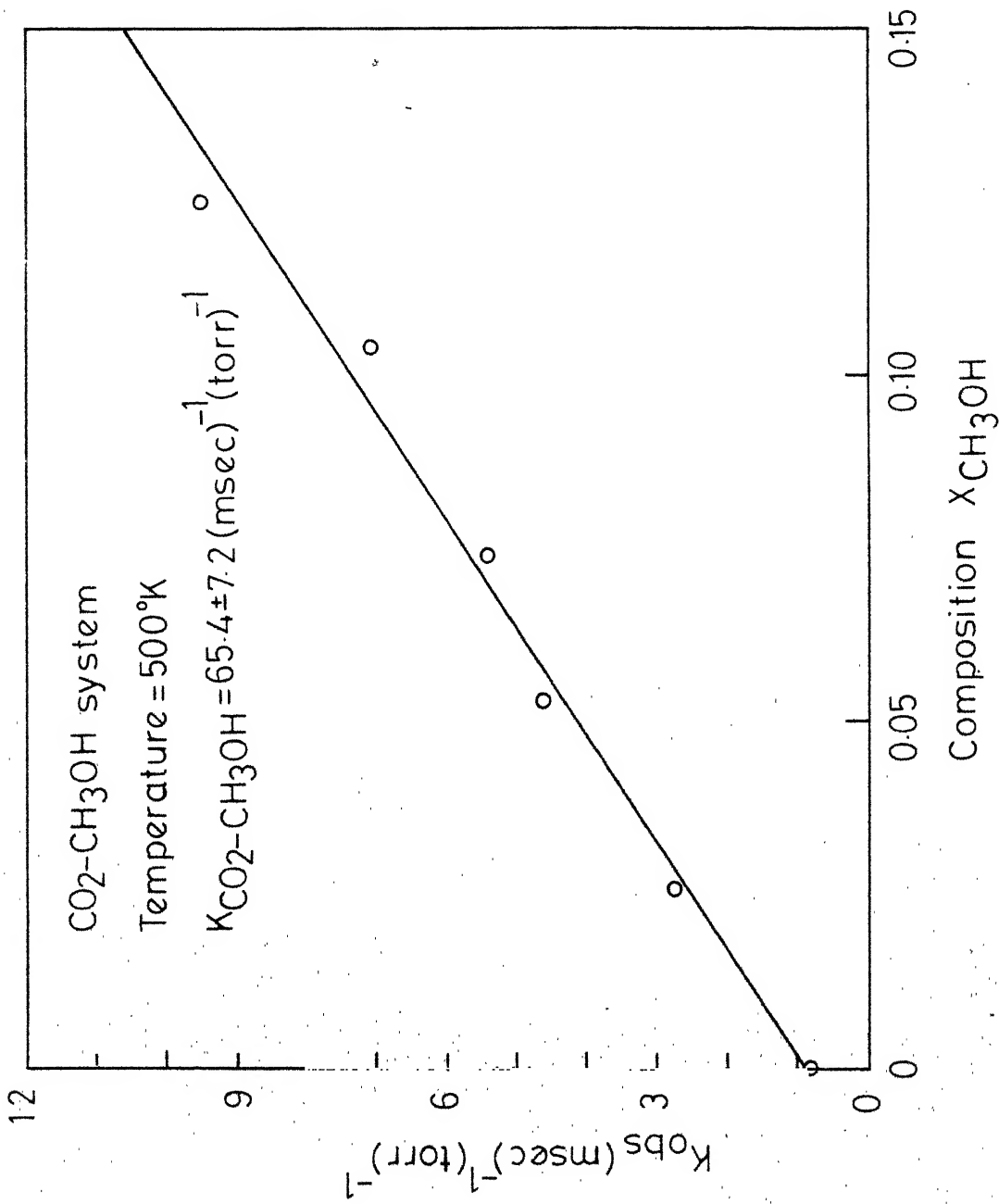


Fig. 6 - Composition dependence of the decay rate constant.

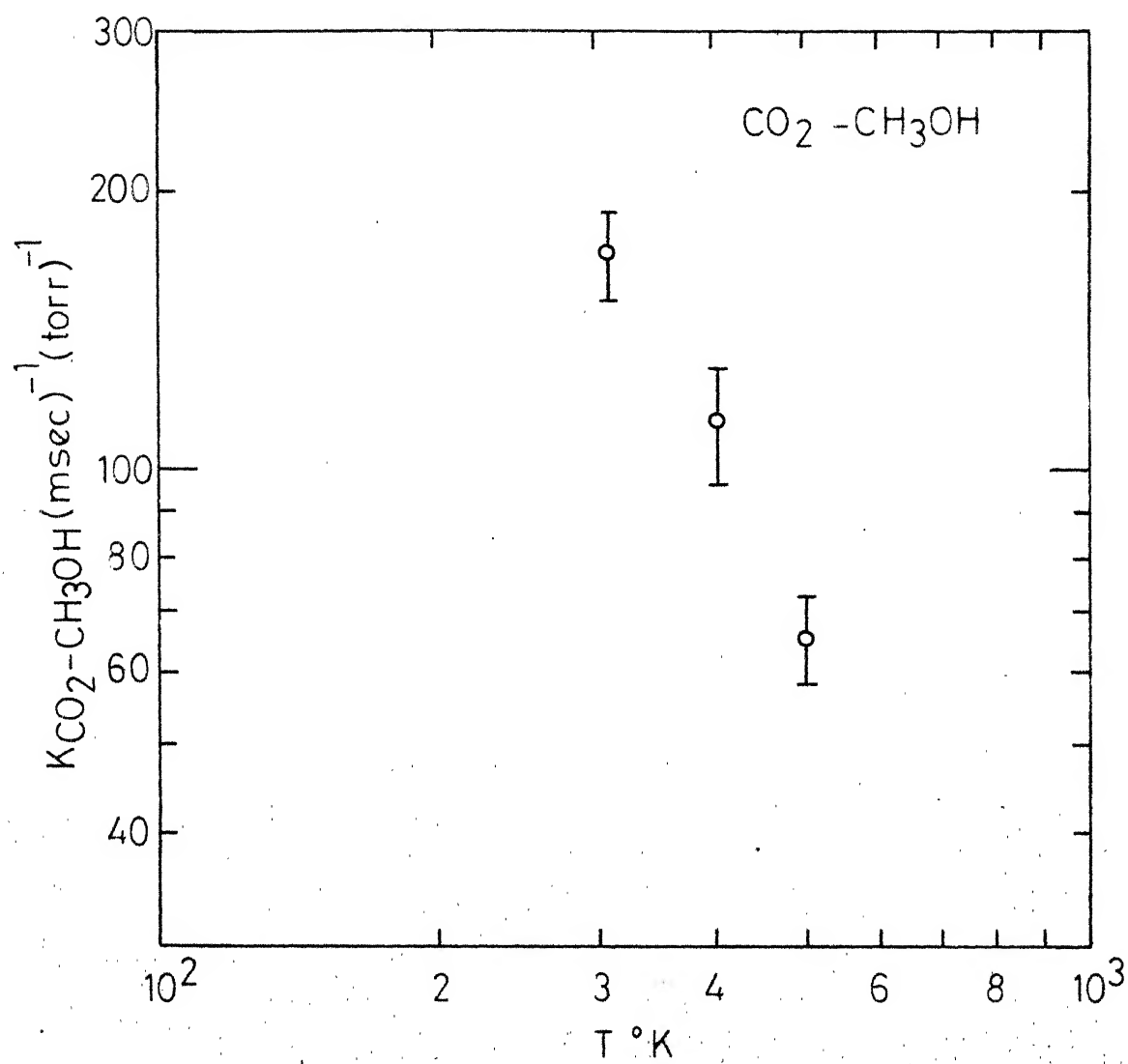


Fig. 7 - Temperature dependence of K_{CO₂-CH₃OH}.

pointed out that Agroskin et al.** measured the deactivation of $\text{CO}_2(00^{\circ}1)$ mode with CH_3OH at 300°K and found a value of $322 \text{ msec}^{-1}\text{torr}^{-1}$ whereas the present measurements resulted in a value of $172 \pm 18 \text{ msec}^{-1}\text{torr}^{-1}$ at 305°K .

Energy transfer cross-section σ and the experimentally derived probability P_{exp} are calculated from the deactivation rate constant $K_{\text{CO}_2-\text{CH}_3\text{OH}}$ at different temperatures using equations 2.4 and 2.5 and are presented in Table 1. The complete experimental data for $\text{CO}_2-\text{CH}_3\text{OH}$ system is presented in Tables 2-4.

Table 1

Rate constants, cross-sections and probabilities of energy transfer from $\text{CO}_2(00^{\circ}1)$ to CH_3OH^*

$T^{\circ}\text{K}$	$K_{\text{CO}_2-\text{M}}(\text{ms}^{-1}\text{torr}^{-1})$	$\sigma \text{ \AA}^2$	$P \times 10^2$
305	172 ± 18	0.92 ± 0.09	2.04 ± 0.22
400	112 ± 15.9	0.69 ± 0.09	1.53 ± 0.22
500	65.4 ± 7.2	0.45 ± 0.05	1.0 ± 0.11

* The error limits correspond to 95% confidence limits.

** This was quoted in Chemical Abstracts 81-70650 h, and the technique with which this was obtained was not mentioned. The original paper is in Russian language and is published in "Khim.Vys. Energ. 8,283 (1974)." This could not be referred to because of unavailability.

TABLE 2

TEMPERATURE (K) = 500.8
(PRESSURE (P) IN Torr AND TOWINVERSE (τ^{-1}) IN INVERSE MILLISEC.)

X = 0.028		X = 0.074		X = 1.052		X = 0.028	
P	τ^{-1}	F	τ^{-1}	P	τ^{-1}	P	τ^{-1}
19.1	301.5	14.7	130.4	21.9	135.9	15.8	81.0
19.5	376.9	14.7	135.0	21.6	136.1	13.6	13.4
19.9	37.9	14.8	93.2	19.2	134.8	13.6	67.6
11.5	142.4	11.5	105.6	19.2	117.0	11.2	54.8
11.9	110.8	9.5	89.1	16.9	109.4	9.8	44.1
11.9	128.6	9.5	79.3	16.9	127.5	9.8	44.8
11.5	77.7	8.2	66.3	14.5	104.0	7.8	39.3
11.5	17.6	8.2	78.3	14.5	119.6	7.8	41.9
11.5	46.4	8.2	73.1	12.2	89.2	6.3	22.1
11.5	94.9	6.9	64.5	12.2	91.5	6.3	31.6
11.5	92.6	6.9	65.6	10.0	78.5	4.9	33.4
11.5	54.0	6.1	54.9	10.0	81.6	4.0	21.7
11.5	52.3	6.1	53.5	8.2	69.8	4.0	23.9
11.5	42.1	5.1	52.2	8.2	12.0	3.1	11.7
11.5	42.1	5.1	56.1	6.6	43.6	3.1	21.9
11.5	43.3	3.9	42.6	6.6	57.2	2.6	17.1
11.5	38.1	3.9	42.3	4.8	45.3	1.6	18.6
11.5	43.6	3.2	42.0	4.8	48.2	4.7	19.6
11.5	31.6	3.2	42.2	3.0	33.3	3.2	21.0
11.5	31.6	3.2	33.0	3.0	35.7	2.2	21.6
11.5	31.6	3.2	31.1				
11.5	31.6	3.2	33.2				

K(CES) = 9.51 ± 0.23 K(CBS) = 7.05 ± 0.08 K(CBS) = 5.40 ± 0.56 K(CES) = 4.50 ± 0.34 K(CBS) = 2.75 ± 1.09

K(CD2-CH3CH) 65.4 ± 7.2 (MILLISEC.TURR)⁻¹

TABLE 3

TEMPERATURE (K) = 400.0 CARBONDIOXIDE-METHYLALCOHOL
PRESSURE (P) IN Torr AND TOWINVERSE (τ^{-1}) IN INVERSE MILLISEC

P	X = 0.104		X = 0.074		X = 0.053		X = 0.026	
	τ^{-1}	P	τ^{-1}	P	τ^{-1}	P	τ^{-1}	P
25.0	206.0	20.2	166.2	15.8	99.2	26.4	94.9	26.4
15.0	200.0	20.2	154.6	15.8	101.2	26.4	91.3	26.4
12.7	174.0	16.2	128.5	12.1	72.2	22.7	74.0	22.7
11.0	140.0	16.2	142.0	10.6	63.2	22.7	71.9	22.7
11.0	156.0	13.0	112.1	10.6	65.6	22.7	77.7	22.7
9.7	137.4	13.0	107.8	8.6	51.2	22.7	70.6	22.7
9.7	145.6	10.6	123.1	8.6	56.4	18.4	56.5	18.4
9.0	105.7	10.6	91.6	6.8	44.0	18.4	60.3	18.4
9.0	112.0	8.6	86.8	6.8	43.5	15.0	52.8	15.0
9.0	96.0	8.6	76.8	5.6	42.1	13.2	57.1	13.2
8.0	97.2	7.0	64.6	5.6	40.4	12.3	57.3	12.3
4.0	10.1	7.0	61.3	4.3	33.0	12.3	55.9	12.3
4.5	91.0	5.6	58.8	4.3	34.0	10.7	39.7	10.7
4.4	62.2	5.6	54.6	3.7	33.6	10.7	41.2	10.7
3.7	56.7	4.6	42.5	3.7	31.8	7.1	35.0	7.1
3.6	34.2	4.6	46.2	3.0	22.4	7.1	34.9	7.1
3.6	38.6	3.7	41.6	3.0	26.0	4.7	29.1	4.7
3.7	72.2	3.7	42.2	2.6	26.2	4.7	29.6	4.7
		3.0	46.3	2.6	25.3	3.2	22.0	3.2
		3.0	40.7			3.2	21.6	
		2.4	32.2					
		2.4	23.2					

K(CBS) = 12.35 ± 0.28

K(CBS) = 7.34 ± 0.01

K(CBS) = 5.32 ± 0.04

K(CBS) = 2.74 ± 0.12

K(CO2-CO+3CH4) = 112 ± 15.9

(MILLI SEC. TORR)⁻¹

TABLE 4

TEMPERATURE (°K) = 301.
 (PRESSURE (P) IN TORR AND TWINVERSE (τ^{-1}) IN INVERSE MILLISEC.)

X = 0.134		X = 0.074		X = 0.052		X = 0.026	
P	τ^{-1}	P	τ^{-1}	P	τ^{-1}	P	τ^{-1}
9.1	113.5	14.2	150.7	15.7	130.0	15.5	83.3
9.1	115.0	16.2	171.0	15.7	130.7	15.5	83.6
8.4	170.0	12.5	172.5	13.6	118.8	13.6	63.8
8.4	182.0	12.5	176.4	10.6	95.7	13.8	74.9
7.7	149.0	9.5	146.9	10.6	89.6	12.1	69.6
6.0	122.0	9.5	122.2	9.8	101.0	12.1	63.2
5.2	127.0	5.6	85.1	9.8	95.4	10.6	66.3
5.2	132.0	6.6	83.9	7.2	73.6	10.6	60.7
5.2	135.0	5.0	67.9	7.2	69.5	10.6	60.7
4.4	85.0	5.0	64.0	6.2	72.4	9.1	57.1
4.4	93.4	4.6	71.1	6.2	77.1	5.1	59.5
4.0	109.0	4.6	69.0	4.8	45.0	5.2	40.3
4.0	102.0	3.6	54.0	4.8	58.5	7.2	44.2
3.6	57.7	3.4	40.4	4.2	52.9	5.9	39.5
3.6	79.5			4.2	47.0	5.0	39.2
3.6	92.0			3.4	32.0	5.0	41.5
2.8	57.5			3.4	36.4	4.1	28.9
2.8	70.5			2.9	39.8	4.1	27.8
2.8	70.5			2.9	39.5	3.4	26.8
						3.4	32.1

K(OBS) = 1.53 ± 0.14 K(OBS) = $12.5 (\pm 0.14)$ K(OBS) = 7.47 ± 0.01 K(OBS) = 4.28 ± 0.04

K(CO₂-CH₂OH) = 172 ± 18 (MILLISEC. TORR)⁻¹

INTERPRETATION OF RESULTS

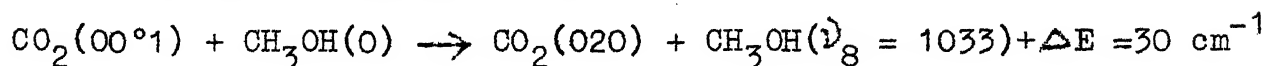
General Comments

Any nonlinear polyatomic molecule contains, in addition to its $3n-6$ (where n is the number of atoms in the molecule) fundamental vibrational bands, a large number of difference, combination and overtone bands. Hence a polyatomic molecule is likely to have several energy levels in any given energy interval and this number increases with the number of atoms in the molecule. Therefore many V-V energy transfer processes may occur during the collision of a $\text{CO}_2(00^01)$ molecule with any polyatomic molecule.

However, all these V-V processes may not contribute significantly to the deactivation of the $\text{CO}_2(00^01)$ mode. The magnitude of the observed deactivation rates and their decrease with temperature suggest that near-resonant V-V energy transfer processes are likely to play a major role in the deactivation of the $\text{CO}_2(00^01)$ mode. An idea of the relative contributions of these processes to the deactivation rate can be had by looking at the four points discussed below.

1. Energy mismatch (ΔE)

In the following V-V process



the energy that has been released by the CO_2 molecule has not been completely taken up by the Methyl alcohol molecule. This difference in the energy exchanged, which has to go into the translational and rotational degrees of freedom of Methyl alcohol, may be called the energy mismatch (ΔE). If ΔE in any process is small, typically less than about 100 to 150 cm^{-1} , that process is called a near-resonant process. Theoretical calculations of Sharma and Brau, as well as the more refined calculations that followed later, indicated that the energy transfer probability falls off steeply in such processes as the energy mismatch increases. Thus, ΔE is one of the important indications of the relative magnitudes of the transition probabilities for different V-V processes, though exceptions to this exist as in the case of Hydrogen Halides in which rotational effects are important²⁴.

2. Transition multipole moments

Sharma and Brau theory has indicated that the energy transfer probability for a near resonant process is proportional to the product of the multipole moments of the transitions involved. Hence, processes involving weak bands, i.e. difference bands, may be neglected in comparison with processes involving strong bands, i.e. fundamentals, other things being the same.

3. Quantum number changes

As Moore³⁹ has pointed out, it may be considered as a rule of thumb that the probability for energy transfer to occur during a collision decreases as the total number of quantum number changes involved in the process increases. Hence, other things being the same, processes that involve less number of quantum number changes are more important.

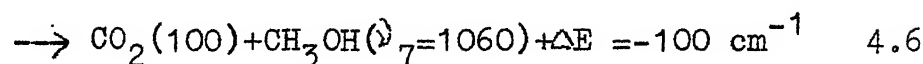
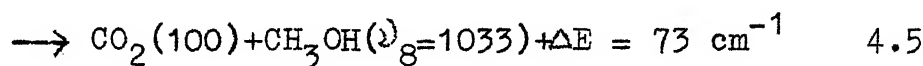
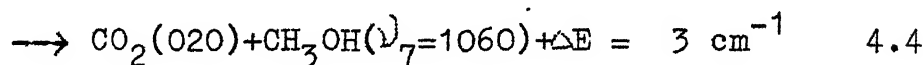
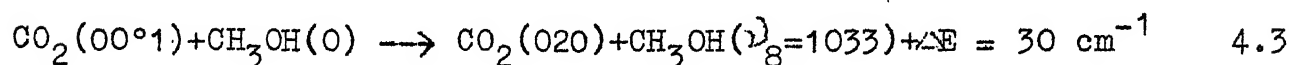
4. Energy level populations

Molecules occupy different energy levels according to the Maxwell-Boltzmann distribution. So, the number of molecules in any energy level decreases exponentially as the energy of that level increases. Thus, possibly except at higher temperatures or when the first vibrationally excited level is close to the ground state, transitions originating from the ground vibrational state of the colliding partner are predominant.

These criteria are used in the following to decide whether a particular process can compete with other possible processes in contributing significantly to the total deactivation probability.

INTERPRETATION OF CO₂-CH₃OH DATA

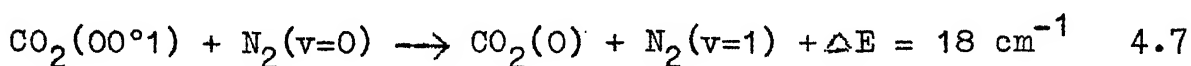
The fundamental vibrational frequencies of Methyl alcohol (CH₃OH) have been tabulated by Shimonouchi⁴⁰. It was observed that this Alcohol is transparent to radiation with frequency around 2349 cm⁻¹(41) which corresponds to the $\nu_3 \rightarrow 0$ transition in CO₂. However, it has a very strong absorption band at 1033 cm⁻¹ (ν_8) identified with the C-O stretch vibration and a weak absorption band at 1060 cm⁻¹ (ν_7) identified with the CH₃ rock. Both these bands are near-resonant with the transitions $\nu_3 \rightarrow 2\nu_2$ and $\nu_3 \rightarrow \nu_1$ in CO₂. Thus, the transitions in CH₃OH corresponding to these bands are likely to play a dominant role in the deactivation of CO₂(00°1) through the following processes



Process 4.6, in addition to involving a weak band (ν_7) of the alcohol, involves a higher energy discrepancy (ΔE) than the other processes. Thus, the contribution of this process to the total deactivation probability may be expected to be small and hence has been neglected in the following calculations.

PROBABILITY CALCULATIONS

Landau and Teller⁴² derived an expression for the temperature dependence of the energy transfer probability during a collision by a purely classical treatment for a vibration to translation (V-T) process. Assuming that only a repulsive exponential potential exists between the colliding molecules, they concluded that the probability varies as $\exp(-T^{-1/3})$. Later Schwartz, Slawsky and Herzfeld (SSH)¹³ derived the same result with an approximate three dimensional quantum mechanical treatment. In the case of V-T processes, where the energy that has to be absorbed by or rejected into the translational degrees of freedom is large, the magnitudes and the temperature dependence of the energy transfer probabilities predicted using this theory are consistent with experimental results in many systems. In the limit of $\Delta E \rightarrow 0$, i.e. for near-resonant processes, this theory predicted a positive temperature dependence. But the process



which is a near-resonant process, exhibited a negative temperature dependence in the range of 300-1000°K³⁸. SSH theory not only failed to predict the observed negative temperature dependence but estimated a value for the probability at room temperature which is four times smaller than that observed.

Later, Sharma and Brau¹² developed a theory which takes into account long range intermolecular forces. This theory successfully predicted the magnitude and temperature dependence of the energy transfer probabilities for the process 4.7. Since then, this theory has been widely used to estimate the energy transfer probabilities for near-resonant processes^{18,43-51}. Even though this theory predicts a negative temperature dependence for a near-resonant process, a positive temperature dependence is also predicted as ΔE is increased but the probabilities are considerably smaller. Recently, Sharma⁵² showed that, refining the earlier theory by using Second order distorted wave Born approximation, does not improve the accuracy of the earlier simpler calculation while requiring a considerably larger computation time. Tam²² has suggested a modification of the simpler theory. However, ~~it is felt that~~ in view of the other approximations in the method (in fact, recently a controversy¹⁹⁻²¹ has arisen about the origin of the T^{-1} dependence obtained in this theory) the SB theory in its original form¹² has been employed in our calculations.

Further, in all the systems we will be considering in the following, none of the transition dipole moments required to calculate the probability by SB theory are available. So, in the following we have inverted the

procedure and estimated the transition moments using the experimentally measured probability. These estimated transition moments are approximate, and their reliability largely rests on the assumption that SB theory reasonably predicts the V-V transfer probabilities in these systems.

The experimentally derived probability can be written as

$$P_{\text{exp}} = \sum_i a_i p_i \quad 4.8$$

where the summation extends over all the possible processes i that cause the energy transfer, a_i is the square of the dipole moment of the transition of M involved in the process i and p_i is the calculated energy exchange probability for the i^{th} process using SB theory but assuming a value of unity for the square of the transition dipole moment of M . Then, a least squares method can be employed to obtain a_i . A similar method has been employed earlier to estimate the transition dipole moment of CS^{51} and those of the $(\nu_3 + \nu_6) \rightarrow 0$ and $(\nu_9 + \nu_{11}) \rightarrow 0$ transitions in $\text{C}_2\text{H}_6^{37}$.

The molecular constants used in the calculations are given in Table 5. Methyl alcohol is assumed to be an oblate symmetric top molecule. The energy transfer probabilities calculated using the SB theory for the processes 4.3 to 4.5 are presented in Table 6.

Table 5

Molecular and other constants used in SB theory calculations

Molecule	Hard sphere dia. σ	Rotational constants cm^{-1}			Ref.
		A	B	C	
CO_2	4.0	0	0.39	0	53,69
CH_3OH	3.585	0.793	0.822	4.26	53,54
CH_3OD	3.585	0.733	0.781	3.65	54
$\text{C}_2\text{H}_5\text{OH}$	4.455	1.11	0.304	0.267	53,56
$\text{C}_2\text{H}_4\text{O}$	4.33	0.85	0.738	0.47	59
CH_3CHO	3.585	1.888	0.339	0.304	68,69
HCOOH	4.455	-	-	-	70 68
CH_3COOH	4.333*	-	-	-	71

The squares of the transition dipole moments of CO_2 are⁷⁰

$$\text{CO}_2 (2_3 \rightarrow 0) = 1.0 \times 10^{-37} \text{ esu}^2 \text{cm}^2$$

$$\text{CO}_2 (2_3 \rightarrow 2_1) = 1.44 \times 10^{-39} \text{ esu}^2 \text{cm}^2$$

$$\text{CO}_2 (2_3 \rightarrow 2_2) = 1.22 \times 10^{-39} \text{ esu}^2 \text{cm}^2$$

* Calculated from critical constant, $V_c = 170.9 \text{ cm}^3/\text{gm.mole}$

Table 6

Calculated Energy Transfer probabilities* for different processes of $\text{CO}_2\text{-CH}_3\text{OH}$ system

T°K	$p_3 \times 10^{35}$	$p_4 \times 10^{35}$	$p_5 \times 10^{35}$
305	1.09	1.33	0.2414
400	0.86	1.01	0.2887
500	0.704	0.809	0.3095

It can be seen from the Table 6 that the sum of the probabilities for processes 4.3 and 4.5, both involving the $\nu_8 \rightarrow 0$ transition in alcohol, is slightly larger than that for process 4.4. In addition to this, it may be inferred from their relative IR absorption intensities⁴⁰ that the transition dipole moment for the process $\nu_7 \rightarrow 0$ is considerably smaller than that of the $\nu_8 \rightarrow 0$ transition. So, the process 4.4 can be neglected. The experimentally derived probability for this system can now be written as

$$P_{\text{exp}} = a (\nu_8 \rightarrow 0) (p_3 + p_5) \quad 4.9$$

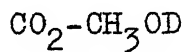
where p_3 , p_5 are the calculated probabilities using SB theory for the processes 4.3 and 4.5 while $a (\nu_8 \rightarrow 0)$ is the square of the dipole moment for the transition $\nu_8 \rightarrow 0$.

* Values are obtained by assuming unity for the unknown transition dipole moments(squares) of M.

A least squares analysis of the data presented in Tables 1 & 6 yielded the following value for a $(\bar{D}_8 \rightarrow 0)$

$$a(\bar{D}_8 \rightarrow 0) = 1.33 \times 10^{-37} \text{esu}^2 \text{cm}^2$$

No attempt has been made to estimate the error limits to the transition dipole moments here and in the subsequent calculations, since the reported values are only approximate. However, more than the errors introduced by the least squares calculations, the limiting factor could be the applicability of SB theory for such calculations in polyatomic molecules. It is likely that short range repulsive forces may also contribute to the total probability when the energy discrepancy is larger ($\Delta E \geq 100 \text{ cm}^{-1}$). But the contribution due to these forces, which may be expected not to be large, has been ignored in this and the subsequent calculations. In the light of these comments the value of the squares of the transition dipole moments estimated in the present work, should be considered only approximate.



The deactivation of CO₂(00°1) mode in collisions with Methyl alcohol-d (CH₃OD) has been studied for different compositions and at five different temperatures in the range of 300-600°K. As in the case of Methyl alcohol, the

fluorescence signal is observed to be a single exponential in all the experiments. The complete experimental data for the system $\text{CO}_2\text{-CH}_3\text{OD}$ is presented in Tables 7 - 11. The analysis of the data is similar to that of Methyl alcohol and hence the details are not repeated here. The temperature dependence of the deactivation rate constant $K_{\text{CO}_2\text{-CH}_3\text{OD}}$ is presented in Fig.8. The collision cross sections and the energy transfer probabilities calculated from this constant according to the equations 2.4 and 2.5 and are presented in Table 12 at different temperatures.

Table 12

Rate constants, cross-sections and probabilities of energy transfer from $\text{CO}_2(00^01)$ to CH_3OD

$T^\circ\text{K}$	$K_{\text{CO}_2\text{-M}}(\text{ms}^{-1}\text{torr}^{-1})$	$\sigma \text{ \AA}^2$	$P_{\text{exp}} \times 10^2$
301	102.5 ± 8.2	0.551 ± 0.05	1.22 ± 0.07
375	93.9 ± 14.7	0.575 ± 0.09	1.25 ± 0.19
450	71.6 ± 11.6	0.471 ± 0.08	1.04 ± 0.17
525	46.4 ± 10.9	0.330 ± 0.08	0.73 ± 0.17
600	57.0 ± 4.4	0.435 ± 0.03	0.96 ± 0.09

TABLE

TEMPERATURE (K) = 600.0 CARBON DIOXIDE-METHYLALCOHOL-D
(PRESSURE (P) IN TORR AND TOWINVERSE (T⁻¹) IN INVERSE MILLISEC.)

X = 0.10		X = 0.075		X = 0.05		X = 0.025	
P	T ⁻¹	P	T ⁻¹	P	T ⁻¹	P	T ⁻¹
10.5	75.1	15.5	99.1	13.9	63.1	21.0	63.0
10.5	76.2	13.5	85.4	13.9	66.1	21.0	64.9
10.5	81.2	13.5	83.6	12.1	63.1	18.9	58.0
9.5	80.9	12.1	70.5	12.1	50.5	18.9	57.8
9.7	53.9	12.1	74.9	10.2	50.4	16.6	48.4
9.0	72.2	10.4	72.2	10.2	57.8	16.6	54.5
9.0	63.0	10.4	57.9	8.2	38.7	14.4	55.7
9.0	89.2	8.7	51.1	8.2	45.1	14.4	45.2
8.0	67.7	8.7	56.6	6.5	31.5	12.6	44.7
8.0	63.1	7.6	48.9	6.5	55.1	12.6	43.6
8.0	85.7	7.6	51.1	4.8	28.6	8.3	37.3
6.9	50.5	6.5	42.0	4.8	28.0	8.3	32.6
6.9	54.5	6.5	38.9	3.4	23.1	6.4	23.0
5.7	49.2	5.0	34.7	3.4	25.7	6.4	22.9
5.7	47.6	5.0	51.6	2.6	28.6	4.8	20.6
4.6	37.6	3.6	28.1	2.2	22.3	4.8	21.7
4.6	37.2	3.6	26.9	2.2	19.1	3.0	17.1
3.6	30.9	2.6	22.2	2.6	21.8	3.0	16.7
3.6	35.3	2.6	22.3	2.2	18.6	2.4	17.7
2.2	23.9	1.9	30.3	2.2	17.5		
2.2	36.6						
1.7	24.8						
1.7	21.5						

K(OBS) = 6.74 ± 0.02 K(OBS) = 5.80 ± 0.05 K(OBS) = 3.99 ± 0.10 K(OBS) = 2.64 ± 0.01

K(CO2-CH2OD) = 56.9 ± 4.4 (MILLISEC. TORR)⁻¹

TABLE 8
TEMPERATURE (K) = 525.0 CARBON DIOXIDE-METHYLALCOHOL-D
(PRESSURE (P) IN TORR AND TOWINVERSE (τ^{-1}) IN INVERSE MILLISEC.)

$\nu = 0.10$		$\nu = 0.075$		$\nu = 0.05$		$\nu = 0.025$	
P	τ^{-1}	P	τ^{-1}	P	τ^{-1}	P	τ^{-1}
13.6	92.6	15.8	81.7	16.2	69.8	19.3	54.3
12.7	89.3	13.7	71.9	14.2	51.5	17.9	53.2
12.3	90.9	13.7	66.7	12.8	48.3	17.9	46.0
11.6	83.0	11.6	58.6	12.6	52.3	16.3	52.7
11.3	87.6	11.8	52.8	12.8	59.2	15.4	47.2
8.6	65.6	10.6	66.8	11.3	46.8	15.4	39.9
7.4	53.9	10.6	57.7	11.3	51.7	14.5	41.6
7.4	54.7	10.6	40.7	9.7	42.4	14.5	39.4
6.6	56.5	6.7	41.6	9.7	43.8	14.5	39.3
6.4	56.7	6.7	49.4	8.2	33.5	11.1	28.9
5.5	47.0	6.7	38.3	8.2	36.1	11.1	31.7
5.3	48.5	5.6	35.8	6.1	29.4	9.6	28.1
4.7	38.7	5.6	43.4	6.1	28.3	9.6	28.7
4.7	45.5	4.2	25.9	4.6	25.7	7.8	24.3
3.1	30.2	4.2	38.1	4.6	21.6	7.8	26.8
3.1	34.3	4.2	33.2	3.0	23.2	6.2	21.7
1.6	19.6	3.0	25.6	3.0	17.7	6.2	21.8
1.6	17.4	3.0	32.7	1.6	12.9	3.4	13.6
0.9	11.8	3.0	32.6	1.6	14.3	3.4	15.3
0.9	12.3	1.7	21.8	2.2	17.5		
2.7	24.6	1.7	19.9				
1.7	24.8						
1.7	21.5						

$$K(\text{OBS}) = 6.0 \pm 0.11$$

$$K(\text{OBS}) = 3.65 \pm 0.10$$

$$K(\text{OBS}) = 3.49 \pm 0.02$$

$$K(\text{OBS}) = 2.49 \pm 0.03$$

$$K(\text{CO}_2\text{-CH}_2\text{OD}) = 46.3 \pm 10.9 \quad (\text{MILLISEC. TORR})^{-1}$$

TABLE 9

TEMPERATURE (K) = 450.0

CARRONDIOXIDE-METHYLALCOHOL-D
(PRESSURE (P) IN TORR AND TOWINVERSE (τ^{-1}) IN INVERSE MILLISEC.)

X = 0.10		X = 0.075		X = 0.05		X = 0.025	
P	τ^{-1}	P	τ^{-1}	P	τ^{-1}	P	τ^{-1}
15.8	129.9	16.9	94.7	15.4	84.2	21.2	58.6
15.8	139.1	14.2	95.4	15.4	70.2	21.2	60.3
15.8	122.0	11.0	64.7	15.4	69.4	18.4	57.9
15.8	149.8	11.0	57.0	12.6	64.5	18.4	58.3
12.2	110.0	11.0	70.1	10.1	45.5	15.2	46.8
12.2	115.7	9.0	62.8	9.8	51.9	12.1	41.0
12.2	116.6	9.0	60.5	8.0	45.6	12.1	42.3
9.8	97.8	7.0	48.5	8.0	45.7	8.7	28.9
9.8	91.7	7.0	52.0	6.4	38.1	8.7	32.9
7.8	75.7	7.0	52.6	6.4	35.6	7.8	33.7
7.8	63.6	5.8	49.2	5.2	31.5	7.8	25.7
6.4	57.9	5.8	46.4	5.2	32.0	5.6	22.3
6.4	57.0	4.6	33.5	4.1	28.1	5.6	22.1
5.0	39.4	4.6	37.5	4.0	30.5	5.0	21.1
5.0	42.1	3.8	33.1	3.4	23.0	5.0	26.7
4.2	46.4	2.9	24.8	3.4	21.0	3.7	17.1
4.2	45.5	2.9	27.5	2.6	24.1	3.7	19.0
3.2	36.6			2.6	21.8	2.4	16.2
3.2	35.7			2.2	18.6	2.4	17.7
2.7	32.5			2.2	17.5		
2.7	33.8						
1.7	24.8						
1.7	21.5						

K(OBS) = 9.18 ± 0.24

K(OBS) = 4.98 ± 0.04

K(OBS) = 4.15 ± 0.05

K(OBS) = 2.44 ± 0.03

K(CO2-CH3OO) = 71.6 ± 11.6 (MILLISEC. TORR)⁻¹

TABLE 10

TEMPERATURE (K) = 375.0

CARBON DIOXIDE-METHYLALCOHOL-D
(PRESSURE (P) IN TORR AND TOWINVERSE (τ^{-1}) IN INVERSE MILLISEC.)

X = 0.10		X = 0.075		X = 0.05		X = 0.025	
P	τ^{-1}	P	τ^{-1}	P	τ^{-1}	P	τ^{-1}
10.4	106.3	12.8	117.2	13.3	61.6	22.6	71.6
10.4	122.5	12.8	131.9	13.3	84.8	14.7	53.1
8.2	92.9	9.9	88.0	11.0	73.4	14.7	47.5
6.9	84.0	9.9	92.5	8.7	65.1	12.5	45.7
6.9	84.1	8.4	73.4	8.7	62.2	9.7	35.3
5.4	59.6	8.4	81.9	5.8	41.8	9.7	37.2
5.4	71.5	6.6	63.4	5.8	41.0	8.3	28.2
4.6	70.4	6.6	64.8	4.8	35.5	8.3	30.6
4.6	48.2	5.4	59.4	4.8	36.1	6.5	28.7
3.5	47.5	5.4	60.0	3.8	36.1	6.5	24.8
3.5	51.3	4.3	46.8	3.8	34.7	5.5	24.6
3.0	45.0	4.3	45.6	3.2	29.1	5.5	25.4
3.0	47.1	3.7	39.3	3.2	29.0	4.4	20.9
2.3	43.1	3.7	40.0	2.6	24.4	4.4	19.2
2.3	43.2	2.9	35.9	2.6	28.6	2.9	19.8
4.2	46.4	2.9	38.5	2.2	23.3	2.9	19.4
4.2	45.5	2.5	31.2	2.2	19.1	3.7	19.0
3.2	36.6	2.5	29.6	2.6	21.8	2.4	16.2
3.2	35.7	1.9	26.9	2.2	18.6	2.4	17.7
2.7	32.5	1.9	30.3	2.2	17.5		
2.7	33.8						
1.7	24.8						
1.7	21.5						

K(OBS) = 9.16 ± 0.17

K(OBS) = 8.51 ± 0.11

K(OBS) = 5.56 ± 0.13

K(OBS) = 2.75 ± 0.05

K(CO2-CH3OD) = 94. ± 14.7 (MILLISEC. TORR)⁻¹

53989

TABLE 11

TEMPERATURE (K) = 301.0 CARBON DIOXIDE-METHYLALCOHOL-
 (PRESSURE (P) IN TORR AND TOWINVERSE (τ^{-1}) IN INVERSE MILLISEC.)

X = 0.05		X = 0.025	
P	τ^{-1}	P	τ^{-1}
14.1	104.9	15.8	62.9
14.1	96.0	15.8	67.2
12.3	94.5	13.8	65.9
12.3	90.0	13.8	61.4
11.3	95.2	11.8	60.7
11.3	86.8	11.8	60.7
10.6	87.1	9.8	55.3
9.9	69.9	9.8	52.9
8.8	75.9	8.8	46.7
8.8	66.9	8.8	52.3
7.8	58.3	6.9	49.5
7.8	75.3	6.9	39.1
7.8	62.0	5.3	43.1
6.0	71.2	5.3	40.9
6.0	70.1	3.8	33.7
6.2	58.3	3.8	37.3
6.4	51.6	2.4	35.5
5.0	14.1	2.4	31.8
5.9	11.8	2.4	33.0
5.9	12.3	1.7	21.8
5.2	24.6	1.7	15.9
5.7	24.8		
5.7	21.5		

K(OBS) = 5.43 ± 0.13

K(OBS) = 2.57 ± 0.00

K(CO2-CH3OD) = 102.5 ± 8.2 (MILLISEC. TORR)⁻¹

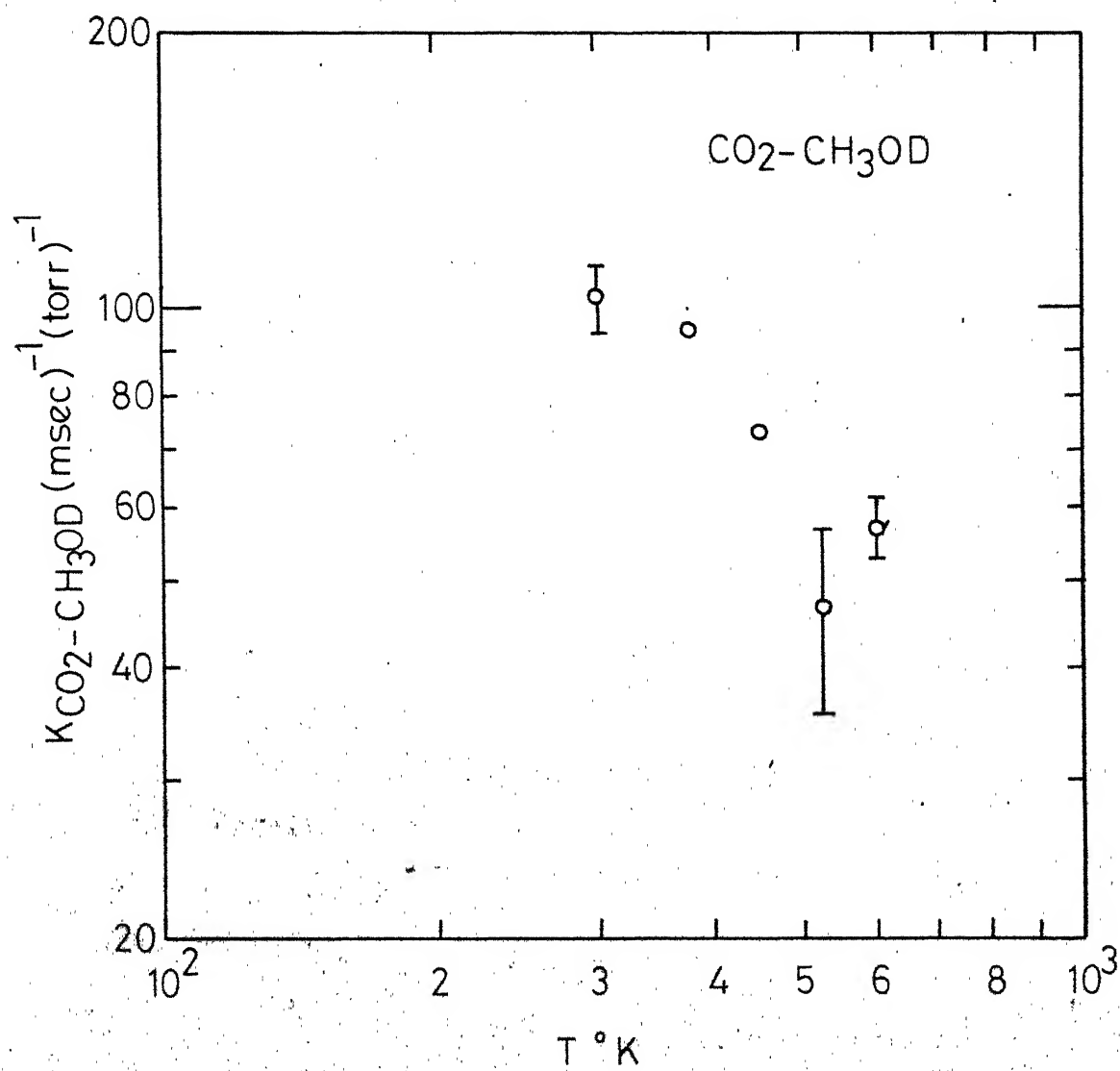
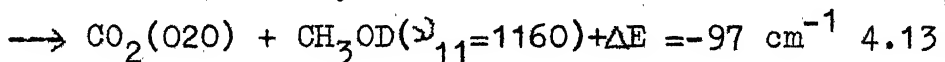
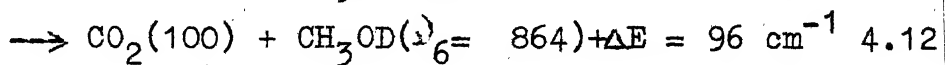
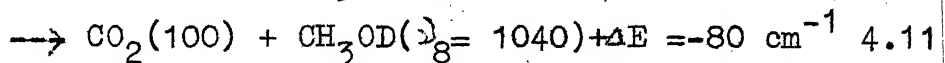
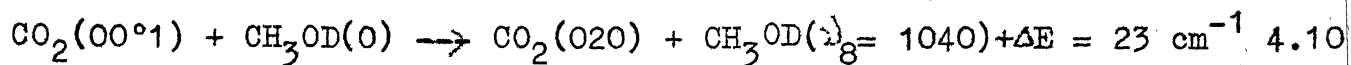


Fig. 8 - Temperature dependence of $K_{\text{CO}_2-\text{CH}_3\text{OD}}$.

INTERPRETATION OF RESULTS

The decrease with temperature and the magnitude of the deactivation rates suggest that long range multipole interactions are primarily responsible for the transfer of energy from the asymmetric stretch mode of CO_2 to Methyl alcohol-d. The fundamental vibrational frequencies of this molecule are tabulated by Shimanouchi⁴⁰. This alcohol is also transparent to radiation with frequency around 2349 cm^{-1} (ν_3) and hence it is unlikely that the transition $\nu_3 \rightarrow 0$ in CO_2 will occur during collisions. The possible deactivation of $\text{CO}_2(00^01)$ can be through the $\nu_3 \rightarrow 2\nu_2$ and $\nu_3 \rightarrow \nu_1$ transitions since there are three fundamental frequencies in CH_3OD that lie in the energy range of these transitions. These are: (i) a very strong band at 1040 cm^{-1} (ν_8) identified as the C-O stretch, (ii) a strong band at 864 cm^{-1} (ν_6) which is the O-D bend and (iii) a very weak band at 1160 cm^{-1} (ν_{11}) named as CH_3 rock. These bands are likely to deactivate the $\text{CO}_2(00^01)$ mode through the following processes



Even though the energy mismatches (ΔE) in processes 4.12 and 4.13 are the same, the transition $v_{11} \rightarrow 0$ is very weak and hence, the process 4.13 involving this transition can be neglected.

PROBABILITY CALCULATIONS

The energy transfer probabilities for the processes shown in 4.10 - 4.12 have been calculated using SB theory taking into account dipole-dipole interactions. The molecular constants used in these calculations are listed in Table 5. The molecular diameter of CH_3OD is assumed to be the same as that of CH_3OH . The transition dipole moments for the transitions involved for this alcohol are not available. The calculated probabilities for the above processes using SB theory, and assuming that this alcohol is an oblate symmetric top as in the case of Methyl alcohol, are presented in Table 13. They decreased with increasing temperature for process 4.10 for which ΔE is small and increased as the temperature is increased for processes 4.11 and 4.12 where the energy mismatch (ΔE) is somewhat larger.

The total deactivation probability for this system can be written as

$$P_{\text{exp}} = a(v_8 \rightarrow 0) (p_{10} + p_{11}) + a(v_6 \rightarrow 0) p_{12} \quad 4.14$$

Table 13

Calculated Energy Transfer probabilities* for different processes of $\text{CO}_2\text{-CH}_3\text{OD}$ system

T°K	$p_{10} \times 10^{35}$	$p_{11} \times 10^{35}$	$p_{12} \times 10^{35}$
301	1.207	0.1921	0.1081
375	0.9842	0.2368	0.1366
450	0.8322	0.2698	0.1641
525	0.7216	0.2909	0.1878
600	0.6373	0.3020	0.2064

where, as earlier, P_i is the probability for the process 4.i and a's are the squares of the transition dipole moments. A least squares analysis of the data presented in Tables 12 & 13 resulted in

$$a(\nu_8 \rightarrow 0) = 0.9 \times 10^{-37} \text{ esu}^2 \text{ cm}^2$$

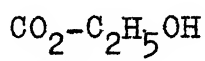
$$a(\nu_6 \rightarrow 0) = 0.16 \times 10^{-37} \text{ esu}^2 \text{ cm}^2$$

These moments are in agreement with the relative intensities of the transitions as reported from spectroscopic measurements⁴⁰. Thus the transition $\nu_8 \rightarrow 0$, which is termed very strong, is 6-7 times larger than that of $\nu_6 \rightarrow 0$ which is designated as strong.

* Values are obtained by assuming unity for the unknown transition dipole moments (squares) of M.

COMMENTS

The introduction of a Deuterium atom in the place of the Hydrogen atom has decreased the rate of the deactivation of the $\text{CO}_2(00^01)$ level by 100%. In Methyl alcohol the C-O stretch $\nu_8 \rightarrow 0$ transition is deactivating the CO_2 asymmetric stretch level through both $\nu_3 \rightarrow 2\nu_2$ and $\nu_3 \rightarrow \nu_1$ transitions. In the Deuterated alcohol, in addition to the above mentioned processes, another strong transition $\nu_6 \rightarrow 0$, the CH_3 rock, is also contributing to the deactivation. It should also be noted that our results indicate that Deuteration has reduced the strength of the C-O stretch band in Methyl alcohol (the transition dipole moment is reduced from 0.366 debye to 0.3 debye). However, both these bands are termed very strong. So the true moments of these bands should perhaps be a little closer.



The quenching of the asymmetric stretching mode of CO_2 in collisions with Ethyl alcohol has been studied at different compositions at five temperatures in the range of 300-600°K. For all the runs taken, the semilogarithmic plot of fluorescence signal intensity versus time exhibited a straight line employing a single exponential decay. The complete experimental data at different temperatures for

this system is presented in Tables 14-18. The data has been analysed in a fashion similar to that of $\text{CO}_2\text{-CH}_3\text{OH}$ system and is not discussed here. The temperature dependence of the deactivation rate $K_{\text{CO}_2\text{-C}_2\text{H}_5\text{OH}}$ is presented in Fig.9. From these rates, the collision cross-sections and the energy transfer probabilities have been calculated and are presented in Table 19 at different temperatures.

Table 19

Rate constants, cross-sections and probabilities of energy transfer from $\text{CO}_2(00^{\circ}1)$ to $\text{C}_2\text{H}_5\text{OH}$

T°K	$K_{\text{CO}_2\text{-M}}(\text{ms}^{-1}\text{torr}^{-1})$	$\sigma \text{ \AA}^2$	$P_{\text{exp}} \times 10^2$
301	209. \pm 23.5	1.27 \pm 0.18	2.27 \pm 0.81
375	141 \pm 5.8	0.96 \pm 0.04	1.72 \pm 0.07
450	101 \pm 18.3	0.75 \pm 0.19	1.35 \pm 0.24
525	77.1 \pm 6.6	0.62 \pm 0.05	1.11 \pm 0.1
600	70.2 \pm 9.4	0.61 \pm 0.08	1.08 \pm 0.14

INTERPRETATION OF RESULTS

A close observation of the deactivation rates presented in Table 19 reveals that the deactivation of the $\text{CO}_2(00^{\circ}1)$ mode in collisions with Ethyl alcohol is again

TABLE 14

TEMPERATURE (K) = 600.0

PRESSURE (P) IN TORR AND TOWINVERSE (τ^{-1}) IN INVERSE MILLISEC.)

X = 0.075		X = 0.05		X = 0.025		X = 0.01	
P	τ^{-1}	P	τ^{-1}	P	τ^{-1}	P	τ^{-1}
15.4	109.1	14.3	74.3	16.1	54.0	24.9	59.6
15.4	110.4	14.3	64.2	16.1	50.8	24.9	53.5
13.0	93.5	12.6	58.5	14.3	46.9	22.0	55.1
13.0	90.7	12.6	67.3	14.3	44.9	22.0	53.6
11.2	71.5	11.3	54.2	13.0	40.5	18.8	49.8
11.2	87.1	11.3	58.7	13.0	49.5	18.8	47.5
9.8	74.0	11.3	48.0	13.0	42.2	15.8	40.5
9.8	66.0	9.7	41.5	11.3	36.3	15.8	41.2
8.3	67.5	9.7	53.7	11.3	39.0	13.6	31.1
8.3	66.4	9.7	50.7	8.0	27.7	13.6	34.8
7.2	50.5	8.3	47.4	8.0	28.7	13.6	34.1
7.2	50.7	8.3	44.5	8.0	27.2	11.2	27.8
5.6	38.9	6.9	40.2	6.9	23.4	11.2	24.8
5.6	35.2	6.9	41.5	6.9	23.6	8.9	24.3
4.1	35.8	5.7	25.0	6.9	25.1	8.9	26.3
4.1	32.0	5.7	27.7	5.1	23.6	6.9	24.7
2.4	21.5	4.2	23.0	5.1	21.7	6.9	22.2
2.4	23.6	4.2	24.1	3.4	16.4	4.9	16.6
2.4	22.3	2.5	22.5	3.4	18.5	4.9	20.6
2.6	25.1	2.5	21.9	3.4	19.3	4.9	16.9
2.6	30.1	3.4	20.9	2.5	15.0	3.4	14.4
2.6	27.7			2.5	13.7	3.4	14.0
				3.8	21.2	4.6	14.4
				2.9	24.5	3.0	14.0
						3.0	14.8

K(OBS) = 6.74 \pm 0.03K(OBS) = 4.21 \pm 0.09K(OBS) = 2.74 \pm 0.01K(OBS) = 2.05 \pm 0.01K(CO2-C2H5OH) = 70.2 \pm 9.4 (MILLISEC. TORR) $^{-1}$

TABLE 15

TEMPERATURE (K) = 525.0

CARBONDIOXIDE-ETHYLALCOHOL

(PRESSURE (P) IN TORR AND TOWINVERSE (τ^{-1}) IN INVERSE MILLISEC.)

X = 0.075		X = 0.05		X = 0.025		X = 0.01	
P	τ^{-1}	P	τ^{-1}	P	τ^{-1}	P	τ^{-1}
15.7	140.1	15.7	82.8	19.2	75.9	27.0	50.1
15.7	109.1	15.7	73.0	19.2	62.2	27.0	51.0
13.1	96.6	14.2	62.0	17.3	59.3	23.9	41.0
13.1	90.2	14.2	78.9	17.3	56.6	23.9	39.8
13.1	83.7	12.6	75.9	15.6	61.0	20.8	37.5
12.0	84.1	12.6	74.2	15.6	47.4	20.8	39.5
12.0	93.1	11.2	53.0	14.3	43.2	18.7	41.3
12.0	92.9	11.2	55.7	14.3	47.9	18.7	39.3
10.1	75.4	9.9	51.4	12.3	45.8	16.6	32.7
10.1	81.9	9.9	47.1	12.3	38.1	16.6	35.4
8.2	69.7	8.6	50.6	10.8	39.6	13.8	32.8
8.2	62.0	7.2	41.5	10.8	38.2	13.8	28.7
7.2	54.0	7.2	41.4	9.2	38.4	10.5	27.4
7.2	56.8	5.8	37.8	9.2	37.8	10.5	26.7
5.4	42.2	5.8	34.8	7.5	27.7	8.2	22.5
5.4	46.8	4.1	30.2	7.5	31.8	8.2	24.2
3.5	39.6	4.1	28.7	7.5	33.6	6.2	25.4
3.5	31.9	2.4	21.8	5.8	25.2	5.8	16.0
3.5	35.9	2.4	21.9	5.8	27.6	5.8	18.1
2.6	25.1	2.4	21.1	5.8	24.0	5.8	16.9
2.6	30.1	3.4	20.9	3.8	20.4	3.7	15.9
2.6	27.7			3.8	21.1	3.7	15.7
				3.8	21.2	4.6	14.4
				2.9	24.5	3.0	14.0
						3.0	14.8

K(OBS) = 6.70 \pm 0.01K(OBS) = 4.31 \pm 0.01K(OBS) = 2.82 \pm 0.02K(OBS) = 1.40 \pm 0.01K(CO2-C2H5OH) = 77.1 \pm 6.6 (MILLISEC. TORR)⁻¹

TABLE 16

TEMPERATURE (K) = 450.0

CARBON DIOXIDE - E.M.

(PRESSURE (P) IN TORR AND TOWINVERSE (τ^{-1}) IN INVERSE MILLISEC.)

X = 0.075			X = 0.05			X = 0.025			X = 0.01		
P	τ^{-1}		P	τ^{-1}		P	τ^{-1}		P	τ^{-1}	
11.7	109.2		13.8	103.6		16.3	51.9		21.3	31.3	
11.8	111.3		13.8	102.3		16.3	63.0		21.3	34.4	
11.8	117.9		12.0	80.6		15.3	51.9		18.8	33.8	
10.6	102.0		12.0	84.0		15.3	50.3		18.8	34.9	
10.6	104.9		11.0	76.5		13.8	54.6		15.9	35.0	
9.3	91.7		9.2	59.8		13.8	49.0		15.9	29.9	
9.3	86.4		9.2	54.5		12.8	54.5		15.9	34.7	
8.0	76.6		7.2	60.3		12.2	47.0		14.2	29.2	
8.0	77.2		7.2	50.4		12.2	51.8		14.2	28.2	
7.2	72.1		6.2	47.2		12.2	44.5		12.3	22.6	
7.2	76.9		6.2	49.1		9.8	41.1		12.3	22.4	
6.2	59.9		5.5	39.5		9.8	34.7		10.8	20.5	
6.2	67.3		5.5	40.3		8.1	34.7		10.8	22.3	
5.3	60.6		4.6	42.2		8.1	31.6		9.6	20.9	
5.3	55.9		4.6	39.2		6.4	27.3		9.6	22.0	
4.3	52.1		3.8	30.4		6.4	29.3		9.6	21.7	
4.3	51.8		3.8	31.4		6.4	31.9		7.8	17.6	
2.4	39.4		2.4	23.0		5.2	27.0		7.8	17.7	
2.4	45.4		2.4	18.9		5.2	26.9		5.8	20.3	
1.8	30.7		2.4	21.1		4.2	22.3		5.8	20.3	
			3.4	20.9		4.2	23.0		3.6	14.9	
						3.0	21.0		3.6	13.6	
						3.0	20.4		4.6	14.4	
						2.9	24.5		3.0	14.0	
									3.0	14.8	

K(OBS) = 7.50 ± 0.25

K(OBS) = 6.59 ± 0.01

K(OBS) = 2.81 ± 0.01

K(OBS) = 1.21 ± 0.02

K(CO2-C2H5OH) = 101 ± 18.3 (MILLISEC. TORR) - 1

TABLE 17

TEMPERATURE (K) = 375.0 CARBON DIOXIDE-ETHYLALCOHOL
(PRESSURE (P) IN TORR AND TOWINVERSE (τ^{-1}) IN INVERSE MILLISEC.)

X = 0.075		X = 0.05		X = 0.025		X = 0.01	
P	τ^{-1}	P	τ^{-1}	P	τ^{-1}	P	τ^{-1}
12.8	131.5	14.6	129.2	16.0	74.0	20.9	43.0
12.8	173.3	14.6	118.1	16.0	75.0	20.9	39.3
12.8	148.5	12.6	104.7	14.4	76.8	20.9	46.5
9.7	117.5	12.6	106.6	14.4	61.2	18.1	42.6
8.5	107.6	11.4	103.8	13.3	58.9	18.1	34.0
3.5	110.0	11.4	98.4	13.3	62.2	15.8	32.5
6.6	75.8	8.4	80.6	12.8	63.8	15.8	33.6
6.6	89.2	8.4	83.6	11.8	62.6	14.1	30.7
5.6	67.7	6.4	52.6	11.8	58.8	14.1	34.1
5.6	69.5	6.4	50.1	10.2	48.3	14.1	35.2
4.9	59.2	6.4	49.9	10.2	49.3	11.9	26.4
4.9	57.7	5.4	54.0	8.0	42.8	11.9	28.0
3.8	60.0	5.4	53.6	8.0	41.3	11.9	25.2
3.8	58.0	4.3	39.5	6.9	37.3	10.5	24.0
3.0	50.0	4.3	38.5	6.9	39.7	10.5	25.0
3.0	51.6	3.6	46.5	5.4	36.9	8.8	20.6
2.6	42.3	3.6	43.6	5.4	35.1	8.8	20.5
2.6	39.2	2.9	34.1	4.6	30.4	7.0	16.8
1.8	31.7	2.9	31.9	4.6	27.3	7.0	17.1
1.8	30.7	2.9	33.0	3.6	21.2	5.8	18.7
		3.4	20.9	3.6	21.8	5.8	18.6
				2.9	24.5	4.6	16.9
				2.9	23.6	4.6	14.4
				2.9	24.5	3.0	14.0
						3.0	14.8

K(OBS) = 10.77±0.04

K(OBS) = 7.76±0.02

K(OBS) = 3.94±0.04

K(OBS) = 1.68±0.03

K(CO2-C2H5OH) = 141 ± 5.8 (MILLISEC. TORR)⁻¹

TABLE 18

TEMPERATURE (K) = 301.0

CARBONDIOXIDE-ETHYLALCOHOL
(PRESSURE (P) IN TORR AND TOWINVERSE (τ^{-1}) IN INVERSE MILLISEC.)

X = 0.015		X = 0.01		X = 0.005	
P	τ^{-1}	P	τ^{-1}	P	τ^{-1}
19.2	73.0	18.3	60.9	22.8	41.2
18.2	76.5	19.3	58.1	20.5	42.1
16.0	75.5	16.8	31.5	20.5	40.6
16.0	72.5	15.8	52.7	18.0	33.7
14.2	68.0	15.8	44.8	15.6	33.4
14.2	65.4	14.5	37.1	15.5	31.8
13.1	51.8	14.5	38.1	13.7	26.6
13.1	60.3	8.8	37.2	13.7	29.1
12.5	53.6	8.8	31.0	12.0	27.1
12.5	51.0	7.3	27.7	12.0	25.9
10.9	51.0	7.3	27.5	10.1	23.8
10.9	55.0	6.1	25.6	10.1	22.8
9.9	44.3	6.1	29.0	10.1	23.4
9.9	50.5	5.0	22.9	8.5	25.1
8.5	40.2	5.0	26.5	8.5	24.4
8.5	40.7	5.0	23.7	7.0	23.3
7.4	38.4	4.2	18.9	7.0	22.0
7.4	38.9	4.2	21.4	7.0	21.0
		3.4	19.5	5.6	19.6
		3.4	21.5	5.6	18.9
		3.4	20.9		

K(OBS) = 3.56 \pm 0.02K(OBS) = 2.09 \pm 0.01K(OBS) = 1.32 \pm 0.01K(CO2-C2+50H) = 209 \pm 28.5 (MILLISEC. TORR)⁻¹

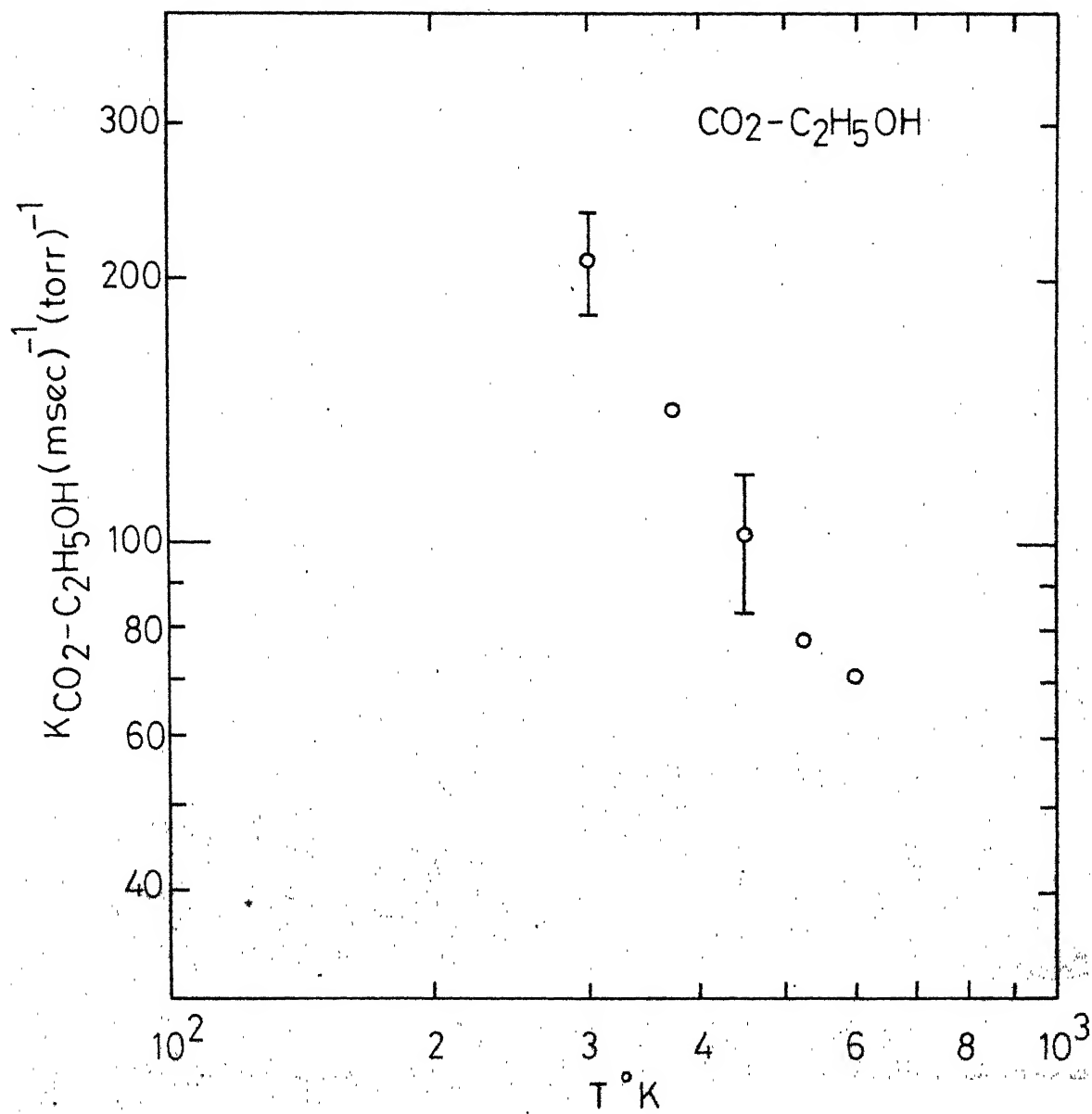


Fig. 9 - Temperature dependence of $K_{\text{CO}_2-\text{C}_2\text{H}_5\text{OH}}$

PROBABILITY CALCULATIONS

The energy transfer probabilities have been calculated at different temperatures using SB theory for process 4.15 by taking into account only the dipole-dipole interactions and assuming a unit value for the two unknown C_2H_5OH transition moments. Then the experimental probability can be written as

$$P_{\text{exp}} = a(\nu_x \rightarrow 0) p_{15} + a(\nu_4 \rightarrow 0) p_{16} \quad 4.18$$

where a 's are squares of the appropriate transition dipole moments. However, both the processes 4.15 and 4.16 have the same energy mismatch ($\Delta E = -4 \text{ cm}^{-1}$) and hence the same temperature dependence. Therefore, their ratio is given by the ratio of the squares of the transition moments of CO_2 as follows.

$$p_{15}/p_{16} = a(\nu_3 \rightarrow 0)/a(\nu_3 \rightarrow 2\nu_2) = 1 \times 10^{-37}/1.22 \times 10^{-39} = 82 \quad 4.19$$

Therefore

$$P_{\text{exp}} = [82 a(\nu_x \rightarrow 0) + a(\nu_4 \rightarrow 0)] p_{16} \quad 4.20$$

The molecular constants used in the calculation of p_{16} are given in Table 5. Ethyl alcohol is assumed to be a prolate symmetric top molecule. The results of the calculations for p_{16} are presented in Table 20. A least square analysis of

this data according to equation 4.20 resulted in a value of $1.95 \times 10^{-37} \text{esu}^2 \text{cm}^2$ for the combined coefficient. Since $\nu_{\text{X}} \rightarrow 0$ is weak and $\nu_4 \rightarrow 0$ is very strong in $\text{C}_2\text{H}_5\text{OH}$, the ratio $a(\nu_4 \rightarrow 0)/a(\nu_{\text{X}} \rightarrow 0)$ is likely to be between 1000 to 100. For these limiting ratios the square of the dipole moment of the C-O stretch can be estimated from equation 4.20 as 1.8×10^{-37} and $1.07 \times 10^{-37} \text{esu}^2 \text{cm}^2$ respectively.

Table 20

Calculated Energy Transfer probabilities* for process 4.16
of $\text{CO}_2\text{-C}_2\text{H}_5\text{OH}$ system

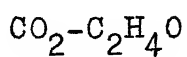
T°K	$p_{16} \times 10^{35}$
301	1.091
375	0.8783
450	0.7354
525	0.6339
600	0.5579

COMMENTS

This study reveals that all the three alcohols are very efficient in deactivating the $\text{CO}_2(00^01)$ mode. In all the three cases studied, it has been observed that the very

* Values are obtained by assuming unity for the unknown transition dipole moments(squares) of M.

strong C-O stretch vibrational transition is mainly responsible for the deactivation. The unknown transition dipole moments for the C-O stretch mode in all the three alcohols studied are estimated though only very approximately for C_2H_5OH . The deactivation rate is about the same for the two alcohols CH_3OH and C_2H_5OH .



The collisional deactivation of $CO_2(00^{\circ}1)$ mode with Ethylene oxide which has the same molecular weight as that of CO_2 , has been studied at four different compositions in the temperature range of 300-650°K. The fluorescence signal intensity again displayed a single exponential decay for all the experimental runs taken. The deactivation rates $K_{CO_2-C_2H_4O}$ are estimated at different temperatures by analysing the data in the same lines as in the case of CO_2-CH_3OH system, and the temperature dependence of the rate is plotted in Fig.10. The complete experimental data has been presented in Tables 21-28 at different temperatures. The experimental cross-sections and the energy transfer probabilities calculated from the deactivation rates by using equations 2.4 and 2.5 are presented in Table 29 along with the rate constants at different temperatures.

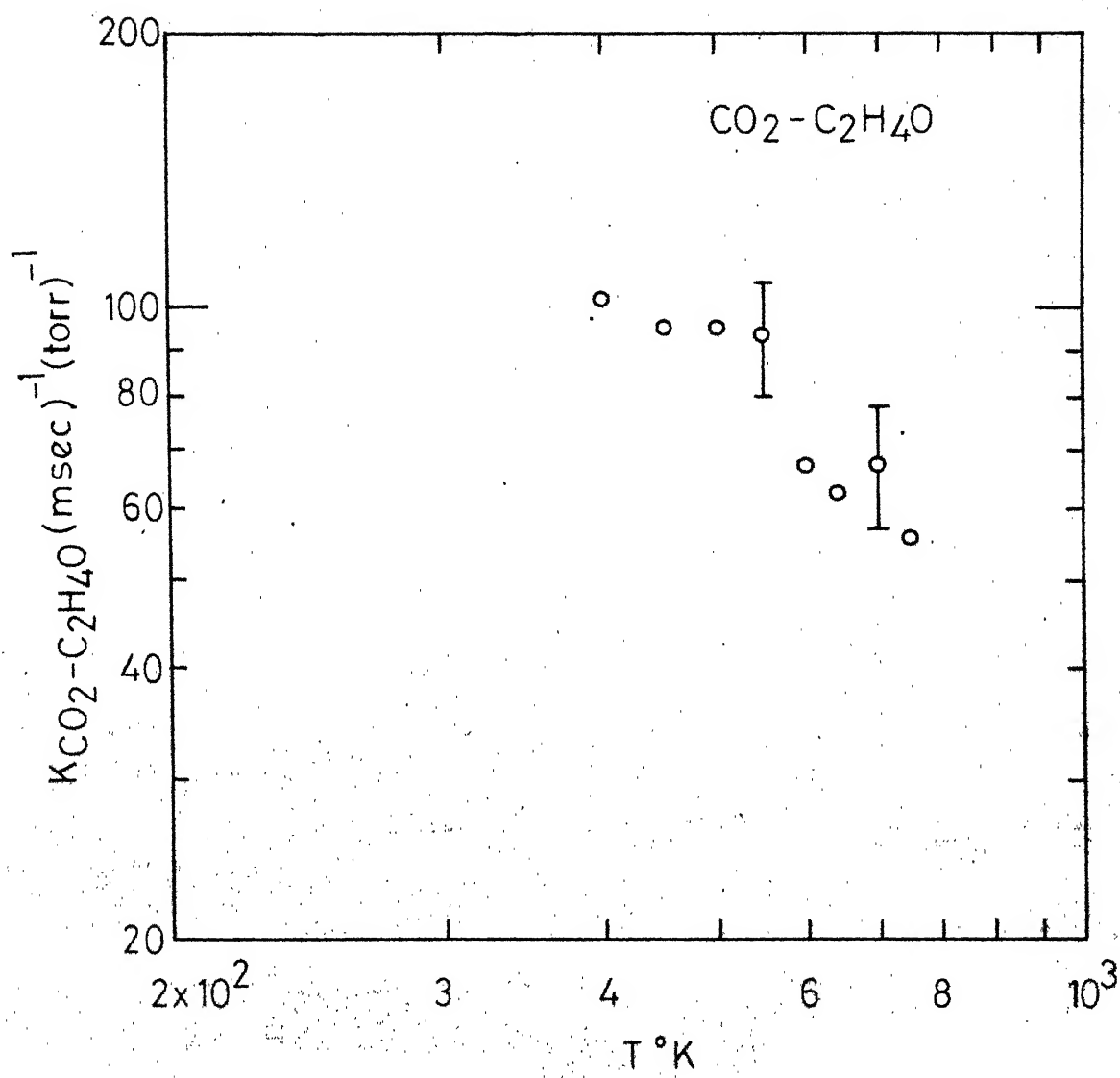


Fig. 10 -Temperature dependence of $K_{\text{CO}_2-\text{C}_2\text{H}_4\text{O}}$

TABLE 2A

TEMPERATURE (K) = 650.0 CARBONDIOXIDE-ETHYLENEOXIDE
(PRESSURE (P) IN TORR AND TOWINVERSE (τ^{-1}) IN INVERSE MILLISEC.)

X = 0.112		X = 0.075		X = 0.026	
P	τ^{-1}	P	τ^{-1}	P	τ^{-1}
13.4	114.0	13.8	82.2	19.8	92.9
13.4	109.8	13.8	92.5	19.8	78.7
12.1	92.5	12.3	84.9	17.8	69.9
12.1	115.3	12.3	90.4	17.8	78.2
10.8	113.6	11.2	67.5	16.0	66.6
10.2	99.7	11.2	62.8	16.0	65.8
9.5	96.1	10.1	66.9	14.0	70.1
9.5	92.9	10.1	68.3	14.0	55.9
8.4	66.3	8.7	57.4	11.5	44.2
8.4	74.7	8.7	61.4	11.5	53.2
7.1	65.7	7.7	49.6	11.5	40.8
7.1	53.1	7.7	56.6	9.9	53.7
6.1	64.1	6.4	47.4	9.9	38.5
6.1	61.4	6.4	49.0	8.0	34.2
5.0	48.5	5.2	41.4	8.0	37.1
5.0	39.9	5.2	39.2	6.2	32.3
5.0	50.4	4.2	30.7	6.2	30.0
3.7	38.7	4.2	29.1	2.5	16.8
3.7	40.7	2.8	24.0	4.3	41.7
2.5	31.6	2.8	25.2	2.5	27.6
2.5	29.6			2.5	22.3

K(OBS) = 8.04 \pm 0.01K(OBS) = 5.84 \pm 0.02K(OBS) = 3.92 \pm 0.04K(CO2-C2H4O) = 55.5 \pm 7.3 (MILLISEC. TORR)

TABLE 230

TEMPERATURE (K) = 540.0 CARBONDIOXIDE-ETHYLENEOXIDE
(PRESSURE (P) IN TORR AND TOWINVERSE (τ^{-1}) IN INVERSE MILLISEC.)

X = 0.027		X = 0.051		X = 0.079		X = 0.115	
P	τ^{-1}	P	τ^{-1}	P	τ^{-1}	P	τ^{-1}
22.8	53.7	22.7	92.1	19.8	102.5	19.5	172.0
22.8	49.1	19.9	78.2	19.8	109.8	18.2	146.0
19.8	44.7	17.5	71.9	17.0	117.0	18.2	150.5
19.8	45.5	17.5	63.4	17.0	104.0	15.3	131.8
17.4	41.4	15.9	55.5	14.8	85.4	12.8	94.5
17.4	41.8	15.9	56.4	14.8	84.4	12.8	103.7
17.4	41.7	12.7	52.1	13.0	77.0	11.1	98.5
16.3	42.4	12.7	53.3	13.0	79.1	11.1	87.5
16.3	46.4	11.2	49.4	10.9	61.4	9.7	74.7
14.5	36.0	11.2	42.2	10.9	70.0	9.7	68.0
14.5	35.8	9.1	28.8	8.2	51.5	8.0	60.5
12.4	43.3	9.1	40.4	8.2	48.4	6.5	57.9
12.4	39.0	7.4	33.4	6.5	40.0	6.6	55.3
10.8	34.4	7.4	32.7	6.5	38.3	4.3	42.8
10.6	31.2	5.6	20.8	4.6	26.3	4.3	36.3
7.4	28.8	5.6	30.0	4.6	28.8	3.2	38.0
7.4	26.6	4.2	21.8	3.0	21.8	3.2	41.0
5.3	18.5	4.2	21.5	3.0	26.2	4.4	45.4
5.3	19.1	4.2	23.2	3.3	34.5	3.4	45.9
3.6	16.8	3.0	22.6	2.8	25.3	3.4	49.0
3.6	14.2	3.0	22.1	2.8	20.7	2.4	32.9
4.0	16.8					2.4	34.1

K(OBS) = 1.78 \pm 0.07K(OBS) = 3.55 \pm 0.05K(OBS) = 5.51 \pm 0.09K(OBS) = 7.90 \pm 0.25K(CO2-C2H4O) = 62.5 \pm 7.2 (MILLISEC. TORR)⁻¹

TABLE 24

TEMPERATURE (K) = 500.0
(PRESSURE (P) IN TORR AND TOWINVERSE (C⁻¹) IN INVERSE MILLISEC.)

CARBON DIOXIDE--ETHYLENEOXIDE

X = 0.027		X = 0.051		X = 0.079		X = 0.115	
P	C ⁻¹	P	C ⁻¹	P	C ⁻¹	P	C ⁻¹
24.2	90.2	22.4	151.0	20.4	126.0	16.5	150.0
24.2	75.6	22.4	147.0	20.4	117.8	16.5	165.0
22.8	69.7	19.2	102.2	17.5	10.0	14.3	154.0
22.8	76.4	19.2	103.2	17.5	06.0	14.3	140.1
19.8	76.3	16.8	109.5	15.9	12.0	12.7	124.5
19.0	70.6	16.8	107.8	15.9	94.2	12.7	136.2
15.9	58.3	15.3	87.3	13.1	76.6	10.6	112.3
15.9	61.8	15.3	86.0	11.0	82.2	10.6	104.7
13.8	48.8	13.0	78.9	11.0	82.3	9.6	103.2
13.8	65.8	11.2	75.3	9.2	58.7	9.6	107.5
11.9	40.4	9.2	55.0	9.2	72.2	8.6	96.3
11.2	43.2	9.2	63.4	8.7	62.2	8.6	98.8
9.5	43.4	7.4	57.2	8.6	64.3	6.5	83.0
9.5	44.4	7.4	53.8	5.8	50.0	6.5	81.0
6.4	24.4	5.8	38.8	5.8	48.6	6.2	63.3
6.4	32.5	5.8	45.0	4.8	38.5	6.2	68.5
5.1	22.9	3.8	36.3	4.8	37.5	4.4	46.6
5.1	27.2	3.8	32.3	3.3	35.1	4.4	45.4
4.0	24.6	4.4	26.2	3.3	34.5	3.4	45.9
4.0	25.6	3.0	22.6	2.8	25.3	3.4	49.0
4.0	24.7	3.0	22.1	2.8	20.7	2.4	32.9
4.0	16.8					2.4	34.1

K(OBS) = 2.95±0.09

K(OBS) = 5.58±0.02

K(OBS) = 5.20±0.01

K(OBS) = 8.97±0.07

K(CO2-C2H4O) = 67. ± 16.5 (MILLISEC. TORR)⁻¹

TABLE 25

TEMPERATURE (K) = 450.0

CARBONDIOXIDE-ETHYLENEOXIDE
(PRESSURE (P) IN TORR AND TOWINVERSE (τ^{-1}) IN INVERSE MILLISEC.)

X = 0.027		X = 0.051		X = 0.079		X = 0.115	
P	τ^{-1}	P	τ^{-1}	P	τ^{-1}	P	τ^{-1}
19.7	68.7	20.1	94.5	19.4	174.0	18.8	202.0
19.7	68.5	18.6	84.5	16.3	140.0	18.9	222.0
17.9	57.8	18.6	87.5	16.3	133.5	16.5	183.8
16.2	56.6	16.2	80.0	16.3	120.4	16.5	172.5
16.2	56.8	16.2	73.0	12.3	107.2	14.1	144.3
14.0	52.6	15.1	76.0	12.3	98.5	14.1	166.9
14.0	48.7	15.1	77.6	11.2	93.2	9.8	108.7
12.2	53.5	13.6	71.4	11.2	95.9	8.0	78.0
12.2	43.1	13.6	69.8	10.0	90.6	8.0	76.4
10.6	39.9	12.4	61.0	10.0	90.6	6.7	71.3
10.6	37.7	12.4	65.4	8.3	90.4	6.7	71.4
10.6	39.0	9.8	52.7	3.3	79.6	5.0	47.7
8.2	27.4	9.8	52.7	7.0	48.4	5.0	53.0
8.2	31.3	8.2	50.9	7.0	47.9	4.3	45.4
6.6	28.4	8.2	52.0	6.0	48.5	4.3	47.9
6.6	28.8	5.9	43.5	6.0	46.2	3.0	40.4
4.7	19.4	5.9	42.4	4.0	34.0	3.0	46.4
4.7	21.6	4.4	32.7	4.0	36.8	4.7	22.3
3.1	20.0	4.4	26.2	2.8	29.6	4.7	28.7
3.0	62.7	3.0	22.6	2.8	25.3	3.6	52.7
2.5	29.6	3.0	22.1	2.8	20.7	2.4	32.9
						2.4	34.1

K(OBS) = 3.05 ± 0.06 K(OBS) = 4.01 ± 0.08 K(OBS) = 8.37 ± 0.08 K(OBS) = 11.04 ± 0.32 K(CO2-C2H4O) = 93.5 ± 12 (MILLISEC. TORR)⁻¹

TABLE 26

TEMPERATURE (K) = 400.0 CARBONDIOXIDE-ETHYLENEOXIDE
(PRESSURE (P) IN TORR AND TOWINVERSE (τ^{-1}) IN INVERSE MILLISEC.)

X = 0.115		X = 0.079		X = 0.051		X = 0.027	
P	τ^{-1}	P	τ^{-1}	P	τ^{-1}	P	τ^{-1}
16.3	204.0	18.9	164.5	17.2	122.0	22.1	99.0
16.3	196.0	18.9	160.5	17.2	131.7	22.1	85.6
13.4	174.0	16.6	149.0	15.8	118.0	18.5	81.7
13.4	192.5	16.6	146.5	15.8	126.0	16.2	63.7
10.2	131.0	13.4	112.4	12.6	92.5	16.2	66.5
10.2	154.0	13.4	107.0	12.6	95.4	15.6	63.3
9.2	111.0	11.6	100.5	11.3	79.8	15.6	69.6
7.8	100.0	11.6	126.8	11.3	76.2	12.8	60.2
7.8	94.0	8.8	94.0	9.5	48.8	12.8	58.8
6.6	92.0	8.8	91.5	9.5	59.8	11.0	59.2
6.6	89.6	7.4	85.4	7.6	44.6	11.0	53.5
5.1	74.6	7.4	71.8	7.6	46.8	10.0	44.8
4.5	77.5	6.2	65.0	6.8	48.8	10.0	49.5
4.6	72.4	6.2	73.3	6.8	54.5	8.0	45.1
4.0	51.0	6.2	45.2	6.0	44.8	8.0	29.1
4.0	52.7	6.2	45.0	6.0	44.9	5.8	26.7
3.4	48.8	4.6	50.2	5.1	36.8	5.3	32.9
3.4	48.3	4.6	64.4	5.1	37.2	4.7	22.3
3.0	61.8	2.5	40.6	2.7	30.1	4.7	28.7
3.0	62.7	2.5	39.1	2.7	33.2	3.6	52.7
2.5	29.6			2.5	22.3	2.4	32.9
						2.4	34.1

K(OBS) = 11.79 ± 0.30

K(OBS) = 7.60 ± 0.03

K(OBS) = 7.21 ± 0.30

K(OBS) = 3.79 ± 0.04

K(CO2-C2H4O) = 94.9 ± 17. (MILLISEC. TORR)⁻¹

TABLE 27

TEMPERATURE (K) = 250.0

CARBON DIOXIDE-ETHYLENE OX. DE
(PRESSURE (P) IN TORR AND TOWINVERSE (τ^{-1}) IN INVERSE MILLISEC.)

X = 0.027 τ^{-1}		X = 0.051 τ^{-1}		X = 0.079 τ^{-1}		X = 0.115 τ^{-1}	
P		P		P		P	
22.1	93.2	18.2	124.5	16.3	154.0	12.7	136.3
22.1	89.5	18.2	126.0	16.3	170.0	12.7	151.7
19.8	80.7	15.8	112.2	13.2	128.5	11.9	144.0
19.8	88.7	15.8	110.0	13.2	138.1	11.9	134.8
15.8	57.8	14.2	94.5	11.2	115.8	11.0	161.5
15.8	62.9	14.2	92.6	11.2	125.0	11.0	115.0
14.2	50.0	12.6	76.6	9.6	84.7	9.9	124.2
14.2	54.5	12.6	82.5	9.6	94.0	9.9	121.5
10.2	48.4	10.8	79.4	8.1	71.0	8.4	119.0
10.2	42.7	10.8	78.6	8.1	81.5	8.4	114.3
8.4	37.4	8.6	58.9	7.2	69.4	6.9	79.6
8.4	37.2	8.6	65.0	7.2	65.6	6.9	94.3
6.9	33.8	7.2	53.8	5.6	53.5	6.0	89.4
6.9	37.4	7.2	61.8	5.6	50.8	6.0	88.0
5.8	30.7	5.9	40.7	4.3	43.1	5.3	87.5
5.8	27.4	5.9	44.2	4.3	34.5	5.3	76.6
4.7	20.2	4.0	32.7	3.1	37.0	4.2	56.6
4.7	22.3	4.0	30.9	3.1	36.0	4.2	59.6
3.2	20.6	2.7	21.6	4.3	41.7	3.6	58.4
3.2	25.0	2.7	27.1	2.5	27.6	3.6	52.7
2.5	29.6	2.7		2.5	22.3	2.4	32.9
						2.4	34.1

K(OBS) = 3.69 ± 0.10

K(OBS) = 6.39 ± 0.06

K(OBS) = 10.13 ± 0.20

K(OBS) = 10.57 ± 0.24

K(CO2-C2H4O) = 94.7 ± 22. (MILLISEC. TORR)⁻¹

TABLE 28

TEMPERATURE (K) = 301.0
 (PRESSURE (P) IN TORR AND TOWINVERSE (τ^{-1}) IN INVERSE MILLISEC.) CARROND/OXIDE-ETHYLENEOXIDE

X = 0.079		X = 0.115		X = 0.051		X = 0.027	
P	τ^{-1}	P	τ^{-1}	P	τ^{-1}	P	τ^{-1}
14.8	168.0	16.8	203.5	15.5	167.0	20.0	92.0
14.5	117.0	16.8	247.0	15.5	174.5	20.0	93.5
14.0	131.0	11.5	180.0	14.0	148.5	18.2	99.5
14.0	131.0	11.5	173.0	14.0	143.0	17.6	85.3
12.8	131.0	9.1	149.0	12.2	139.0	17.5	86.7
12.8	133.0	9.1	149.0	10.8	95.0	13.7	75.2
10.9	122.3	8.0	135.0	10.8	102.5	13.7	70.8
10.5	107.0	8.0	139.5	8.0	91.7	11.1	57.2
10.5	121.4	6.0	106.5	9.0	101.0	9.2	49.3
10.2	101.0	5.6	88.0	7.0	90.3	7.8	43.2
10.2	108.0	5.6	89.0	7.0	81.4	7.8	55.6
7.4	81.0	4.0	81.0	6.2	75.3	6.4	35.7
7.4	89.0	4.0	85.6	6.2	84.8	6.4	56.0
7.2	72.0	3.8	69.5	5.0	60.3	4.2	27.5
7.2	101.0	3.8	66.3	5.0	61.7	4.2	31.3
5.0	56.6	2.2	53.0	4.0	61.0	3.0	36.8
5.0	56.6	2.2	49.7	4.0	60.5	3.0	34.4
3.4	45.3	4.2	21.5	3.0	45.8	2.9	32.3
3.4	46.9	4.2	23.2	3.0	46.4	3.4	45.9
2.6	41.5	3.0	22.6	2.8	25.3	3.4	49.0
2.6	41.3	3.0	22.1	2.8	20.7	2.4	32.9
2.6	37.8					2.4	34.1

K(OBS) = 8.58±0.08 K(OBS) = 12.25±0.19 K(OBS) = 9.21±0.01 K(OBS) = 3.82±0.13

K(CO2-C2H4O) = 101 ± 31 (MILLISEC.TORR)⁻¹

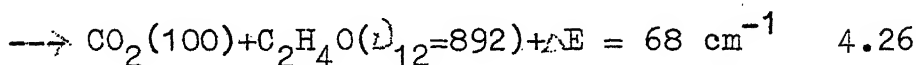
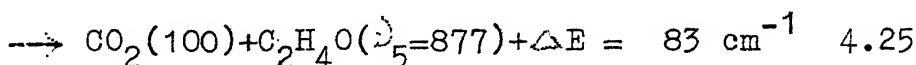
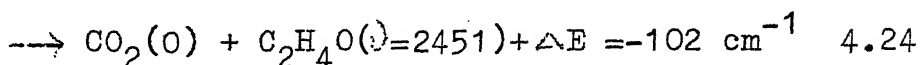
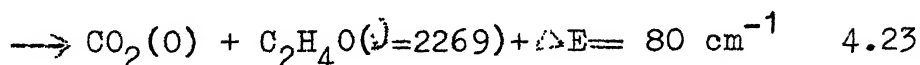
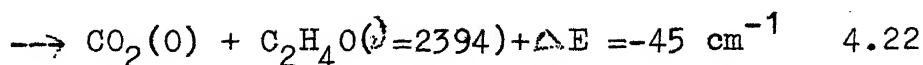
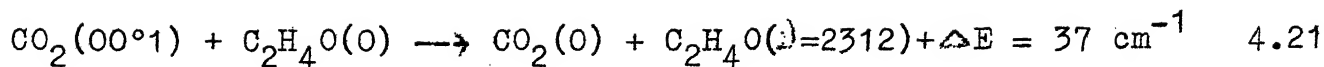
Table 29

Rate constants, cross-sections and probabilities of energy transfer from $\text{CO}_2(00^{\circ}1)$ to $\text{C}_2\text{H}_4\text{O}$

$T^{\circ}\text{K}$	$K_{\text{CO}_2-\text{M}}(\text{ms}^{-1}\text{torr}^{-1})$	$\sigma \text{ \AA}^2$	$P_{\text{exp}} \times 10^2$
301	101 ± 31	0.59 ± 0.18	1.08 ± 0.33
350	94.7 ± 22.4	0.594 ± 0.14	1.09 ± 0.33
400	94.9 ± 17.7	0.64 ± 0.12	1.17 ± 0.26
450	93.5 ± 12.8	0.675 ± 0.09	1.22 ± 0.22
500	67.0 ± 16.5	0.502 ± 0.13	0.92 ± 0.17
540	62.5 ± 7.2	0.49 ± 0.06	0.90 ± 0.23
600	67.2 ± 10.4	0.552 ± 0.08	1.01 ± 0.1
650	55.5 ± 7.3	0.474 ± 0.06	0.87 ± 0.16

INTERPRETATION OF RESULTS

Ethylene oxide is also an efficient collision partner with a rate comparable to that of Methanol-d. Such high energy transfer rates and their decrease with increasing temperature suggest that near-resonant V-V energy transfer processes are of primary importance in the deactivation of the $\text{CO}_2(00^{\circ}1)$ mode. Following the vibrational assignments of Lord and Nolin⁵⁷ and Thompson and Cave⁵⁸ for Ethylene oxide molecule the following processes need to be considered.



The transitions in $\text{C}_2\text{H}_4\text{O}$ in the first four processes (ie. equations 4.21 - 4.24) are weak whereas those in processes 4.25 and 4.26 are very strong.

PROBABILITY CALCULATIONS

The dipole moments of Ethylene oxide transitions for none of the above processes are available. The energy transfer probabilities for all the above processes are calculated using SB theory where only the dipole-dipole interactions are assumed to contribute and are presented in Table 30. It is assumed that Ethylene oxide may be approximated by an oblate symmetric top molecule and the molecular constants used are given in Table 5. A close look at the probabilities in Table 30 reveals that the probabilities decrease with increasing temperature for processes 4.21 and 4.22 where ΔE is 37 and -45 cm^{-1} respectively,

Table 30

Calculated Energy Transfer probabilities* for different processes of $\text{CO}_2\text{-C}_2\text{H}_4\text{O}$ system

T°K	$p_{21} \times 10^{35}$	$p_{22} \times 10^{35}$	$p_{23} \times 10^{35}$	$p_{24} \times 10^{35}$	$p_{25} \times 10^{35}$	$p_{26} \times 10^{35}$
301	57.35	47.29	15.2	3.768	0.1836	0.3914
350	49.49	42.66	17.13	4.596	0.2105	0.4025
400	43.78	38.91	18.96	5.86	0.2373	0.4072
450	39.11	35.55	19.97	7.084	0.2543	0.4013
500	35.31	32.61	20.43	8.158	0.2638	0.3891
540	32.72	30.49	20.38	8.766	0.2656	0.3618
600	29.51	27.72	20.19	9.678	0.2664	0.3394
650	27.25	25.84	19.72	10.15	0.2623	0.3300

* Values are obtained by assuming unity for the unknown transition dipole moments (squares) of M.

shows a broad maximum around 500°K for process 4.23 where ΔE is 80 cm^{-1} and finally shows a positive temperature dependence as ΔE is further increased to 102 cm^{-1} in process 4.24. The probability for process 4.24 increases by 3 times from 300 to 650°K whereas for processes 4.21 and 4.22 the decrease is by about a factor of two in the same temperature range. The experimentally derived probability for this system can be written as

$$P_{\text{exp}} = \sum_i a_i p_i + a_{25} p_{25} + a_{26} p_{26} \quad 4.27$$

where the summation extends over the first four weak processes. It is a common practice to report the combined coefficients for weak bands⁶⁰. Using a similar approach, equation 4.27 can be rewritten as

$$P_{\text{exp}} = a_{\text{weak}} \sum_i p_i + a(\nu_{5 \rightarrow 0}) p_{25} + a(\nu_{12 \rightarrow 0}) p_{26} \quad 4.28$$

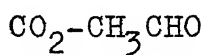
The experimental probabilities at different temperatures are used to find out the dipole moment squares for the transition shown in processes 4.21 - 4.26. The values obtained using least squares analysis are

$$a_{\text{weak}} = 0.17 \times 10^{-39} \text{esu}^2 \text{cm}^2$$

$$a(\nu_{5 \rightarrow 0}) = 0.66 \times 10^{-37} \text{esu}^2 \text{cm}^2$$

$$a(\nu_{12 \rightarrow 0}) = 1.8 \times 10^{-37} \text{esu}^2 \text{cm}^2$$

These values are in accordance with the relative spectroscopic absorption intensities^{57,58}. Thus the calculated value, for the combined strength of the four bands which are reported to be weak, is about three orders of magnitude smaller than the very strong $\nu_{12} \rightarrow 0$ transition. However, the values for $a(\nu_5 \rightarrow 0)$ and $a(\nu_{12} \rightarrow 0)$ are differing by a factor of about 2.3 even though both are reported to be very strong.



The deactivation of the $\text{CO}_2(00^01)$ mode in collisions with Acetaldehyde, whose molecular weight is the same as that of CO_2 and $\text{C}_2\text{H}_4\text{O}$ has been studied for different compositions in the temperature range of 300-650°K. In all the experimental runs the deactivation of this mode followed a single exponential decay which is deduced from the semilogarithmic plot of fluorescence signal intensity versus time. The deactivation rate constant $K_{\text{CO}_2\text{-CH}_3\text{CHO}}$ is deduced along the same lines as has been described previously and its temperature dependence is presented in Fig.11. The complete experimental data taken on this system is presented in Tables 31-36 at different temperatures. The collision cross-sections and the energy transfer probabilities calculated using equations 2.4 and 2.5 are presented in Table 37 along with the deactivation rate at different temperatures.

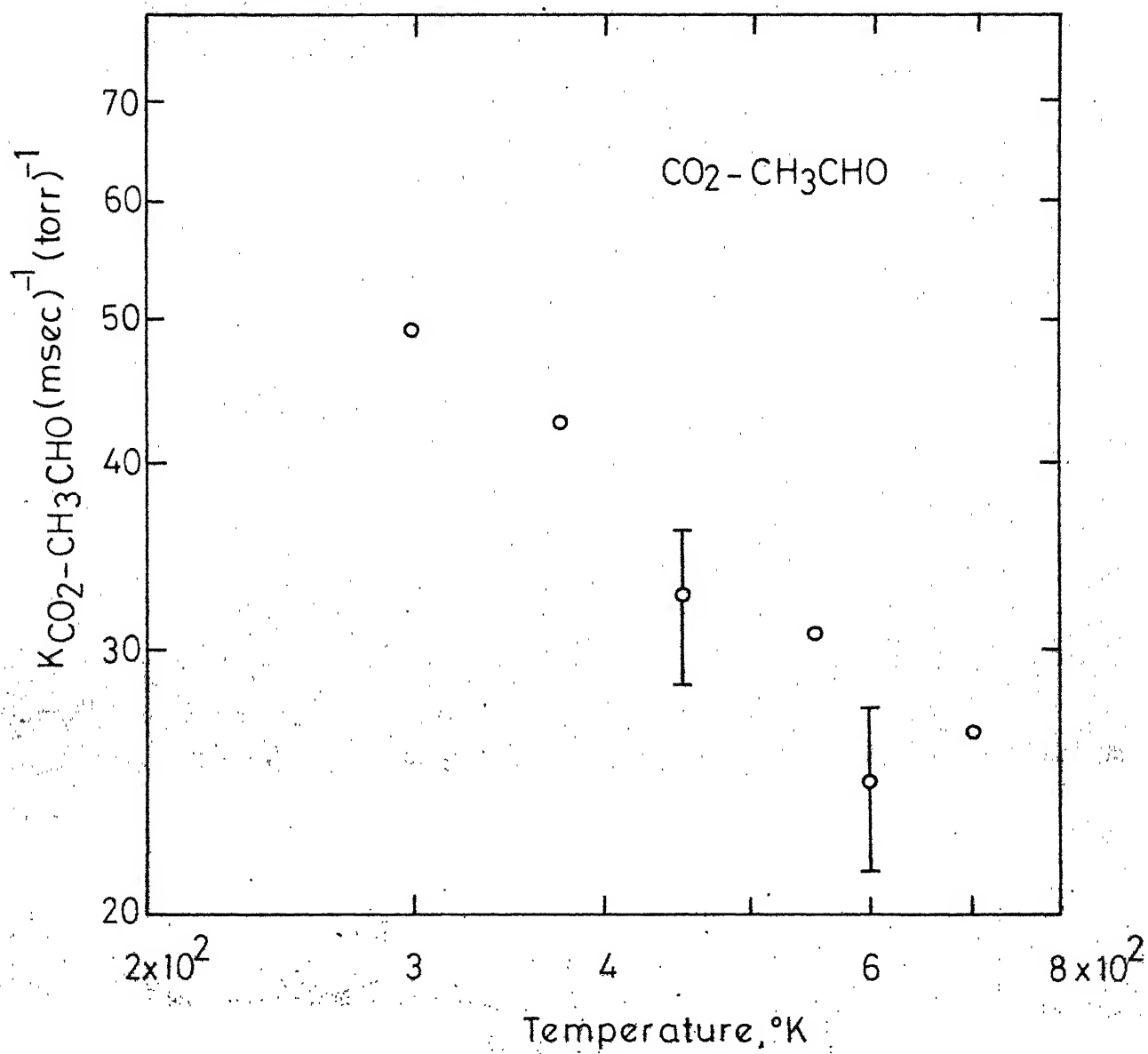


Fig 11 - Temperature dependence of $K_{\text{CO}_2-\text{CH}_3\text{CHO}}$

TEMPERATURE (K) = 650.0

CARBONDIOXIDE-ACETALDEHYDE

(PRESSURE (P) IN TORR AND τ IN INVERSE MILLISECS.)

$X = 0.030$		$X = 0.059$		$X = 0.089$		$X = 0.113$	
P	τ^{-1}	P	τ^{-1}	P	τ^{-1}	P	τ^{-1}
24.1	69.9	16.2	55.0	14.4	69.4	16.3	91.4
18.8	61.1	15.2	55.5	14.4	59.4	16.3	72.2
18.8	53.3	14.1	50.1	12.8	52.5	13.5	64.3
15.3	50.0	12.3	45.9	12.3	57.1	11.3	60.8
14.4	50.1	12.3	42.7	11.5	52.9	11.3	61.7
12.8	45.9	10.6	34.3	10.1	41.8	11.0	50.1
12.8	40.0	9.4	35.4	10.1	41.5	11.0	61.9
11.2	36.7	9.4	35.0	8.5	37.4	11.0	61.9
11.2	48.2	7.8	28.4	8.5	44.0	9.4	47.9
9.4	34.0	7.8	28.3	8.6	39.7	9.4	52.8
9.4	34.1	5.2	24.2	7.0	32.3	7.3	39.4
7.7	29.8	5.2	30.5	7.0	30.1	7.3	40.5
7.7	28.8	5.2	33.4	5.1	25.4	6.5	37.8
6.3	27.4	4.8	28.7	5.1	24.4	5.5	34.9
6.3	26.4	4.8	25.5	4.9	25.5	4.7	23.3
4.3	23.6	3.7	19.3	4.9	24.1	4.7	23.9
4.3	24.8	3.7	19.9	3.4	24.6	3.3	23.3
4.8	26.6	2.2	15.2	3.4	22.2	3.3	20.4
3.2	16.9	2.2	15.2				
3.2	15.2						

K(OBS) = 2.50 ± 0.07 K(OBS) = 2.54 ± 0.02 K(OBS) = 3.88 ± 0.11 K(OBS) = 4.57 ± 0.04 K(CO2-CH3CHO) = 26.5 ± 4.9 (MILLISECS.TORR)⁻¹

TABLE 32

TEMPERATURE (K)= 600.0 CARBON DIOXIDE-ACETALDEHYDE
(PRESSURE (P) IN TORR AND TOWINVERSE (τ^{-1}) IN INVERSE MILLISEC.)

X = 0.030		X = 0.059		X = 0.089		X = 0.113	
P	τ^{-1}	P	τ^{-1}	P	τ^{-1}	P	τ^{-1}
23.4	63.2	21.8	62.1	17.5	80.8	16.2	70.2
23.4	57.3	21.8	70.1	17.5	73.0	16.2	69.0
21.0	60.8	18.4	64.9	13.8	52.5	14.4	64.7
21.0	54.8	17.0	51.6	13.8	47.5	14.4	72.2
19.4	47.1	17.0	50.9	11.6	54.6	12.8	67.8
19.4	51.5	14.7	47.8	11.6	51.8	12.8	63.7
16.9	52.9	14.7	51.8	10.0	44.7	11.4	52.2
16.9	42.2	14.7	54.4	10.0	52.1	11.4	57.3
14.9	40.4	13.4	44.0	8.6	42.6	11.4	57.0
14.9	47.4	13.4	47.8	8.6	38.2	9.8	45.9
12.5	37.7	12.1	39.9	8.6	33.8	9.8	44.8
12.5	46.4	12.1	41.3	7.0	38.8	8.6	44.5
10.2	32.6	10.2	37.8	7.0	29.1	8.6	45.7
10.2	31.5	10.2	39.4	7.0	27.3	7.4	36.1
7.7	26.5	6.6	30.1	5.3	23.3	7.4	44.7
7.7	27.8	6.6	32.3	5.3	22.2	6.1	37.7
7.7	26.1	4.3	19.7	3.3	23.3	6.1	32.7
5.5	23.1	4.3	21.1	3.3	24.3	4.6	27.2
5.5	21.3	2.6	16.9	1.8	16.3	4.6	29.0
3.7	16.9	2.6	17.3	1.8	15.4	3.0	22.4
3.7	17.1					3.0	20.8
3.7	16.8						

K(OBS)= 2.20±0.02

K(OBS)= 2.58±0.01

K(OBS)= 3.67±0.03

K(OBS)= 3.90±0.04

K(CO2-CH3CHO)= 24.4±3.1 (MILLISEC.TORR)⁻¹

TABLE 33

TEMPERATURE (K) = 525.0
 (PRESSURE (P) IN TORR AND TOWINVERSE (τ^{-1}) IN INVERSE MILLISEC.)

CARBON DIOXIDE-ACETALDEHYDE

X = 0.030		X = 0.059		X = 0.089		X = 0.113	
P	τ^{-1}	P	τ^{-1}	P	τ^{-1}	P	τ^{-1}
20.3	43.2	20.9	51.6	17.3	69.2	13.3	67.4
20.3	41.6	17.7	58.1	17.3	68.1	13.3	62.8
17.3	36.3	17.7	56.9	14.3	58.6	11.9	62.6
17.3	33.8	15.8	46.8	14.3	55.1	11.9	60.3
14.8	32.6	15.8	45.6	12.2	40.9	9.4	50.4
14.8	40.6	14.3	48.4	12.2	41.5	8.2	40.7
12.8	33.4	14.3	42.3	10.0	46.1	8.2	40.4
12.8	31.9	13.1	40.8	10.0	46.9	7.3	41.3
10.6	25.3	13.1	42.1	8.6	34.4	7.3	40.4
10.6	25.9	11.2	39.3	8.6	36.5	6.6	35.3
8.2	29.9	11.2	37.8	7.4	35.8	6.6	42.8
8.2	25.4	9.7	38.8	7.4	33.7	5.2	27.0
6.8	19.4	9.7	35.8	7.4	30.9	5.2	32.2
6.8	20.2	8.2	33.3	5.7	19.3	5.2	30.7
5.2	21.3	8.2	31.7	5.7	20.8	4.1	28.3
5.2	21.9	6.6	29.4	4.6	18.1	4.1	28.6
3.8	13.1	6.6	25.0	4.6	18.4	3.2	27.3
3.8	13.9	4.2	20.4	3.6	18.2	3.2	25.0
5.5	21.3	4.2	22.4	3.6	17.9	4.6	29.0
3.7	16.9	2.6	17.3	2.5	14.0	3.0	22.4
3.7	17.1			2.5	14.0	3.0	20.8
3.7	16.8						

K(OBS) = 1.55 \pm 0.06K(OBS) = 2.15 \pm 0.02K(OBS) = 3.69 \pm 0.03K(OBS) = 4.09 \pm 0.04K(CO₂-CH₃CHO) = 30.9 \pm 5.(MILLISEC. TORR)⁻¹

TABLE 349

TEMPERATURE (K) = 450.0
 (PRESSURE (P) IN TORR AND TOWINVERSE (τ^{-1}) IN INVERSE MILLISEC.)

CARBONDIOXIDE-ACETALDEHYDE

X = 0.030		X = 0.059		X = 0.089		X = 0.113	
P	τ^{-1}	P	τ^{-1}	P	τ^{-1}	P	τ^{-1}
25.2	53.0	20.2	69.9	20.2	81.4	12.6	58.6
25.2	48.1	17.7	53.7	15.4	62.2	12.5	56.2
21.1	40.9	15.2	50.9	15.4	62.5	10.7	55.9
21.1	40.9	15.2	52.9	13.0	57.1	10.7	57.6
18.6	37.4	13.0	49.1	9.9	49.4	9.2	53.3
18.6	41.2	11.4	39.3	9.9	46.1	9.2	49.6
15.8	35.2	11.4	39.1	9.9	50.5	7.4	41.4
15.6	35.5	9.9	31.9	8.5	42.9	7.4	42.7
13.6	31.7	9.9	34.7	8.5	37.0	5.9	33.9
13.6	32.6	8.4	38.4	6.6	30.1	5.9	39.9
12.0	30.7	8.4	39.5	6.6	30.6	4.6	29.1
12.0	33.4	6.6	27.0	5.6	28.8	4.6	30.6
10.2	26.5	6.6	27.4	5.6	28.8	3.7	22.8
10.2	28.8	5.6	24.5	4.3	24.3	3.7	25.4
8.3	22.9	5.6	24.2	4.3	23.5	3.0	21.2
8.3	22.9	3.6	18.6	3.0	18.5	3.0	23.0
6.6	23.6	3.6	19.7	3.0	20.7	3.2	27.3
6.6	21.1	4.2	20.4	3.6	18.2	3.2	25.0
4.5	17.1	4.2	22.4	3.6	17.9	4.6	29.0
4.5	16.0	2.6	17.3	2.5	14.0	3.0	22.4
3.7	17.1			2.5	14.0	3.0	20.8
3.7	16.8						

K(OBS) = 1.51±0.04 K(OBS) = 2.80±0.01 K(OBS) = 3.63±0.02 K(OBS) = 4.04±0.02

K(CO2-CH3CHO) = 32.4±3.8 (MILLISEC.TORR)⁻¹

TABLE 35A

TEMPERATURE (K) = 375.0 CARBONDIOXIDE-ACETALDEHYDE
(PRESSURE (P) IN TORR AND TOWINVERSE (τ^{-1}) IN INVERSE MILLISEC.)

X = 0.030		X = 0.059		X = 0.089		X = 0.113	
P	τ^{-1}	P	τ^{-1}	P	τ^{-1}	P	τ^{-1}
25.1	50.0	19.9	68.4	15.0	70.0	11.8	70.9
25.1	50.5	19.9	69.2	13.8	67.2	11.8	74.5
21.0	43.2	16.6	59.6	13.8	77.0	9.0	50.6
21.0	43.1	16.6	50.2	10.7	48.0	7.2	52.5
16.8	38.0	13.1	42.5	10.7	50.4	7.2	56.6
16.8	37.6	13.1	42.8	9.4	43.4	7.2	51.4
13.6	34.3	11.0	35.2	9.4	50.6	5.8	38.5
13.6	30.0	11.0	36.2	7.8	42.5	5.8	44.8
11.1	24.5	8.7	34.3	7.8	41.5	4.8	41.2
11.1	26.8	8.7	32.4	6.2	36.1	4.8	35.8
9.0	24.9	8.7	33.4	6.2	38.1	3.8	29.3
9.0	23.9	7.3	26.6	5.1	30.8	3.8	25.1
7.4	27.3	7.3	27.9	5.1	30.8	3.2	30.9
7.4	18.1	5.9	24.4	4.1	29.5	3.2	28.3
5.9	20.0	5.8	22.2	4.1	30.4	2.6	25.0
5.9	18.8	4.9	18.9	3.4	22.6	2.5	24.0
5.0	16.6	4.9	21.8	3.4	22.7	3.2	27.3
5.0	20.1	3.9	21.3	2.7	23.2	3.2	25.0
4.1	16.1	3.9	23.4	2.7	25.5	4.5	29.0
4.1	15.8	3.9	22.1	2.5	14.0	3.0	22.4
3.7	17.1	2.6	17.5	2.5	14.0	3.0	20.8
3.7	16.8	2.6	17.7				

K(OBS) = 1.60±0.01 K(OBS) = 2.84±0.04 K(OBS) = 4.01±0.09 K(OBS) = 5.18±0.05

K(CO2-CH3CHO) = 42.4±1.2 (MILLISEC.TORR)⁻¹

TABLE 36

TEMPERATURE (K) = 300.0
(PRESSURE (P) IN TORR AND TOWINVERSE (τ^{-1}) IN INVERSE MILLISEC.)

CARBONDIOXIDE-ACETALDEHYDE

X = 0.030		X = 0.059		X = 0.089		X = 0.113	
P	τ^{-1}	P	τ^{-1}	P	τ^{-1}	P	τ^{-1}
24.2	59.8	21.0	77.1	18.8	115.5	16.6	110.7
24.2	58.6	21.0	73.8	18.8	108.8	14.6	93.5
20.2	48.6	18.2	70.3	16.6	83.8	12.3	96.8
20.0	41.5	18.2	71.1	16.6	95.5	12.8	89.9
16.5	46.7	15.9	66.0	14.3	64.0	11.2	70.4
16.5	46.0	15.9	63.0	14.3	97.2	9.9	70.6
13.5	38.3	14.2	50.4	12.8	63.6	9.9	65.9
13.6	36.4	14.2	49.5	12.8	83.0	8.6	66.8
11.3	31.5	12.0	53.5	11.3	57.2	8.6	75.8
11.3	29.1	12.0	45.4	11.3	56.9	7.6	60.8
9.3	22.4	9.8	38.1	9.8	54.6	7.5	60.9
9.3	26.7	9.8	38.3	9.8	51.7	6.8	48.0
7.8	22.1	8.0	37.1	8.7	48.0	6.8	48.0
7.8	20.6	8.0	36.6	8.7	42.4	5.9	55.5
7.8	21.8	6.6	34.1	7.7	47.0	5.9	55.7
6.4	25.4	6.6	30.8	7.7	37.7	4.7	46.2
6.4	28.7	5.5	24.7	6.6	41.3	4.7	44.7
6.4	27.3	5.5	29.2	6.6	44.0	4.7	49.1
5.4	18.1	4.6	25.0	5.8	34.8	4.6	29.0
5.4	23.3	4.6	22.1	5.8	38.7	3.0	22.4
5.4	17.4	2.6	17.5	2.5	14.0	3.0	20.8
4.4	18.2	2.6	17.7				
3.7	17.2						
3.7	18.7						

K(OBS) = 1.97±0.02

K(OBS) = 3.23±0.04

K(OBS) = 5.63±0.14

K(OBS) = 5.30±0.13

K(CO2-CH3CHO) = 48.6±10.7 (MILLISEC.TORR)⁻¹

Table 37

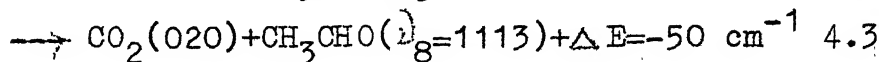
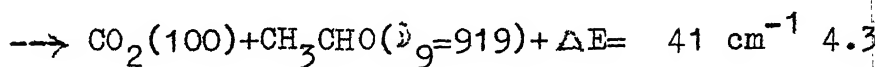
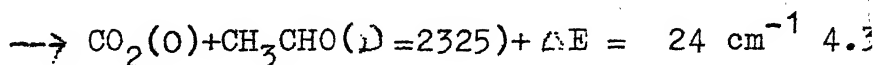
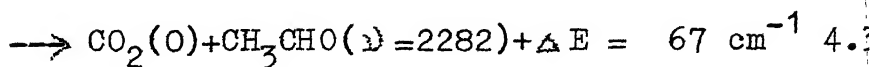
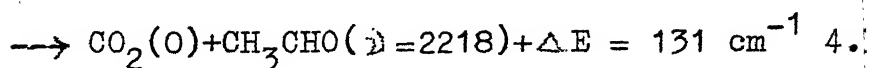
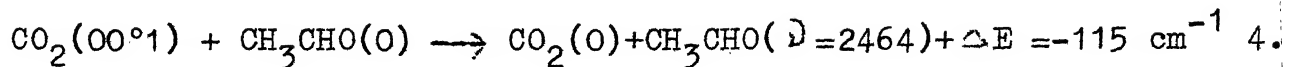
Rate constants, cross-sections and probabilities of energy transfer from $\text{CO}_2(00^{\circ}1)$ to CH_3CHO

$T^{\circ}\text{K}$	$K_{\text{CO}_2-\text{M}}(\text{ms}^{-1}\text{torr}^{-1})$	$\sigma \text{ \AA}^2$	$P_{\text{exp}} \times 10^2$
301	48.6 ± 10.7	0.28 ± 0.06	0.61 ± 0.134
375	42.4 ± 1.2	0.28 ± 0.01	0.594 ± 0.017
450	32.4 ± 3.8	0.23 ± 0.03	0.498 ± 0.059
525	30.9 ± 5.0	0.23 ± 0.04	0.504 ± 0.083
600	24.4 ± 3.1	0.20 ± 0.03	0.432 ± 0.055
650	26.5 ± 4.9	0.23 ± 0.04	0.488 ± 0.091

INTERPRETATION OF RESULTS

Among the seven molecules studied in the present work, Acetaldehyde is the least efficient in deactivating the $\text{CO}_2(00^{\circ}1)$ mode by collisions. The deactivation rates decrease as the temperature is increased. The negative temperature dependence of the deactivation rates may be ascribed to near-resonant V-V energy transfer processes. Based on the vibrational frequencies, tabulated by Shimonouchi⁴⁰ for the fundamental bands, and those of Evans and Bernstein⁶¹ and Morris⁶² for mixed and over-tone bands, it appears that a number of processes

contribute to the total deactivation rate. These are given below.



PROBABILITY CALCULATIONS

The calculation of energy transfer probabilities using SB theory has been carried out at different temperatures for all the processes shown above. In these calculations it is assumed that the contribution due to dipole-dipole interactions is dominant and the procedure followed to estimate the unknown transition moments is the same as before. The molecular constants used in these calculations are presented in Table 5 and Acetaldehyde molecule is approximated by a prolate symmetric top. The molecular diameter of CH_3CHO is assumed to be the same as that of CH_3OH as is done by Stephenson⁶⁸. The calculated probabilities are presented in Table 38. These probabilities show a negative temperature dependence for processes 4.32 and

Table 38

Calculated Energy Transfer probabilities* for different processes of $\text{CO}_2\text{-CH}_3\text{CHO}$ system

T°K	$p_{29} \times 10^{35}$	$p_{30} \times 10^{35}$	$p_{31} \times 10^{35}$	$p_{32} \times 10^{35}$	$p_{33} \times 10^{35}$	$p_{34} \times 10^{35}$
301	2.112	1.387	15.82	107.0	0.9502	0.3800
375	2.521	1.706	18.88	89.09	0.8892	0.4167
450	2.882	1.980	21.37	76.58	0.8179	0.4306
525	3.228	2.226	23.13	67.32	0.7504	0.4296
600	3.582	2.457	24.2	60.18	0.6902	0.42
650	3.871	2.636	21.37	56.51	0.6457	0.4138

* Values are obtained by assuming unity for the unknown transition dipole moments (squares) of M.

4.33 where ΔE is 24 and 41 cm^{-1} respectively, exhibit a maximum at around 600°K and 450°K for processes 4.31 and 4.34 as ΔE is increased to 67 and -50 respectively and finally shows a positive temperature dependence as ΔE is further increased to -115 and 131 cm^{-1} respectively for processes 4.29 and 4.30. No attempt has been made to estimate the contribution of short range forces to these processes. The experimentally derived probability for this system can be written as

$$P_{\text{exp}} = a_{\text{weak}} \sum_i p_i + a(\nu_9 \rightarrow 0) p_{33} + a(\nu_8 \rightarrow 0) p_{34} \quad 4.35$$

The first four processes 4.29-4.32 involve weak transitions and their coefficients are combined as in the case of $\text{C}_2\text{H}_4\text{O}$. The three transition moments in 4.35 are then obtained by the least squares method. The values obtained are

$$a_{\text{weak}} = 0.3 \times 10^{-39} \text{esu}^2 \text{cm}^2$$

$$a(\nu_9 \rightarrow 0) = 0.15 \times 10^{-37} \text{esu}^2 \text{cm}^2$$

$$a(\nu_8 \rightarrow 0) = 0.21 \times 10^{-37} \text{esu}^2 \text{cm}^2$$

The relative magnitudes of these numbers are in accord with the spectroscopic observation^{40,61,62} that $\nu_8 \rightarrow 0$ transition is strong, $\nu_9 \rightarrow 0$ is medium while the remaining four are weak.

COMMENTS

All the three molecules CO_2 , $\text{C}_2\text{H}_4\text{O}$ and CH_3CHO have the same molecular weight. However, they differ considerably in their rate of deactivation of $\text{CO}_2(2_3)$, Ethylene oxide being two times more efficient than Acetaldehyde. The higher rate of deactivation by $\text{C}_2\text{H}_4\text{O}$ is due to the two very strong fundamental bands at 892 and 877 cm^{-1} with high transition dipole moments. In Acetaldehyde, in addition to the four weak bands, the bands ν_8 and ν_9 designated as $\text{C}=\text{O}$ stretch and CH_3 rock are responsible for the deactivation. The latter two are characterised as only strong and medium respectively. Thus, the transition dipole moment squares in Acetaldehyde are much smaller than that in Ethylene oxide and hence the lower rate compared to Ethylene oxide.

$\text{CO}_2\text{-HCOOH}$

The rate of quenching of the $\text{CO}_2(00^01)$ mode in collisions with Formic acid has been studied at three different temperatures namely 301, 350 and 400°K at different compositions. It should be noted that due to the large deactivation rates only mixtures with less than 1.5% at 301°K and less than 5% at 400°K could be studied. For all the experimental runs the fluorescence decay is observed to be a single exponential.

The data is analysed along the same lines as for the $\text{CO}_2\text{-CH}_3\text{OH}$ system. The complete experimental data on $\text{CO}_2\text{-HCOOH}$ system is presented in Tables 39-41 at different temperatures. The temperature dependence of the deactivation rate constant $K_{\text{CO}_2\text{-HCOOH}}$ is shown in Fig.12. These rates along with the collision cross-sections and the energy transfer probabilities calculated using equations 2.4 and 2.5 are presented in Table 42 at different temperatures. However, it is shown below that because of dimer formation $K_{\text{CO}_2\text{-HCOOH}}$ obtained above can not be attributed to collisions between CO_2 and HCOOH .

Table 42

Rate constants, cross-sections and probabilities of energy transfer from $\text{CO}_2(00^01)$ to HCOOH

$T^\circ\text{K}$	$K_{\text{CO}_2\text{-M}}(\text{ms}^{-1}\text{torr}^{-1})$	$\frac{\sigma^2}{\text{\AA}}$	$P_{\text{exp}} \times 10^2$
301	336 ± 23	1.98 ± 0.14	3.52 ± 0.25
350	249 ± 50	1.58 ± 0.32	2.82 ± 0.56
400	140 ± 22	0.94 ± 0.15	1.69 ± 0.27

TEMPERATURE (K)= 400.0
 (PRESSURE (P) IN TORR AND TOWINVERSE (τ^{-1}) IN INVERSE MILLISEC.) CARBONDIOXIDE-FORMICACID

X = 0.050			X = 0.025			X = 0.014			X = 0.005			X = 0.010		
P	τ^{-1}	P	τ^{-1}	P	τ^{-1}	P	τ^{-1}	P	τ^{-1}	P	τ^{-1}	P	τ^{-1}	P
11.6	111.5	15.1	78.7	15.5	52.9	25.5	34.9	15.8	37.5	15.8	37.5	15.8	37.5	15.8
11.6	104.7	13.6	74.6	15.5	55.2	24.8	28.7	15.8	39.7	15.8	39.7	15.8	39.7	15.8
10.6	116.8	12.2	65.3	13.9	48.9	22.6	33.3	14.2	32.6	14.2	32.6	14.2	32.6	14.2
9.0	93.5	12.2	74.9	13.9	52.0	22.6	35.7	14.2	34.5	14.2	34.5	14.2	34.5	14.2
9.0	87.4	12.2	72.5	12.0	41.8	16.8	26.5	14.2	33.5	14.2	33.5	14.2	33.5	14.2
7.6	82.5	8.1	46.2	12.0	45.0	16.8	31.9	11.4	33.3	11.4	33.3	11.4	33.3	11.4
7.6	79.3	8.1	45.9	10.2	39.8	15.4	25.0	11.4	35.1	11.4	35.1	11.4	35.1	11.4
6.8	86.7	4.9	36.9	10.2	37.4	15.4	29.5	11.4	29.9	11.4	29.9	11.4	29.9	11.4
6.8	66.5	4.9	36.5	8.6	35.9	13.4	23.8	9.8	31.3	9.8	31.3	9.8	31.3	9.8
6.8	65.2	4.1	25.4	8.6	33.7	13.4	27.3	9.8	32.4	9.8	32.4	9.8	32.4	9.8
5.3	59.9	4.1	28.1	7.2	32.6	13.4	25.7	8.1	28.1	8.1	28.1	8.1	28.1	8.1
5.3	69.6	4.1	32.7	7.2	31.6	11.8	23.1	8.1	25.5	8.1	25.5	8.1	25.5	8.1
5.3	67.5	3.0	26.7	5.5	25.3	11.8	20.7	6.2	19.6	6.2	19.6	6.2	19.6	6.2
3.9	56.0	3.0	26.0	4.2	21.9	8.5	20.6	6.2	21.1	6.2	21.1	6.2	21.1	6.2
3.9	58.6	2.2	18.4	4.2	18.7	8.5	19.6	4.5	16.1	4.5	16.1	4.5	16.1	4.5
3.9	58.9	2.2	18.1	2.7	16.0	6.5	17.6	4.5	20.6	4.5	20.6	4.5	20.6	4.5
4.1	30.2	5.8	29.8	2.7	17.1	6.5	17.0	3.3	20.3	3.3	20.3	3.3	20.3	3.3
3.2	23.5	4.5	28.6	2.1	16.8	4.2	12.3	3.3	20.6	3.3	20.6	3.3	20.6	3.3
3.2	24.5	4.5	26.3	11.0	34.7	4.2	11.9	2.3	17.0	2.3	17.0	2.3	17.0	2.3
2.2	26.0	4.1	25.6	11.0	33.1			2.3	16.4	2.3	16.4	2.3	16.4	2.3
2.2	24.0	4.1	26.0	9.8	14.8			1.6	17.3	1.6	17.3	1.6	17.3	1.6
		4.1	24.8	9.8	15.7			1.6	19.3	1.6	19.3	1.6	19.3	1.6
		3.3	16.5	8.4	21.3									
		3.3	17.6	8.4	26.9									
				8.4	22.5									

 $K(\text{OBS}) = 7.12 \pm 0.16$ $K(\text{OBS}) = 4.77 \pm 0.07$ $K(\text{OBS}) = 2.94 \pm 0.00$ $K(\text{OBS}) = 0.98 \pm 0.05$ $K(\text{OBS}) = 1.51 \pm 0.05$
 $K(\text{CD}_2\text{-HCCOH}) = 140 \pm 22$ (MILLISEC.TORR) $^{-1}$

TABLE 40

TEMPERATURE (K)= 350.0 CARBON DIOXIDE-FORMIC ACID
(PRESSURE (P) IN TORR AND TOWINVERSE (τ^{-1}) IN INVERSE MILLISEC.)

X = 0.025			X = 0.014			X = 0.010			X = 0.005		
P	τ^{-1}	P	P	τ^{-1}	P	P	τ^{-1}	P	P	τ^{-1}	P
13.6	105.4	17.9	68.3	47.8	16.4	16.4	47.8	16.4	16.4	35.2	16.4
13.6	106.6	17.9	60.4	52.6	16.4	16.4	52.6	16.4	16.4	34.7	16.4
12.7	95.4	15.9	56.0	39.2	12.2	12.2	39.2	15.3	15.3	30.9	15.3
12.7	98.1	14.4	50.2	42.8	12.2	12.2	42.8	15.3	15.3	30.2	15.3
13.7	92.0	14.4	56.1	34.1	12.2	12.2	34.1	13.8	13.8	28.4	13.8
10.7	90.7	13.2	58.3	42.6	10.6	10.6	42.6	13.8	13.8	29.0	13.8
9.4	65.7	13.2	55.9	35.7	10.6	10.6	35.7	12.3	12.3	29.1	12.3
9.4	63.5	12.0	43.1	31.4	7.4	7.4	31.4	12.3	12.3	25.9	12.3
6.2	52.9	12.0	48.6	29.7	7.4	7.4	29.7	10.4	10.4	24.3	10.4
6.2	53.3	10.7	44.6	27.5	6.5	6.5	27.5	10.4	10.4	24.0	10.4
5.0	41.3	10.7	43.0	20.1	6.5	6.5	20.1	8.1	8.1	18.9	8.1
5.0	39.0	9.6	46.2	22.2	4.5	4.5	22.2	8.1	8.1	19.4	8.1
4.2	45.8	9.6	48.8	17.7	4.5	4.5	17.7	7.0	7.0	21.0	7.0
4.2	48.2	7.4	37.2	17.9	3.2	3.2	17.9	7.0	7.0	20.1	7.0
4.7	31.7	7.4	36.8	16.4	3.2	3.2	16.4	5.2	5.2	13.7	5.2
4.1	29.2	5.8	29.2	16.8	3.2	3.2	16.8	5.2	5.2	12.6	5.2
4.1	30.2	5.8	29.8	34.7	2.1	2.1	34.7	4.0	4.0	13.1	4.0
3.2	23.5	4.5	28.6	33.1	2.1	2.1	33.1	4.0	4.0	14.9	4.0
3.2	24.5	4.5	26.3	14.8	11.0	11.0	14.8				
2.2	26.0	4.1	25.6	15.7	9.8	9.8	15.7				
2.2	24.0	4.1	26.0	21.3	9.8	9.8	21.3				
		3.3	16.5	26.9	8.4	8.4	26.9				
		3.3	17.6	22.5	8.4	8.4	22.5				

K(OBS)= 6.79±0.35 K(OBS)= 2.71±0.05 K(OBS)= 2.38±0.01 K(CBS)= 1.52±0.03

K(CO2-HCOOH)= 249±50 (MILLISEC.TORR)⁻¹

TABLE 41

CARBONDIOXIDE-FORMICACID

TEMPERATURE (K) = 301.0
(PRESSURE (P) IN TCRR AND TOWINVERSE (τ^{-1}) IN INVERSE MILLISEC.)

X = 0.014		X = 0.010		X = 0.005	
P	τ^{-1}	P	τ^{-1}	P	τ^{-1}
14.7	63.9	15.1	37.5	21.0	24.0
14.7	67.0	15.1	36.0	21.0	22.3
12.0	66.0	13.8	43.4	19.8	26.8
12.0	58.5	12.8	45.8	19.8	27.5
12.0	55.4	12.1	39.3	17.9	32.7
10.1	50.9	12.1	38.5	17.9	33.7
10.1	48.4	12.1	40.1	16.0	35.8
8.1	45.2	10.4	26.9	16.0	33.4
8.1	46.0	10.4	28.4	14.2	19.3
6.5	46.4	10.4	30.0	14.2	19.0
5.0	37.7	8.8	38.0	14.2	15.7
5.0	39.4	8.8	37.7	13.5	20.5
5.0	37.3	8.8	30.8	13.5	19.7
4.7	32.3	7.2	22.0	12.2	20.6
4.7	31.7	7.2	24.4	12.2	24.4
4.1	29.2	6.0	29.0	12.2	34.2
4.1	30.2	6.0	27.2	11.0	26.9
3.2	23.5	4.9	20.3	11.0	26.5
3.2	24.5	4.9	21.1	11.0	34.7
2.2	26.0	4.1	25.6	11.0	33.1
2.2	24.0	4.1	26.0	9.8	14.8
2.2		4.1	24.8	9.8	15.7
		3.3	16.5	8.4	21.3
		3.3	17.6	8.4	26.9
				8.4	22.5

K(CBS) = 2.50 ± 0.00

K(OBS) = 1.88 ± 0.06

K(CBS) = 0.35 ± 0.02

K(CO2-HCCFH) = 336 ± 23.

(MILLISEC.TCRR) = 1

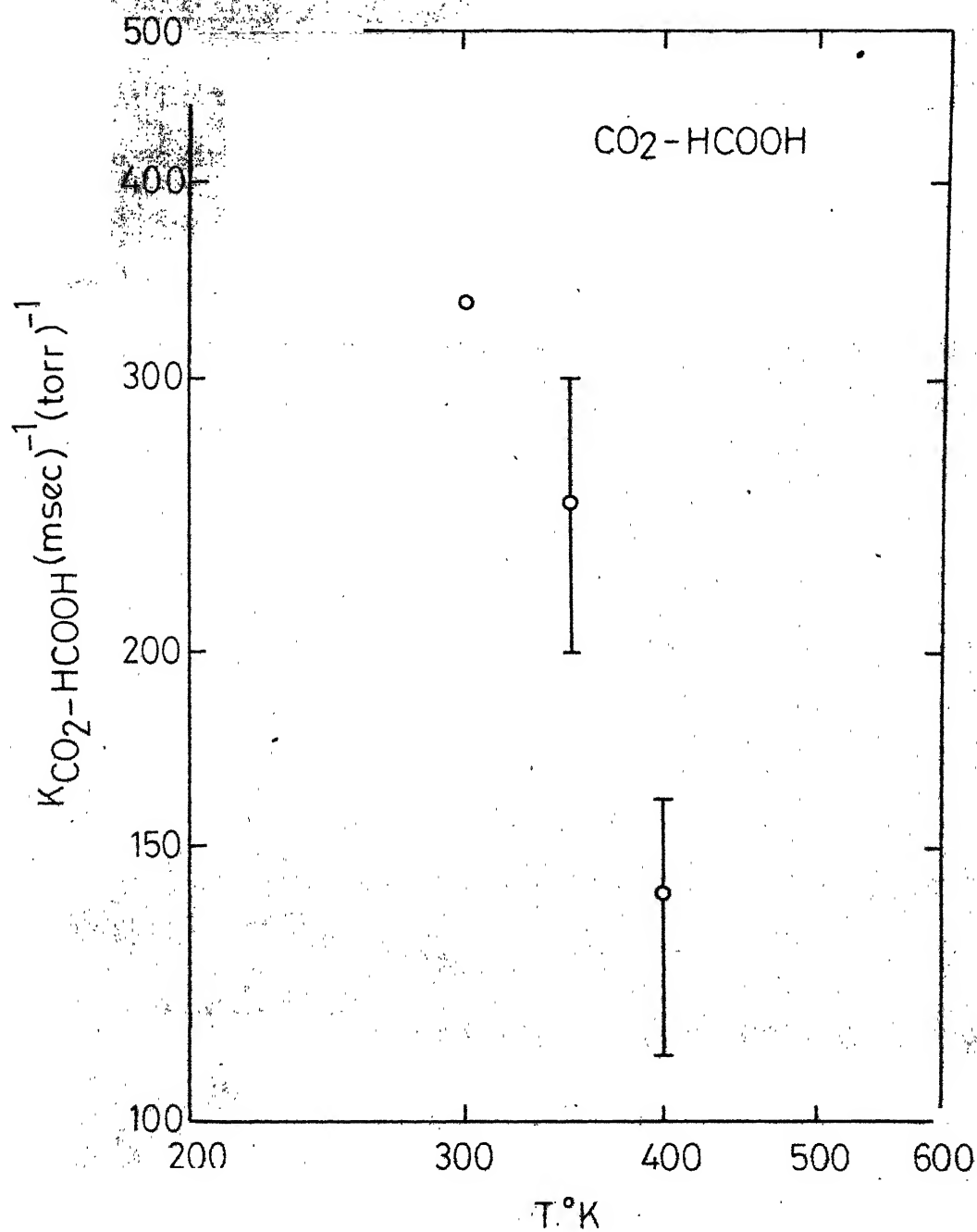
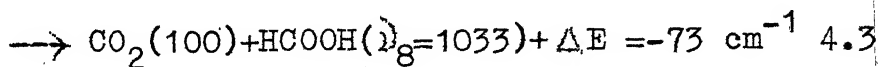
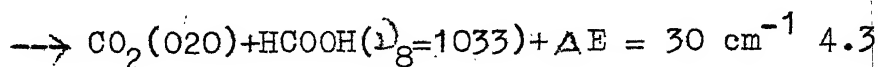
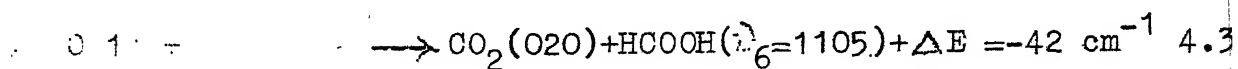
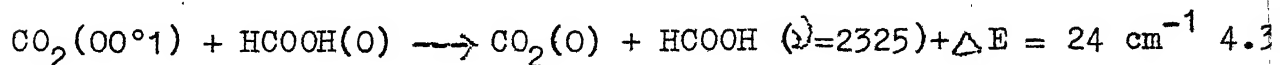


Fig. 12. - Temperature dependence of $K_{\text{CO}_2\text{-HCOOH}}$.

INTERPRETATION OF RESULTS

In the following we first ignore the dimer formation. The deactivation rate of the $\text{CO}_2(00^{\circ}1)$ mode in collisions with Formic acid (HCOOH) is about two orders of magnitude higher than that with CO_2 itself at room temperature and the rates decrease as the temperature increases. This again suggests that near-resonant V-V energy transfer processes could play the dominant role in the deactivation of $\text{CO}_2(00^{\circ}1)$ mode. The fundamental vibrational frequencies of Formic acid are tabulated by Shimonouchi⁴⁰. There is no fundamental band to quench the $\text{CO}_2(00^{\circ}1)$ to the ground state, but there is a weak mixed band at $2325\text{ cm}^{-1}(63)$. The $\text{CO}_2(00^{\circ}1)$ can also be deactivated by a strong fundamental band at $1105\text{ cm}^{-1}(\nu_6)$ identified as the C-O stretch band and a weak band at $1033\text{ cm}^{-1}(\nu_8)$ through the $\nu_3 \rightarrow 2\nu_2$ and $\nu_3 \rightarrow \nu_1$ transitions in CO_2 . Hence the likely processes occurring in the deactivation of $\text{CO}_2(00^{\circ}1)$ level are



No attempt has been made to obtain the dipole moments of the transitions of HCOOH involved in the above processes for the following reasons.

1. The experiments could not be carried out beyond 425°K, at which temperature Formic acid starts dissociating.
2. More importantly, even within the temperature range studied, part of the Formic acid exists in dimeric form because of association. The associative nature of this molecule is well studied⁶⁴ and it has been observed that the dissociation constant K of the dimers is related to the temperature as

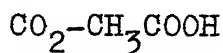
$$\text{Log } K = 10.755 - 3090/T \quad 4.40$$

in the temperature range 283-430°K. Here K is in mmHg and T is in °K. Simple calculation from this relation revealed that at room temperature about 64% of the Formic acid is present in the dimeric form and dimer concentration falls to about 1.0% at 400°K at a total pressure of 5 torr.

Further, the dimer concentration increases somewhat with increasing pressure. Due to this pressure dependence of the concentration of dimers the determination of $(P \tau_{\text{coll}})^{-1}$ from the graph of τ^{-1} versus P is not reliable.

Evidently the observed decay constant K_{obs} represents the deactivation of $\text{CO}_2(00^01)$ mode by monomers as well as dimers and their individual rate contributions could not be separated. In view of this, the value of $K_{\text{CO}_2\text{-HCOOH}}$ obtained by extrapolation of K_{obs} to 100% of HCOOH cannot be attributed to collisions between CO_2 and HCOOH . Thus

the processes 4.36 - 4.39 represents the deactivation of $\text{CO}_2(00^{\circ}1)$ only due to collisions occurring in the mixture with HCOOH monomers. To get a complete picture of the deactivation processes the energy exchange between CO_2 and HCOOH dimers must also be included.



The collisional deactivation of the $\text{CO}_2(00^{\circ}1)$ mode with Acetic acid has been studied at different compositions and several temperatures in the range of 300-750°K. As in the case of the previous systems the fluorescence decay is a single exponential. The complete experimental data has been presented in Tables 43-50 for different temperatures. The deactivation rate constant has been estimated from the fluorescence signals as for the other systems. The temperature dependence of this deactivation rate constant $K_{\text{CO}_2\text{-CH}_3\text{COOH}}$ is presented in Fig.13. The collision cross-sections and the energy transfer probabilities calculated using equations 2.4 and 2.5 at different temperatures are presented in Table 51 along with the deactivation rate constant. As in the case of Formic acid, there is a difficulty in the interpretation of $K_{\text{CO}_2\text{-CH}_3\text{COOH}}$ also, though only at temperatures below 500°K.

TABLE 4B

TEMPERATURE (K) = 750.0

CARBONDIOXIDE-ACETIC ACID

(PRESSURE (P) IN TORR AND TOWINVERSE (T) IN INVERSE MILLISEC.)

X = 0.010		X = 0.025		X = 0.050		X = 0.075	
P	T	P	T	P	T	P	T
16.0	63.6	14.6	57.5	12.5	67.9	12.2	96.6
16.0	79.4	14.6	48.6	12.5	62.8	12.2	84.7
14.6	70.6	13.8	46.3	11.4	69.2	11.1	79.0
14.6	66.6	13.8	48.1	11.4	61.2	11.1	91.4
13.2	47.4	12.2	45.7	10.2	57.2	9.8	79.7
13.2	48.3	12.2	48.2	10.2	52.2	9.8	77.8
13.2	45.0	10.8	44.0	9.1	55.7	8.1	66.9
12.1	46.7	10.8	50.1	8.9	43.4	8.1	73.7
12.1	53.0	9.8	49.1	8.0	59.2	6.7	68.1
10.6	59.5	9.8	45.4	8.0	43.8	6.7	63.0
10.6	55.5	8.2	35.0	6.9	53.9	5.6	63.3
9.0	45.0	8.2	41.6	6.9	54.4	5.6	49.0
9.0	35.6	6.9	36.8	5.4	36.2	5.6	51.2
7.4	31.6	6.9	33.2	5.4	40.0	4.5	42.2
7.4	33.2	5.6	31.4	4.3	33.2	4.5	42.4
5.0	22.7	5.6	32.2	4.3	29.7	3.3	36.9
5.0	19.8	4.0	26.3	3.2	24.1	3.3	32.2
4.0	24.2	4.0	27.8	3.2	26.5	1.8	27.5
4.0	13.3	2.5	23.0	1.8	18.6	1.8	25.0
2.4	15.8	2.5	17.8	1.8	19.3	2.7	27.2
2.4	15.1	4.4	26.3	2.8	35.2	2.7	29.6
3.2	12.8	4.4	24.8			2.7	30.2
		3.4	23.2				
		3.4	20.8				
		2.0	16.3				
		2.0	17.1				

K(CBS) = 4.00±0.06

K(CBS) = 2.49±0.16

K(CBS) = 4.36±0.06

K(CBS) = 6.31±0.11

K(CC2-CH3CCCH) = 45.8±26.7 (MILLISEC.TORR)⁻¹

TABLE 44

TEMPERATURE (K) = 700.0 CARBON DIOXIDE-ACETIC ACID
PRESSURE (P) IN TORR AND TOWINVERSE (τ^{-1}) IN INVERSE MILLISEC.

X = 0.010		X = 0.025		X = 0.050		X = 0.075	
P	τ^{-1}	P	τ^{-1}	P	τ^{-1}	P	τ^{-1}
15.4	73.5	20.2	91.0	21.6	94.4	12.6	85.5
15.4	55.4	15.7	71.3	19.8	78.9	12.6	95.9
13.6	53.4	15.7	68.3	19.8	76.8	11.1	79.1
13.8	50.0	13.9	72.7	15.4	63.8	11.1	66.1
12.7	33.2	13.9	71.2	15.4	72.2	11.1	68.2
12.7	42.0	12.4	63.2	13.8	73.0	10.1	66.3
12.7	41.1	12.4	72.7	13.8	65.3	10.1	84.2
11.6	44.3	10.3	39.6	11.8	61.3	8.9	58.3
11.6	43.7	10.3	52.9	11.8	50.7	8.9	43.6
10.7	38.7	10.1	79.7	10.0	42.8	8.6	47.9
10.7	34.0	8.5	37.8	10.0	55.0	8.6	43.1
9.0	33.5	8.5	39.0	7.6	43.0	6.5	31.5
9.0	30.3	6.5	33.0	7.6	40.6	6.5	45.3
7.5	27.5	6.5	33.9	6.2	41.2	5.6	34.0
7.5	28.4	4.8	24.2	6.2	37.9	5.6	38.1
6.7	29.8	4.8	24.3	4.2	33.1	4.6	36.2
6.7	33.3	3.2	20.2	4.2	27.9	4.6	38.3
5.0	20.0	3.2	21.3	3.8	44.6	3.8	34.0
5.0	17.0	1.7	16.2	3.8	44.2	3.8	28.0
3.2	13.7	1.7	15.2	2.8	23.4	2.7	27.2
3.2	22.0	4.4	26.3	2.8	35.2	2.7	29.6
3.2	12.8	4.4	24.8			2.7	30.2
		3.4	23.2				
		3.4	20.8				
		2.0	16.3				
		2.0	17.1				

OBS) = 3.38±0.03 K(OBS) = 4.43±0.02 K(OBS) = 3.31±0.08 K(OBS) = 5.86±0.20

K(CO2-CH3COOH) = 39.7±23.9 (MILLISEC.TORR)⁻¹

TABLE 45

TEMPERATURE (K) = 650.0
(PRESSURE (P) IN TORR AND TOWINVERSE (τ^{-1}) IN INVERSE MILLISEC.)

Y = 0.010		X = 0.025		X = 0.050		X = 0.075	
P	τ^{-1}	P	τ^{-1}	P	τ^{-1}	P	τ^{-1}
16.0	54.3	12.5	54.1	11.7	91.4	11.4	94.4
16.0	45.7	12.5	59.0	10.7	71.0	10.3	88.1
14.2	49.4	11.3	47.0	9.8	79.3	10.3	93.7
14.2	48.7	11.3	60.8	8.3	70.5	9.5	98.7
12.6	45.0	10.0	46.2	8.8	71.3	9.5	82.9
12.4	38.2	10.0	45.2	7.7	60.0	8.6	93.7
11.1	41.9	8.7	46.2	7.7	57.9	8.5	83.0
11.1	41.2	8.7	42.7	6.2	45.2	7.9	89.1
9.6	35.9	7.6	35.5	6.2	47.0	7.9	79.8
9.6	32.6	6.3	38.7	5.1	35.6	6.1	74.8
7.0	24.3	6.3	35.4	5.1	43.5	6.1	62.8
7.3	21.0	5.2	34.1	4.0	33.3	4.6	58.7
6.2	22.7	5.2	34.9	4.0	36.5	4.6	54.2
6.2	22.0	4.0	22.3	2.8	23.2	3.6	44.1
4.3	15.7	4.0	22.8	2.8	21.5	3.5	47.3
4.3	20.3	2.8	17.5	1.9	23.7	2.3	33.2
3.2	15.8	2.8	18.8	1.9	20.8	2.3	33.2
3.2	14.0	2.8	18.1	3.8	44.6	1.8	27.6
2.0	12.9	1.7	16.2	3.8	44.2	3.1	44.0
2.0	11.8	1.7	15.2	2.8	28.4	2.2	32.2
		4.4	26.3	2.8	35.2	2.2	36.7
		4.4	24.8				
		3.4	23.2				
		3.4	20.8				
		2.0	16.3				
		2.0	17.1				

$K(OBS) = 2.95 \pm 0.02$ $K(OBS) = 3.88 \pm 0.02$ $K(OBS) = 7.04 \pm 0.07$ $K(OBS) = 7.22 \pm 0.21$
 $K(CO_2-CH_3COOH) = 78.9 \pm 20.$ (MILLISEC. TORR)⁻¹

TEMPERATURE (K) = 600.0 CARBONDIOXIDE-ACETIC ACID
 (PRESSURE (P) IN TORR AND TOWINVERSE (τ^{-1}) IN INVERSE MILLISEC.)

T	X = 0.010		X = 0.025		X = 0.050		X = 0.075	
	P	τ^{-1}	P	τ^{-1}	P	τ^{-1}	P	τ^{-1}
22.0	12.9	62.9	12.9	58.7	9.9	100.4	8.3	86.3
19.0	12.9	53.3	12.9	63.6	9.9	89.1	8.3	93.6
19.0	11.9	53.5	11.9	58.0	9.3	87.7	7.6	92.1
18.0	11.9	40.0	11.9	60.0	8.2	82.4	7.6	82.1
13.0	11.5	42.3	11.5	54.0	8.2	86.7	6.3	79.3
12.0	11.5	36.5	11.5	59.2	7.6	68.7	6.8	81.0
12.0	11.5	35.4	11.5	59.3	5.6	57.2	6.1	72.3
13.0	10.5	31.0	10.5	59.8	5.6	53.4	6.1	69.0
10.0	10.5	30.6	10.5	53.0	4.7	54.0	5.1	73.9
9.0	9.6	30.7	9.6	47.8	4.7	51.9	5.1	63.7
9.0	9.6	28.2	9.6	45.0	3.9	41.7	4.5	58.5
6.0	9.0	23.5	9.0	44.6	3.9	39.8	4.5	56.6
6.0	9.0	22.7	9.0	45.4	2.9	36.0	3.7	54.3
4.0	8.0	16.8	8.0	43.8	2.9	33.9	3.7	45.5
4.0	8.0	16.7	8.0	41.4	1.8	22.1	2.9	35.0
2.0	8.0	13.2	8.0	41.4	1.8	22.4	2.9	39.1
2.0	6.8	8.9	6.8	43.9	4.6	42.6	1.3	35.6
2.0	6.8	18.0	6.8	34.9	3.8	44.6	1.3	27.6
2.0	5.5	18.9	5.5	32.1	3.8	44.2	3.1	44.0
	5.5		5.5	27.0	2.8	28.4	2.2	32.2
	4.4		4.4	26.3	2.8	35.2	2.2	36.7
	4.4		4.4	24.8				
	3.4		3.4	23.2				
	3.4		3.4	20.8				
	2.0		2.0	16.3				
	2.0		2.0	17.1				

K(OBS) = 2.47±0.02 K(OBS) = 4.30±0.02 K(OBS) = 8.85±0.07 K(OBS) = 9.48±0.22

K(CO2-CH3COOH) = 118±26 (MILLISEC.TORR)⁻¹

TABLE 487

TEMPERATURE (K) = 550.0
(PRESSURE (P) IN TORR AND TOWINVERSE (T⁻¹) IN INVERSE MILLISEC.)

CARBON DIOXIDE-ACETIC ACID

X = 0.010		X = 0.025		X = 0.050		X = 0.075	
P	T ⁻¹	P	T ⁻¹	P	T ⁻¹	P	T ⁻¹
12.5	41.2	10.9	36.0	11.5	96.1	10.0	95.3
12.5	49.7	9.5	27.9	11.5	102.9	10.0	128.1
11.1	41.9	9.5	27.0	10.4	55.2	8.7	86.5
11.1	41.2	8.1	23.0	10.4	67.1	8.7	82.2
10.2	40.4	8.1	27.1	10.4	65.5	8.2	113.0
10.2	35.8	7.0	22.8	9.4	58.6	8.2	106.3
8.9	32.1	7.0	22.2	9.4	49.1	7.0	103.3
7.6	27.1	6.1	18.6	8.5	67.9	7.0	102.6
7.6	24.7	6.1	17.4	8.5	68.3	6.3	94.5
5.3	21.8	5.0	20.4	7.4	61.6	6.3	85.6
5.3	19.8	5.0	20.8	7.4	63.3	5.5	66.0
4.1	16.1	3.8	18.7	6.5	52.9	5.6	81.2
4.1	17.1	3.8	16.7	6.5	50.3	5.5	79.2
3.2	19.3	3.1	17.2	5.4	50.3	4.8	69.6
3.2	19.1	3.1	18.3	5.4	53.9	4.8	71.5
2.5	13.2	2.2	10.7	4.6	40.0	4.1	50.8
2.5	8.9	2.2	13.4	4.6	42.6	4.1	56.3
2.6	18.0	2.4	18.6	3.8	44.6	3.1	40.2
2.5	18.9			3.8	44.2	3.1	44.0
				2.8	28.4	2.2	32.2
				2.8	35.2	2.2	36.7

K(OBS) = 3.29 ± 0.07 K(OBS) = 2.07 ± 0.01 K(OBS) = 5.22 ± 0.03 K(OBS) = 10.07 ± 0.12

K(CO2-CH3COOH) = 109 ± 36 (MILLISEC. TORR)⁻¹

TABLE 48

TEMPERATURE (K) = 500.0 CARBON DIOXIDE-ACETIC ACID
 (PRESSURE (P) IN TORR AND TOWINVERSE (τ^{-1}) IN INVERSE MILLISEC.)

ρ	$X = 0.010$	τ^{-1}	P	$X = 0.025$	τ^{-1}	P	$X = 0.050$	τ^{-1}	P	$X = 0.075$	τ^{-1}
15.0	40.7	12.7	63.2	7.9	73.4	7.8	112.4				
15.0	44.8	12.7	62.0	7.9	64.4	7.8	113.3				
13.5	34.8	11.2	50.6	7.9	68.9	7.2	112.0				
13.5	36.7	11.2	39.7	7.0	57.5	7.2	97.2				
12.0	35.5	9.9	36.1	7.0	54.6	6.7	102.5				
12.0	33.4	9.9	33.5	6.1	56.7	6.7	113.6				
10.9	27.1	8.6	29.8	5.4	47.3	6.2	99.9				
9.1	23.4	8.6	41.9	5.4	55.1	6.2	99.3				
9.1	29.2	6.4	29.2	4.8	40.2	5.4	78.6				
8.3	24.9	6.4	33.6	4.8	50.8	5.4	86.8				
8.3	24.3	5.1	25.6	4.5	47.3	5.0	73.4				
8.3	22.8	5.1	25.5	4.5	39.2	5.0	80.8				
7.5	25.7	4.0	21.8	4.0	43.3	4.0	71.4				
7.5	21.4	4.0	29.2	4.0	43.7	4.0	66.7				
5.4	19.0	3.2	26.5	3.0	39.4	3.3	52.0				
3.9	18.3	3.2	22.6	3.0	33.4	3.3	58.3				
3.2	20.4	2.4	14.1	2.2	24.7	2.4	41.7				
2.6	18.0	2.4	18.6	2.2	24.6	2.4	43.7				
2.6	18.9			1.6	30.1	1.5	34.3				
				1.6	26.5	1.6	31.1				

K(OBS) = 2.51 ± 0.05

K(OBS) = 3.44 ± 0.03

K(OBS) = 6.52 ± 0.04

K(OBS) = 13.38 ± 0.12

K(CO2-CH3COOH) = 156 ± 33 (MILLISEC. TORR)⁻¹

TABLE 69

TEMPERATURE (K) = 400.0

CARBON DIOXIDE-ACETIC ACID
(PRESSURE (P) IN TORR AND TOWINVERSE (τ^{-1}) IN INVERSE MILLISEC.)

X = 0.010		X = 0.025		X = 0.050		X = 0.075	
P	τ^{-1}	P	τ^{-1}	P	τ^{-1}	P	τ^{-1}
14.0	40.4	12.3	90.0	9.1	195.3	6.4	118.4
16.0	35.6	12.3	92.3	9.1	173.3	6.4	113.5
14.0	32.6	11.1	81.2	8.2	147.7	3.7	75.7
14.0	32.5	11.1	87.8	8.2	151.1	3.7	69.8
12.0	33.3	8.1	59.9	7.9	119.6	2.4	52.7
12.0	32.3	8.1	67.4	4.9	75.9	2.4	56.2
12.0	34.3	7.3	55.8	4.9	78.6	1.6	40.3
10.0	30.0	7.3	66.7	3.8	78.1	1.6	36.2
10.0	31.5	4.8	42.9	3.8	83.2		
8.0	25.5	4.8	46.7	3.0	54.0		
8.0	23.0	3.2	41.6	3.0	54.4		
6.5	23.8	3.2	36.4	2.0	45.8		
6.4	22.0	2.1	27.2	1.2	46.5		
5.4	22.6	2.1	30.2	1.2	39.1		
5.4	19.0						
3.0	18.3						
3.0	20.4						
2.6	18.0						
2.6	18.9						

K(OBS) = 1.50 ± 0.04

K(OBS) = 5.98 ± 0.02

K(OBS) = 17.06 ± 0.42

K(OBS) = 15.92 ± 0.49

K(CO2-CH3COOH) = 239 ± 81 (MILLISEC.TORR)⁻¹

TABLE 29

TEMPERATURE (K) = 301.0 CARBON DIOXIDE-ACETIC ACID
(PRESSURE (P) IN TORR AND TOWINVERSE (τ^{-1}) IN INVERSE MILLISEC.)

X = C.C10		X = 0.025	
P	τ^{-1}	P	τ^{-1}
3.7	20.6	10.5	124.0
3.7	17.9	10.5	164.0
2.8	19.4	9.6	130.9
2.8	16.7	9.6	149.6
		8.7	142.5
		8.7	123.5
		7.9	118.8
		7.9	114.7
		7.2	105.3
		7.2	102.4
		6.2	115.9

K(OBS) = 1.36 \pm 1.53K(OBS) = 10.09 \pm 1.74K(CO2-CH3COOH) = 405 \pm 152 (MILLISEC.TORR) $^{-1}$

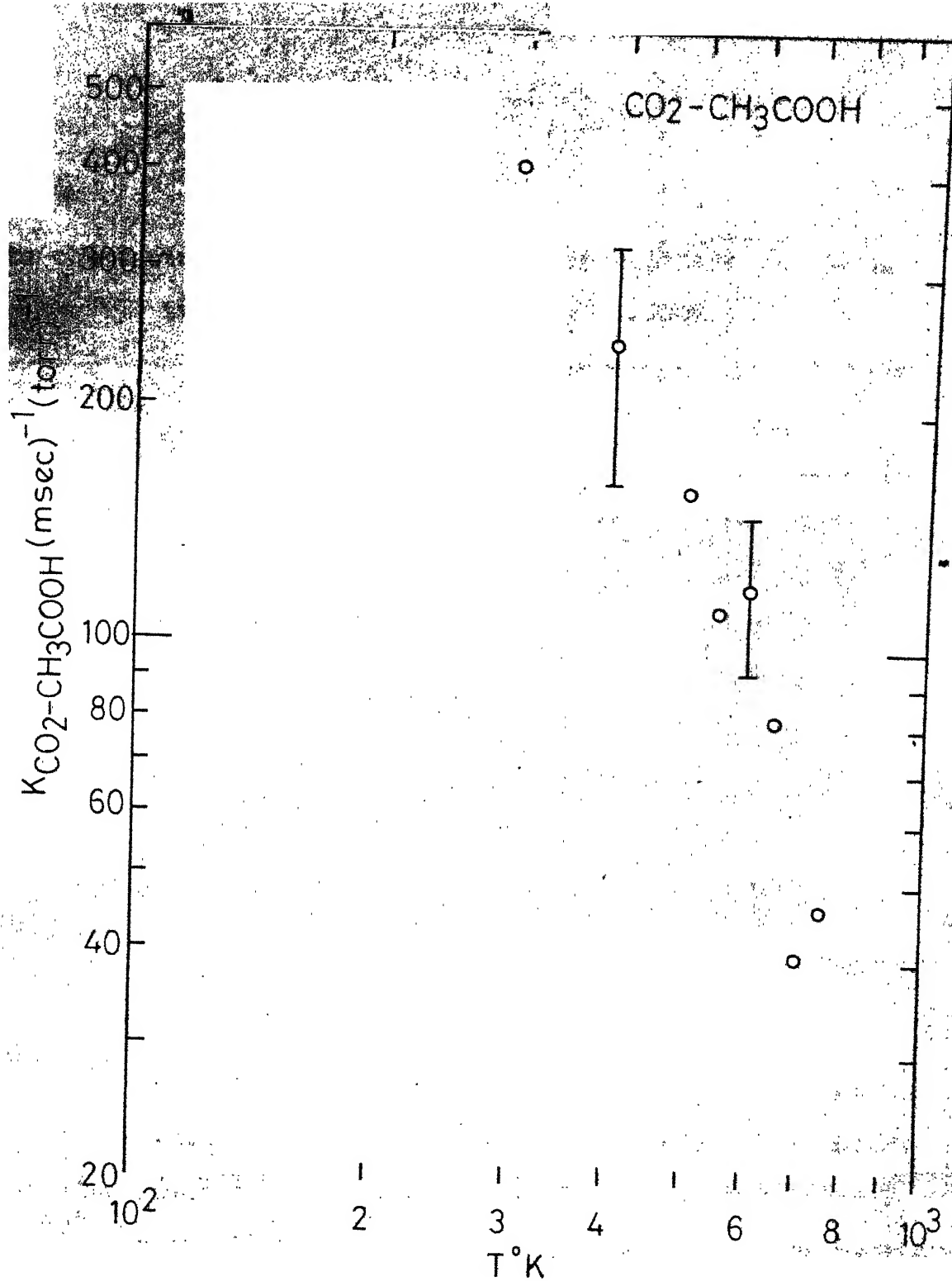


Fig. 13 - Temperature dependence of $K_{\text{CO}_2\text{-CH}_3\text{COOH}}$.

Table 51

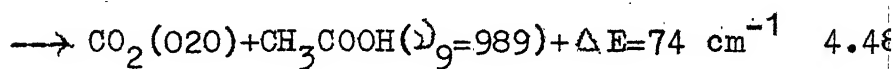
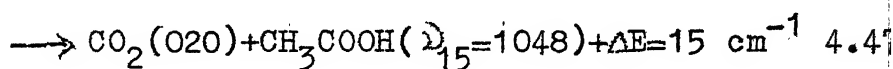
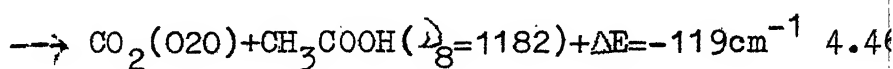
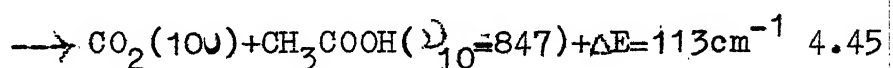
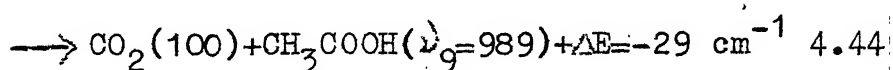
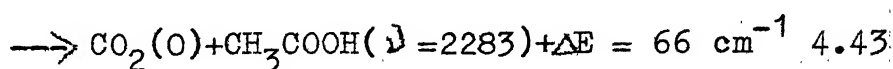
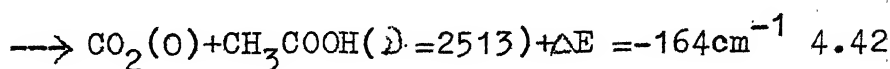
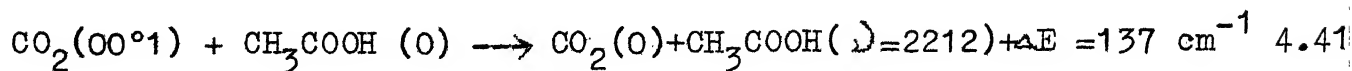
Rate constants, cross-sections and probabilities of energy transfer from $\text{CO}_2(00^{\circ}1)$ to CH_3COOH

$T^{\circ}\text{K}$	$K_{\text{CO}_2-\text{M}}(\text{ms}^{-1}\text{torr}^{-1})$	$\sigma \text{ \AA}^2$	$P_{\text{exp}} \times 10^2$
301	405 ± 152	2.47 ± 0.93	4.18 ± 1.57
400	239 ± 81	1.68 ± 0.57	2.85 ± 0.96
500	156 ± 33	1.23 ± 0.26	2.08 ± 0.44
550	109 ± 36	0.89 ± 0.3	1.52 ± 0.5
600	118 ± 26	1.02 ± 0.22	1.72 ± 0.37
650	78.9 ± 20.0	0.70 ± 0.18	1.2 ± 0.3
700	39.7 ± 23.9	0.37 ± 0.22	0.62 ± 0.38
750	45.8 ± 26.7	0.44 ± 0.23	0.74 ± 0.04

INTERPRETATION OF RESULTS

Again we first ignore dimer formation in this molecule also. The magnitude and the temperature dependence of the deactivation rates for this system are similar to those for Formic acid. So, as in the case of Formic acid, near-resonant processes must be dominant in the deactivation of the CO_2 asymmetric mode by Acetic acid molecules. The vibrational frequencies of the fundamental bands of Acetic acid are reported by Shimanouchi⁴⁰

and those of the mixed and overtone bands by Wilmschurt⁶⁵. Based on these frequencies, the following processes may be expected to cause the deactivation of the $\text{CO}_2(00^01)$ mode.



All the three mixed mode transitions of Acetic acid in processes 4.41 and 4.42 and 4.43 are weak. Even though 4.41 and 4.42 involve a large energy mismatch, they can not be dropped because the $\nu_3 \rightarrow 0$ transition of CO_2 is very strong and their contribution might be comparable to that of 4.43. The $\nu_9 \rightarrow 0$ transition in 4.44 and 4.45 is of medium strength. Even though the CO_2 transitions involved in these are less intense, these processes could not be dropped because the energy mismatches are not large. The transition $\nu_{10} \rightarrow 0$ in process 4.45

is weak with a large energy mismatch and a less intense CO_2 transition. Hence this process can be neglected. Process 4.46 involving larger energy mismatch cannot be dropped since the $\nu_{18} \rightarrow 0$ (C-O stretch) transition is strong. The transition $\nu_{15} \rightarrow 0$ in process 4.47 is weak but can not be dropped because this involves a small energy mismatch. Hence except process 4.45, all the others are likely to contribute to the total deactivation.

No attempt has been made to estimate the transition moments for this system also because of the following reasons.

1. A large number of processes are involved in the deactivation of $\text{CO}_2(00^01)$.
2. Acetic acid, like Formic acid, is highly associative at room temperature and the dissociation constant of dimers is given by^{66,67}

$$\text{Log } K = 11.789 - 3590/T \quad 4.49$$

in the temperature range of 298-728°K,

where K is the dimer dissociation constant in mmHg and T is the temperature in °K.

At room temperature and a pressure of 5 torr about 82% of this acid exists as dimers and this concentration falls to 1.5% at 400°K and is negligible at 500°K and the

concentration of dimers increases as the pressure is increased. Hence, part of the measured deactivation rate is due to dimers at 300 and 400°K. Therefore, all the comments made regarding the interpretation of K_{obs} and $K_{\text{CO}_2\text{-M}}$ in the case of $\text{M}=\text{HCOOH}$ are also applicable to Acetic acid at temperatures where the dimer concentration is appreciable.

Thus the temperature range that can be used for estimating the transition moments is narrowed down to 500-750°K. It is felt that this temperature range is too small to estimate the transition moments in view of the large number of processes involved.

CHAPTER V

CONCLUSIONS

The Laser Induced Fluorescence technique has been used to measure the deactivation rates of the asymmetric stretch mode of CO_2 in collisions with polyatomic molecules. The polyatomic molecules studied are CH_3OH , CH_3OD , $\text{C}_2\text{H}_5\text{OH}$, $\text{C}_2\text{H}_4\text{O}$, CH_3CHO , HCOOH and CH_3COOH . These measurements have been carried out at those temperatures where no dissociation of these molecules occurred in the range of 300-750°K. The studies have been limited to lean mixtures of the polyatomic molecules, all below 12.5%, due to the limitations imposed by the time constant of the detector and the associated electronic circuitry, which is $< 2 \mu\text{sec}$. The lean mixture data is extrapolated to 100% of polyatomic gas composition to get the deactivation rate $K_{\text{CO}_2-\text{M}}$ of CO_2 with the polyatomic molecule M. The measured deactivation rates are in the range of 20-400 $\text{msec}^{-1}\text{torr}^{-1}$ and decreased with increasing temperature.

The deactivation rates of the $\text{CO}(v=1)$ mode with the above polyatomic molecules (with the exception of CH_3OD and $\text{C}_2\text{H}_4\text{O}$) are measured⁶⁸ at room temperature and are 5.9, 5.9, 4.7, 11.7 and 20 $\text{msec}^{-1}\text{torr}^{-1}$ for CH_3OH , $\text{C}_2\text{H}_5\text{OH}$, CH_3CHO , HCOOH and CH_3COOH respectively. These rates are quite small since only the bands around 2150 cm^{-1} , which are all weak,

can cause deactivation of $\text{CO}(v=1)$. The corresponding rates of deactivation of $\text{CO}_2(00^{\circ}1)$ mode obtained in the present work are about 17, 35, 10, 28 and 20 times faster than those for the $\text{CO}(v=1)$ deactivation by the same molecules respectively. These enhanced rates are due to the additional deactivation channels available in CO_2 for the transfer of energy through $(00^{\circ}1 \rightarrow 020, 100)$ transitions and the existence of very strong/strong fundamental vibrational bands in the polyatomic molecules to take the energy by near-resonant V-V processes. In the alcohols it is the very strong C-O stretch which is responsible for the enhanced rate while in $\text{C}_2\text{H}_4\text{O}$ two very strong ring deform vibrations are responsible and in CH_3CHO the strong C-C stretch and the medium CH_3 rock bands are responsible. Since only strong and medium bands are responsible for the deactivation in the case of CH_3CHO , it is the least efficient of the seven polyatomic molecules studied.

In the case of the two acids, the deactivation rates are even larger. However, because of dimer formation in the vapor phase, the reliability of $K_{\text{CO}_2\text{-HCOOH}}$ and $K_{\text{CO}_2\text{-CH}_3\text{COOH}}$ obtained by extrapolation to zero percent of CO_2 is uncertain.

The dipole moments of the transitions involved in the polyatomic molecules are estimated. This is done with the

help of the experimentally derived probabilities at different temperatures and the SB theory. These estimated transition moments are approximate to the extent that the SB theory is approximate. However, these moments are in agreement with the relative intensities of the transitions as reported from spectroscopic measurements⁴⁰. If these transition moments can be measured independently, these calculations can be used to test the validity of the SB theory for such calculations in polyatomic molecules.

The useful temperature range for the above calculations in the case of the Carboxylic acids is reduced due to association at the lower temperatures. Considering the fact that the number of processes involved in these molecules is relatively large with respect to the available temperature range, no attempt has been made to calculate the transition moments.

REFERENCES

1. C.K.N. Patel, Phys.Rev. Letts., 12, 588 (1964) and 13, 617 (1964)
2. C.K.N. Patel, W.L.Faust and R.A. McFarlane, Bull. Amer. Phys. Soc., 9, 500 (1964)
3. C.K.N. Patel, P.K.Tien and J.H. McFee, Appl. Phys. Letts, 7, 290 (1965)
4. G.Moeller and J.D. Rigden, Appl. Phys.Letts, 7, 274 (1965)
5. O.P. Judd, Appl. Phys. Letts, 22, 95 (1973)
6. E.T. Gerry, IEEE Spectrum, 7(11), 51 (1970)
7. C.K.N. Patel in "Lasers" Vol.2, ed. Levine, chapter 1, Marcel Dekker, New York (1968)
8. N.V. Karlov, Appl. Optics, 13, 310 (1974)
9. J.C. Stephenson and S.M. Freud, J.Chem.Phys., 65, 1893 (1976)
10. J.M.Press, R.E. Weston Jr and G.W. Flynn, Chem.Phys.Letts 46, 69 (1977)
11. C.B. Moore in "Fluorescence" ed. by Gilbault, chapter 3, Marcel Dekker, New York (1967)
12. R.D. Sharma and C.A. Brau, J.Chem.Phys., 50, 924 (1969)
13. R.N. Schwartz, Z.I. Slawsky and Herzfeld, J.Chem. Phys., 20, 1591 (1952)
14. F.I. Tanczos, J.Chem.Phys., 25, 439 (1956)
15. F.H. Mies, J.Chem.Phys., 42, 2709 (1965)
16. J.L. Stretton in "Transfer and storage of energy by molecules" ed. by G.M. Burnett and A.M. North, chapter 2, John Wiley (1969)
17. K.F. Herzfeld and T.F. Litovitz in "Absorption and dispersion of Ultrasonic waves", Academic Press, London (1959)

18. C.B. Moore in "Advances in Chem.Phys.", ed. by I.Prigogine and S.A. Rice, Vol.23, chapter 2, John Wiley (1972)
19. J.D. Stettler and N.M. Witriol, Chem.Phys.Letts, 23, 95 (1973)
20. P.D. Gait, Chem.Phys.Letts. 41, 236 (1976)
21. J.D. Stettler and N.M. Witriol, Chem.Phys.Letts. 41, 241 (1976)
22. W.G. Tam, Chem.Phys.Letts. 15, 113 (1972)
23. R.D. Sharma, Chem.Phys. Letts. 30, 261 (1975)
24. T.A. Dillon and J.C. Stephenson J.Chem.Phys. 58, 2056, 3849 (1973) and 60, 4286 (1974)
25. R.C. Amme in "Advances in Chem.Phys.", ed. by I.Prigogine and S.A. Rice, Vol.28, Chapter 3, John Wiley (1975)
26. Stephen Ormonde, Rev. Modern Phys. 47, 193 (1975)
27. L.O. Hocker, M.A. Kovacs, C.K. Rhodes, G.W. Flynn and A. Javan, Phys.Rev.Letts. 17, 233 (1966)
28. J.T. Yardley and C.B. Moore, J.Chem.Phys. 45, 1066 (1966)
29. G.W. Flynn in "Chemical and biological applications of lasers" ed. by C.B. Moore, chapter 6, Academic Press (1974)
30. E.Weitz and G.W. Flynn in "Annual Rev.Phys.Chem.", ed. by H.Eyring, Vol.25, Annual review incorp. Co.(1974)
31. A.J. Andrews and C.J. S.M. Simpson, Chem.Phys. Letts 41, 565 (1976)
32. R.J. Pirkle and T.A.Cool, Chem.Phys.Letts, 42, 58 (1976)
33. L.A. Gamss, B.H. Kohn, M.I. Pollack and A.M. Ronn, Chem. Phys. 18, 85 (1976)
34. M.A.Kovacs, D.R. Rao and A.Javan, J.Chem.Phys. 48, 3339 (1968)
35. Y.V.Chalapathi Rao, V.Subba Rao and D. Ramachandra Rao, Chem.Phys.Letts. 17, 531 (1972) and Y.V. Chalapati Rao, Ph.D. Thesis, I.I.T.Kanpur, 1972

36. P. Ramamohana Rao, Y.V.Chalapathi Rao, S.V.Babu and V.Subba Rao, Ind. J.Phys. 50, 259 (1976) and Proceedings of the "DAE Chemistry Symposium on Fast reactions, chemistry and measurement" held at VSSC, Trivandrum, February 17-21, 1977, to be published.
37. I.V.Rao, Ph.D. Thesis, I.I.T. Kanpur (1976)
38. W.A. Rosser Jr, A.D. Wood and E.T. Gerry, J.Chem.Phys., 50, 4996 (1969)
39. C.B. Moore, Acc. Chem. Research 2, 103 (1969)
40. T. Shimanouchi, Tables of molecular vibrational frequencies, consolidated Volume I, NSRDS-NBS 39 (National Bureau of Standards, Washington, 1971)
41. M.Filk and E. Whalley, J.Chem.Phys. 34, 1554 (1964)
42. L.Landau and E.Teller, Z.Phys. Sowjetunion, 10, 34 (1936)
43. I. Burak, Y.Noter, A.M. Ronn and A.Szoke, Chem.Phys.Letts, 16, 306 (1972)
44. R.D. Sharma, H.L. Chen and A. Szoke, J.Chem.Phys., 58, 3519 (1973)
45. W.Q. Jeffers and J.D. Kelly, J.Chem.Phys. 55, 4433 (1971)
46. R.D. Sharma, Phys.Rev., 177, 102 (1969)
47. B.M. Hopkins, H.L. Chen and R.D. Sharma, J.Chem.Phys. 59, 5758 (1973)
48. W.A. Rosser Jr, R.D. Sharma and E.T. Gerry, J.Chem.Phys. 54, 1196 (1971)
49. D.Frankel, J.I. Steinfeld, R.D. Sharma and L. Poulsen, Chem.Phys.Letts. 28, 485 (1974)
50. R.D. Sharma and C.W. Kern, J.Chem.Phys., 55, 1171 (1971)
51. I.W.M. Smith and C. Morley, Trans. Farad Soc., 67, 2575 (1971)
52. R.D. Sharma, R.B.Malk, R.R.Hart and R.H. Picard, Chem. Phys.Letts. 35, 286 (1975)

53. J.O. Hirschfelder, C.F.Curtiss and R.B. Bird, Molecular Theory of Gases and Liquids (Wiley, New York, 1954)
54. P.Venkateswarlu and W. Gordy, J.Chem.Phys., 23, 1200 (1955)
55. E.K. Plyler, J.Research NBS, 48, 281 (1952)
56. L.M.Imanov, Ch.O.Kadzhar and I.D.Isaev, Optics and spectroscopy 18, 194 (1965)
57. R.C.Lord and N.B.Nolin, J.Chem.Phys., 24, 656 (1956)
58. H.W.Thompson and W.T.Cave, Trans.Farad Soc. 47, 946 (1951)
59. JANAF Thermochemical Tables (U.S.Dept. of Commerce, NBS, 1965)
60. S.M. Sverdlov, M.A.Kovner and E.P.Krainov, Vibrational spectra of polyatomic molecules, John Wiley (1974)
61. J.C. Evans and H.T. Bernstein, Can.J. Chem. 34, 1084 (1956)
62. J.C. Morris, J.Chem.Phys., 11, 230 (1943)
63. L.G.Boner and R.Hofstadter, J.Chem.Phys. 6, 531 (1938)
64. A.S. Coolidge, J.Amer.Chem.Soc. 50, 2166 (1928)
65. J.K.Wilshurst, J.Chem. Phys., 25, 1171 (1956)
66. F.M.Mac Daugall, J.Amer.Chem.Soc. 58, 2585 (1936)
67. R.M. Badger and S.H.Bauer, J.Chem.Phys., 5, 605 (1937)
68. J.C.Stephenson and E.R. Mosburg, J.Chem.Phys., 60, 3562 (1974)
69. G.Herzberg, Electronic spectra of polyatomic molecules (Von Nostrand Publishing Co., New York (1966))
70. J.C.Stephenson and C.B. Moore, J.Chem.Phys., 52, 2333 (1970)
71. J.M. Prausnitz, Molecular Thermodynamics of Fluid Phase Equilibria, Prentice Hall, New Jersey (1969)

ACKNOWLEDGEMENTS

With deep sense of gratitude, I would like to express my sincere thanks to Dr. S.V. Babu and Dr. Y.V.Chalapathi Rao for their valuable guidance throughout the course of this work. Dr. Y.V.C. Rao not only introduced me to the exciting field of lasers but his experimental expertise has been a constant source of help, without which this work could not have been progressed at all. My discussions with Dr. S.V. Babu at various stages assisted me in the theoretical analysis and interpretation of the experimental results.

I would like to thank Professor D. Ramachandra Rao, of physics Department for his unreserved help and encouragement during the course of this work. The discussions I had with him has helped me a lot in the final preparation of the manuscript. Thanks are also due to Professor V.Subba Rao for his help and encouragement.

The unassuming help I have received from Mr. K.M.S.Prasad in the working of the electronic equipment can not be over emphasised. Mr. L.S.Rao and Mr. Ansari of workshop and Mr. C.M. Sharma of glass blowing deserve a special mention for their valuable help all throughout. I am grateful to all of them.

Thanks are due to my friends, Mr. Ramakrishna for many useful discussions and his assistance in computer programming, Mr. K.B.K.Rao, Mr. L.V.Sivaji and Mr. V.Sasidhar for their help in the experimental work and Mr. K.K.Rao for his assistance in computer programming at various stages.

The timely services of Mr. R.P.Yadav and the neat typing of Mr. M.M.Beg are acknowledged.

I owe an apology rather than effusive thanks to my wife Bharati who, while tolerating immense difficulties, remained a constant source of inspiration and encouragement throughout the course of this work.

Now, my wife joins me with our son Rajeev, in recalling the happy times we spent at IIT/Kanpur with many of our friends, in particular Madhava Raos, Satyanarayan, Captain (Major), NS Rao, Radha Krishna (popularly known as Mathes teacher), Babu, Gandhi, DP Rao, LS Rao, Govardhan, Hari Babu, KK Rao, Ramakrishna, Srihari, KBK, Chhatrapati, Anjaneyalu, Narasaiah, Sita, Monica, Professor etc., and their families.

Finally, the financial grant by CSIR in the form of a Senior Research Fellowship is gratefully acknowledged.

(Ramamohana Rao)